Comparison of regge models of pion-nucleon scattering and related processes

R. A. Swetman

COMPARISON OF REGGE MODELS OF PION-NUCLEON SCATTERING AND RELATED PROCESSES.

COMPARISON OF REGGE MODELS OF PION-NUCLEON SCATTERING AND RELATED PROCESSES.

THESIS SUBMITTED TO THE UNIVERSITY OF DURHAM.

BY

R.A.SWETMAN

FOR THE DEGREE OF DOCTOR OF PHILOSOPHY

DEPARTMENT OF PHYSICS
UNIVERSITY OF DURHAM

DECEMBER 1972

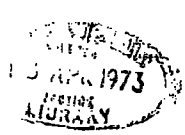

ABSTRACT

A phenomenological analysis of pion nucleon scattering at high energies is presented in terms of several absorptive models for the πN amplitudes. In the past there have been two popular versions - the weak-cut model and the strong-cut model. In general it was difficult to choose between these two very different approaches. However the whole absorptive approach was thrown into doubt when better information about the polarization in $\pi^- p \to \pi^0 n$ at larger $|t|$ became available last year. The new data in fact accords with the predictions of the $\rho + \rho'$ pole fit of Barger and Phillips. More recently measurements of the R parameter in $\pi^{\pm} p \to \pi^{\pm} p$ have enabled the phases of the πN amplitudes to be determined, and again these agree with the Barger-Phillips (B.P) predictions but contradict both types of absorption model.

We assume that the B.P $I_t = 0$ amplitudes are a reliable representation of these amplitudes, and we fit these with a somewhat simpler parameterization. For our $I_t = 1$ amplitudes we find that a t-channel parameterization plus crossing was much preferred to the usual direct s-channel parameterization. We find, by correctly taking into account the real parts of the $I_t = 0$ non-flip amplitude i.e essentially, by including a $\rho \otimes P'$ cut contribution in the $I_t = 1$ amplitudes, that our fits improved considerably, especially the charge-exchange polarization.

We find that the fixed-pole coupling model is by far the best. In general the data is reasonably well fitted apart from the high $|t|$ region of our elastic polarization. This is traced back to our rather poor representation of the real parts of the $I_t = 1$ amplitudes. It is unlikely that a better representation

of the $I_t = 0$ amplitudes will remedy this defect. The imaginary parts of these amplitudes are in good agreement with amplitude analysis. We conclude that the absorption prescription, with any hypothesis about the choosing mechanism of the ρ pole is not completely successful in explaining the $I_t = 1$ amplitudes. It works well for the imaginary parts and less so for the real parts, and we indicate possible reasons for this.

ACKNOWLEDGEMENTS

I should like to thank my supervisor Dr.P.D.B.Collins for his friendly help and patient guidance during the preparation of this work.

I have benefitted also from discussions with many people, in particular Dr.P.K.Hutt.

The work was supported by a Science Research Council Research Studentship.

PREFACE

Part of the work reported here has been done in collaboration with Dr.P.D.B.Collins and is published in Lettere al Nuovo Cimento vol.5 n.12, 793 (1972).

No part of the work presented in this thesis has previously been submitted for a degree in this or any other University.

CONTENTS

CHAPTER 1

INTRODUCTION

The theoretical study of the interactions between elementary particles, over a hundred of which have been discovered, involves various standpoints and techniques. These can roughly be divided into three branches:-

(a) Quantum Field Theory, which describes particle interactions by means of an interaction Lagrangian constructed from the field operators.

(b) S-matrix theory, which attemts to describe interactions in terms of measurable quantities only e.g energy, momenta, spin etc.

(c) Symmetries. These include Lorentz covariance, crossing symmetry, spin and isospin groups and SU_3 symmetry.

Field theoretic models have been outstandingly successful for electromagnetic interactions, but not so far for the strong interactions. For this reason the latter are almost exclusively studied using the S-matrix approach, although some ideas from field theory are sometimes incorporated.

Since this thesis concerns itself with certain aspects of the high energy physics of the strongly interacting particles we shall be adopting the S-matrix approach.

The S-matrix is simply a matrix of the transition amplitudes for the strong interactions. A typical list of important properties which the S-matrix ought to satisfy would be :-

(a) the superposition principle

(b) Lorentz covariance

(c) conservation of probability

(d) short -range character of the forces

(e) transition amplitudes are the real-boundary values of analytic functions.

Some consequences of these are the 'connectedness' of the S-matrix, the unitarity of the S-matrix

$$SS^{+} = S^{+}S = 1 \ , \qquad (1.1)$$

and the fact that the matrix elements depend on the four-momenta only through their invariant scalar products. Property (e), together with the hypothesis that there exists a "physical sheet" of a given invariant, states that on this sheet continuation to the real axis from above (the +ie prescription) gives us the physical transition amplitudes. Implicit in this postulate is the idea of 'crossing', which is the property that transition amplitudes for different regions of the variables are connected by analytic continuation.

The above list of properties of the S-matrix, and their consequences, are generally agreed to be the basic requirements of an S-matrix theory. However so far the theory does not have much dynamical content. To remedy this two slightly more controversial postulates are added as requirements of the S-matrix. They are usually called Maximal Analyticity of the First and Second kinds (hereafter abbreviated to MA1 and MA2) (see ref. 4).

MA1 postulates that the only singularities in the complex energy variables of the invariant amplitudes derived from the connected parts of the S-matrix are the poles corresponding to stable and unstable particles, together with those singularities generated from these poles by the requirements of

unitarity and crossing.

MA2 postulates that the S-matrix is continuable throughout the complex angular-momentum plane, with only isolated singularities.

The consequences of these postulates for general scattering processes (connected parts) is quite complicated (ref. 5) and far reaching. By far the most common and useful applications so far have been to the 2 particle - 2 particle process (the four-line connected part).

As the energy is increased more and more 'communicating' channels become open, and since each appears discontinuously it implies that the scattering amplitude A(s,t) has cuts at these thresholds. In terms of the usual s,t,u Mandelstam variables, MA1 gives the scattering amplitude A(s,t) the analytic structure depicted in fig.(1),(for fixed t).

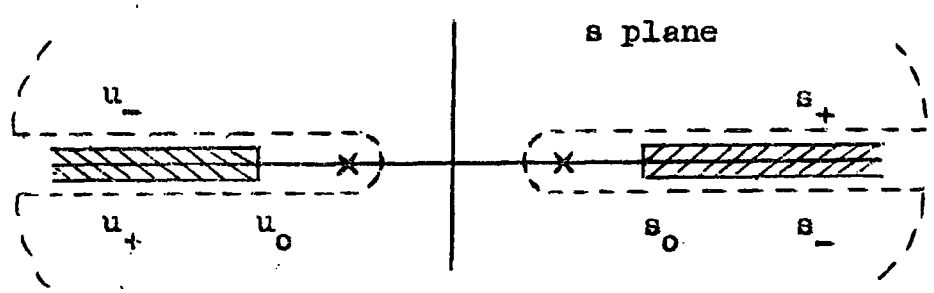

fig.(1)

(fixed t)

We can then write a dispersion relation for A(s,t) (see refs.1,2,3)

$$A(s,t) = \sum \text{poles} + \frac{1}{\pi}\int_{z_R}^{\infty} \frac{D_s(z'_t,t)\,dz'_t}{z'_t - z_t} + \frac{1}{\pi}\int_{-z_L}^{-\infty} \frac{D_u(z'_t,t)\,dz'_t}{z'_t - z_t} \qquad (1.2$$

in the z_t ($=\cos\theta_t$) plane, where D_s is the discontinuity across the R.H cut, D_u the discontinuity across the L.H cut, and z_R corresponds to s_0, z_L to u_0. The above form assumes that $|A(s,t)| \longrightarrow 0$ as $s \longrightarrow \infty$.

If the asymptotic behaviour of $A(s,t)$ is $|A(s,t)| \longrightarrow |s|^{N-\varepsilon}$ $(\varepsilon \geqslant 0)$ as $|s| \to \infty$ then we can now write a dispersion integral for $A(s,t)/s^N$. We get, neglecting the pole terms for the moment, and with $z = z_t$

$$A(s,t) = \sum_{n=0}^{N-1} \gamma_n(t) z^n + \frac{z^N}{\pi} \left\{ \int_{z_R}^{\infty} \frac{D_s(z',t)\,dz'}{z'^N (z'-z)} + \int_{-z_L}^{-\infty} \frac{D_u(z',t)\,dz'}{z'^N (z'-z)} \right\} \qquad (1.3)$$

The $\gamma_n(t)$ are the subtraction constants and are essentially arbitrary. However MA2 tells us how to remove this arbitrariness, and thus completes the dynamical content given to the theory by MA1.

Using s-channel unitarity, Froissart (ref.7) has shown that for finite range strong interaction forces we have the bound

$$|A(s,t)| \leqslant \text{constant} \times s \log^2 s \ , \qquad \text{for } t \leqslant 0, \qquad (1.4)$$

which implies that we need only two subtractions.

PARTIAL WAVE AMPLITUDES AND THE COMPLEX ANGULAR MOMENTUM PLANE

The amplitude $A(s,t,u)$ can be expanded in a series of any set of complete orthogonal funtions, but the most common and convenient choice is the set of angular momentum eigenfunctions. Thus a t-channel partial wave amplitude is defined by the 'partial wave projection', (for spinless particles)

$$A_l(t) = \frac{1}{32\pi} \int_{-1}^{+1} A\left(s(z_t,t), t\right) P_l(z_t)\, dz_t \qquad (1.5)$$

for $l = 0, 1, 2, \ldots$.

The corresponding partial wave series is

$$A(s,t) = 16\pi \sum_{l=0}^{\infty} (2l+1)\, A_l(t)\, P_l(z_t). \qquad (1.6)$$

This representation will break down at the nearest s or u singularity. However we can still define the partial wave amplitudes by (1.5) even when (1.6) diverges. If we substitute (1.3) into (1.5) we obtain (see ref.2)

$$A_l(t) = \frac{1}{16\pi^2}\int_{z_0}^{\infty}\left\{D_s(z',t) + (-1)^l D_u(-z',t)\right\}Q_l(z')\,dz' \quad (1.7)$$

which is valid for $l > N$. Here $z_0 = \min(z_R, z_L)$.

Because of the factor $(-1)^l$ the R.H side of (1.7) is not suitable for continuation in the complex angular momentun plane. This difficulty is overcome by defining the "signatured partial wave amplitudes"

$$A^{\pm}(t,l) = \frac{1}{16\pi^2}\int_{z_0}^{\infty}\left\{D_s(z',t) \pm D_u(-z',t)\right\}Q_l(z')\,dz' \quad (1.8)$$

which are now suitable for continuation in l. Equation (1.8) is known as the 'Froissart-Gribov' projection. The actual amplitude is then given by

$$A(z,t) = \frac{1}{2}\left[A^+(z,t) + A^+(-z,t)\right] + \frac{1}{2}\left[A^-(z,t) - A^-(-z,t)\right] \quad (1.9)$$

The partial wave projection (1.8) introduces kinematical zeros and sometimes branchpoints over and above the dynamical singularities. It is often desirable to remove these threshold singularities by defining the 'reduced' partial wave amplitudes (ref.2, also refs.11,12,13)

$$B_l^{\pm}(t) = A_l^{\pm}(t) \,/\, q_t^{2l} \quad (1.10)$$

In terms of partial wave amplitudes elastic unitarity takes the simple form

$$\mathrm{Im}\; A_l^{aa}(t) = \frac{2q_t}{\sqrt{t}}\left|A_l^{aa}(t)\right|^2 \quad (1.11)$$

and so we can write

$$A_\ell^{aa}(t) = \frac{e^{2i\delta_\ell(t)} - 1}{2i\rho} \qquad (1.12)$$

where $\rho = 2q_t/(t)^{\frac{1}{2}}$, and $\delta_\ell(t)$ is a relativistic phase shift.

To continue to complex l we make use of MA2. The first step is to perform a Sommerfeld-Watson transformation (refs.1.2) on each of the amplitudes $A^{\pm}(s,t)$ separately. Although $A^{\pm}(t,l)$ have been shown to be analytic in l only for Re $l > N$, MA2 allows us to assume that $A^{\pm}(t,l)$ can be continued to the left at least as far as Re $l = -\frac{1}{2}$, even though they may have singularities in this new region. MA2 tells us to expect contributions from isolated singularities and it is these which are then identified with the subtraction terms in the dispersion relation (1.3). For relativistic scattering the expected singularities are poles and cuts. In this way we obtain

$$A^{\pm}(s,t) = 8\pi i \int_{-\frac{1}{2}-i\infty}^{-\frac{1}{2}+i\infty} (2\ell+1) A^{\pm}(t,\ell) \frac{P_\ell(-z_t)}{\sin\pi\ell}\, d\ell.$$

$$+ 8\pi i \int_{cut}^{\alpha_c^{\pm}(t)} (2\ell+1) \Delta^{\pm}(\ell,t) \frac{P_\ell(-z_t)}{\sin\pi\ell}\, d\ell \qquad (1.13)$$

$$- 16\pi^2 \sum_i (2\alpha_i^{\pm}(t)+1)\, \beta_i^{\pm}(t)\, P_{\alpha_i^{\pm}}(-z_t) / \sin\pi\alpha_i^{\pm}(t).$$

where we have exhibited only one cut with branch point at $\alpha_c^{\pm}(t)$ and with discontinuity $\Delta^{\pm}(l,t)$. The behaviour of this cut term depends on the behaviour of the discontinuity Δ at the branch point $\alpha_c(t)$. If Δ is finite there we get an asymptotic behaviour of $s^{\alpha_c(t)}/\log s$. If $\Delta \sim [\ell - \alpha_c(t)]^{\delta}$ $(\delta > 0)$ then the cut term is $\sim s^{\alpha_c(t)}/(\log s)^{1+\delta}$

The last term of (1.13) is the contribution from the 'Regge'

poles (ref.14), with positions and residues $\alpha_i^{\pm}(t)$ and $\beta_i^{\pm}(t)$ respectively. If we have just a single Regge pole of definite signature $\mathcal{S}$ then its contribution to the full amplitude is

$$A^R(s,t) = \frac{1}{2}\left[A^{\mathcal{S}}(z_t,t) + \mathcal{S}\,A^{\mathcal{S}}(-z_t,t)\right]$$
$$\underset{s\to\infty}{\sim} -\gamma(t)\left(\frac{s}{s_0}\right)^{\alpha(t)}\left[\frac{e^{-i\pi\alpha} + \mathcal{S}}{\sin\pi\alpha}\right] \qquad (1.14)$$

where s_0 is a quantity with the dimensions of s.

CHAPTER 2

THE IMPORTANCE OF CUTS

It was originally thought that cut contributions to an amplitude were not very important, and most of the early theory and phenomenological fits concentrated on Regge poles only. However it became increasingly obvious, both theoretically and phenomenologically, that the pure Regge pole model was deficient in many respects. These discrepancies and/or inadequacies are most 'naturally' explained by including these cut contributions. As will be shown later, a Regge cut contribution has the form

$$F(t)\, s^{\alpha(t)} / \log s \qquad (2.1)$$

and without assuming a specific model for cuts, very little is known about the size nor the t dependence of the function F(t). The obvious difference between poles and cuts is the factor log s. However for the energy range that has been experimentally explored, and with the errors involved, this factor is so 'mild' that its presence is difficult to detect. Thus if F(t) turned out to be 'large' we would not be able to disentangle the pole from the cut. To resolve this difficulty we must decide what properties to impose on Regge poles. These will be summerized briefly :

(a) Connection of poles with particles.

It seems reasonable to use only Regge pole trajectories which contain established resonances. An exception is the Pomeron, which may or may not be associated with the f or f'. Thus we exclude the use of such poles as the ρ', ω', P'' etc. for which there is doubtful evidence.

(b) Phase.

This is given by the signature factor $\xi + e^{-i\pi\alpha}$ and thus depends on α alone. This is the same for all helicity amplitudes.

(c) Energy dependence.

$$d\sigma/dt \propto s^{2\alpha(t)-2}, \quad \sigma \propto s^{\alpha(t)-1}$$

(d) Factorisation.

If ab → cd is the t channel process then the t channel Regge residue factorises :

$$\beta(t) = \beta_{ab}(t)\beta_{cd}(t).$$

This property relates different processes.

(e) Exchange degeneracy.

The argument for this comes from duality, which requires the choosing nonsense mechanism. However this is not finally settled.

(f) Wrong signature nonsense zeros.

If the residue $\beta(t)$ has a zero then via factorisation these propogate to other processes. This causes difficulties in the understanding of cross-over phenomena in $\bar{K}N$, KN and $\bar{N}N$, NN elastic scattering.

Given these properties there are several features of experimental data which cause trouble for the pure pole model. We mention briefly a few of them.

(a) CEX polarization.

Since the ρ is the only known particle which can be exchanged in $\pi^- p \to \pi^0 n$ then the helicity amplitudes have the same phase, and so the polarization should be zero. This is contrary to data. For $\pi^- p \to \eta^0 n$ one can appeal to a second A_2 trajectory i.e a split A_2 , to give us a non-zero polarization.

(b) Crossover mechanism.

The crossover between $d\sigma/dt(\bar{p}p)$ and $d\sigma/dt(pp)$ is explained by a zero in the ω non-flip residue. Using factorisation it can be shown that this must be a universal zero. It is observed in $K^{\pm}p$ scattering but not universally.

(c) Pion conspiracy.

For both $pn \to np$ and $\gamma p \to \pi^+ n$ a pion-conspirator c as well

as a π exchange are required to fit the data, but the zero (or deep minimum) needed in the π residue is again propogated by factorisation, which contradicts other data.

(d) Missing dips.

WSNZ give a neat explanation of dips. However some reactions do not have dips and unsatisfactory arguments have to be invoked to explain this (e.g important contributions from Λ_γ or N_γ)

(e) Serpukhov data (25-65 Gev/c).

Regge pole theory predicts a steady decrease of σ_T but the data is essentially flat. A sum of Regge poles gives

$$\sigma_T = \sum_i \sigma_i \, s^{\alpha_i(0)-1}$$

We expect the pomeron P to have $\alpha_p(0) = 1$ and other leading pole corrections to have $\alpha_i(0) \approx 0.5$. However the data suggests a contribution with $\alpha(0) \approx 0.8$ and is thus incompatible with the known Regge trajectories.

(f) Exotic exchanges.

There are no known Regge poles for exchanges with "exotic" quantum numbers i.e those not included in the usual $\bar{q}q$ and qqq Quark model configurations. Multi-Regge cuts can have exotic quantum numbers, so one might expect these reactions to be pure 'Regge cut'. An example is $\pi^- p \to \pi^+ \Sigma^-$ (double charge exchange) with leading cut $\rho \otimes \rho$.

The inclusion of cuts remedies several of these defects. From a theoretical standpoint cuts are not only desirable but necessary. This is most clearly exhibited by considering the left-hand discontinuity of the signatured partial wave amplitudes. We show explicitly in Appendix A that

$$\mathrm{Im}\left[B^{\pm}(\ell,t)\right]_{L.H} = \frac{1}{32\pi}\int_{4m^2}^{4m^2-t} \frac{ds'}{2q^2}\frac{1}{(-q^2)^{\ell}} P_{\ell}\left(-1-\frac{s'}{2q^2}\right) D_s^{\pm}(s',t-i0)$$

$$+\frac{1}{16\pi^2}\int_{U_-(t)}^{U_+(t)} \frac{ds'}{2q^2}\frac{1}{q^{2\ell}} Q_{\ell}\left(1+\frac{s'}{2q^2}\right)\left(1\mp e^{-i\pi\ell}\right)\rho_{su}(s',4m^2-t-s') \qquad (2.2)$$

for the scattering of spinless, equal mass particles. Here ρ_{su} is the so-called 'third double spectral function' (third dsf) and $U_{\pm}(t)$ are given by

$$U_{\pm}(t) = \frac{1}{2}(4m^2-t) \pm \sqrt{t(t+8m^2)} \qquad (2.3)$$

An analogous result holds for the general case with unequal masses and spin (see ref.1) -

$$\mathrm{Im}\, A^{\delta}_{HJ}(t)\Big|_{L.H} = \frac{1}{32\pi}\int_{-1}^{z_t(s,t_c)} dz_t \Big\{ D_{sH}(s,t)\,\xi_{\lambda\lambda'}(z_t)\, d^{J}_{\lambda\lambda'}(z_t)$$

$$+ \delta(-1)^{\lambda-\nu} D_{uH}(s,t)\,\xi_{\lambda-\lambda'}(z_t)\, d^{J}_{\lambda-\lambda'}(-z_t)\Big\}$$

$$+\frac{1}{16\pi^2}\int_{a(t)}^{b(t)} dz_t\, \rho^{su}_{H}(s,u)\, e^{J}_{\lambda\lambda'}(z_t)\left[\frac{1-\delta e^{-i\pi(J-\nu)}}{2}\right] \qquad (2.4)$$

The equation (2.2) is important for two reasons:-

(a) the appearance of the third dsf ρ_{su} in the second term of (2.2) This term vanishes for physical l values i.e at right signature points, but is finite at wrong signature points. Also since the third dsf does not exist for non-relativistic scattering then this latter term is a purely relativistic effect.

(b) the finite ranges of integration.

This is very important since it implies that the L.H. discontinuity is a regular function of l in the whole finite plane, except for the poles of Q_l (at negative integer values of l) in the second term. Having finite ranges means that (2.2) can be continued as it stands below Re $l > N$, right down to Re $l < \emptyset$. This is not necessarily true for the R.H. discontinuity since this involves an infinite range of integration (see Appendix A), and so, 'a priori', it is only defined for Re $l > N$.

Thus it appears that the L.H. discontinuity of $B^{\pm}(l,t)$ (and therefore of $A^{\pm}(l,t)$) has fixed poles at the wrong signature (WS) negative integers (nonsense l). It can be shown that the remainder of the L.H. cut and the R.H. cut cannot give a cancelling contribution except possibly at isolated values of t. Since the L.H. discontinuity in t of $A^{\pm}(l,t)$ has fixed poles at nonsense l it follows that $A^{\pm}(l,t)$ itself has these fixed l plane poles at nonsense WS l.

It is well known that fixed poles contradict the elastic unitarity equation (continued)(see (1.11))(since the L.H. side of (1.11) is a simple pole and the R.H. side a double pole) in the absence of cuts. If we iterate this procedure we end up with an essential singularity (the so-called 'Gribov disease').

We can get round this difficulty by postulating a Superconvergence relation (SCR) i.e that the residue of the fixed pole vanishes. However it can be shown, at least for some values of t, that this requirement can not be met (refs.1,2). Thus in general these wrong signature fixed poles (commonly called Gribov-Pomeranchuk (G.P) poles (ref.8)) cannot be made to disappear by S.C.R. For this reason unitarity then demands that cuts should exist, since the R.H. terms of (1.11) then have to be evaluated on

different sides of the cut, so that the pole will only appear in one term (with the cut shielding the other).

Apart from violating unitarity these fixed poles cause trouble when we consider the scattering of particles with spin. In this case, the first fixed pole now occurs at $J = \max(\sigma_1 + \sigma_2, \sigma_3 + \sigma_4) - 1 \equiv \sigma - 1$ instead of at $J = -1$ for the spinless case. But a fixed pole at $J = \sigma - 1$ gives an asymptotic behaviour $s^{\sigma-1}$ and so for particles with $\sigma > 2$ we get an immediate contradiction with the Froissart bound (eqn.(1.4)).

We mention here that these fixed poles do not contribute to the asymptotic behaviour of the physical amplitude. This follows immediately from eqn.(1.9).

In the preceding analysis of the continuation of (2.2) from Re $l > N$ down to the left the effects of moving cuts was neglected. In the presence of these cuts it might be possible that as J is reduced another cut in the t plane might overlap the L.H. cut and so $\text{Disc}_t B^{\pm}(l,t)\Big|_{L.H}$ now might not be given by the R.H. side of (2.2) alone, and the reasoning leading to the G.P poles might no longer be valid. Similarly for the essential singularity argument. However as shown by Mandelstam and Wang (ref.15) the movements of the cuts are not such as to affect the G.P fixed poles argument but they do get rid of the essential singularity argument. This agrees with the work of Jones and Teplitz (ref.16), who approached the problem via the N/D method.

GENERAL PROPERTIES

We can gain further insight into the relationship between l and t plane singularities by considering the Froissart-Gribov projection in more detail. Using (1.10) eqn. (1.8) can be written

$$B^{\pm}(\ell,t) = \frac{1}{16\pi^2}\int_{4m^2}^{\infty} \frac{D_s^{\pm}(s,t)}{q^{2\ell}}\, Q_\ell\left(1+\frac{s}{2q^2}\right)\frac{ds}{2q^2}$$

$$= \frac{1}{16\pi^2}\left(\int_{4m^2}^{a^2} + \int_{a^2}^{\infty}\right) \equiv E^{\pm}(\ell,t) + D^{\pm}(\ell,t)\,, \text{ say} \quad (2.5)$$

where $$D_s^{\pm}(s,t) = D_s(s(z,t),t) \pm D_u(s(-z,t),t)$$

Here $E^{\pm}$ is defined by a finite integral and so is meromorphic in the whole ℓ plane except for poles at the negative integers. All other singularities of $B^{\pm}$ come from $D^{\pm}$. Since a^2 can be as large as we please we see that these singularities depend only on the asymptotic behaviour of $D^{\pm}(s,t)$ for $s\to\infty$ i.e the high energy behaviour of the absorptive parts in the s and u channel.

The above representation is valid for Re $\ell > N$, and in general, of course, N is a function of t, $N = \alpha(t)$.

Thus suppose $D_s(s,t) \sim s^{\alpha(t)}(\log s)^{\delta(t)}$ $(s\to\infty)$ then we get the integral

$$\int_{a^2}^{\infty} ds\, s^{-\ell-1+\alpha(t)}(\log s)^{\delta(t)}$$

which gives singularities in the ℓ plane of the form

$$\frac{b(t)}{(\alpha(t)-\ell)^{1+\delta}} \quad + \text{ other terms , for Re } \delta(t) \neq -1$$

$$\text{and} \quad b(t)\log(\alpha(t)-\ell) \quad \text{for Re } \delta(t) = -1 \qquad (2.6)$$

and these of course correspond to cuts in the ℓ plane.

Thus $A(s,t) \sim s^{\alpha(t)}/\log s$ corresponds to a cut in the ℓ plane of the form $b(t)\log(\alpha(t)-\ell)$. Notice that this is infinite at the branch point. This feature is discussed below.

Similar considerations apply when $A(s,t)$ is a continuous superposition of Regge poles e.g

$$D_s \sim \int^{\alpha_c(t)} \rho(\ell',t)\, s^{\ell'}\, d\ell'$$

which gives a singularity like

$$\int^{\alpha_c(t)} dl' \frac{\rho(l',t)}{l'-l} \qquad + \text{other terms,}$$

and this is the form of a Regge cut in the l plane starting at $\alpha_c(t)$

As it stands (2.5) is a valid representation for Re $l > N$ and in this case D has branch points only for $t \geq 4m^2$. In the continuation of D to Re $l < N$ we encounter new singularities in the t plane. These must be l-dependent singularities otherwise they could not disappear suddenly from the physical sheet of the t plane as Re l is increased above N. This follows from the continuity theorem for functions of two or more complex variables. These new singularities thus must be singular surfaces $t = \phi(l)$. These can disappear (as Re l increases above N) from the physical sheet only through the branch points on the real axis. Conversely as l is reduced singularities in the t plane will emerge from the inelastic thresholds. In particular, cuts in the l plane will manifest themselves as cuts in the t plane, which will emerge from the inelastic thresholds.

Not much of a general nature can be said about these l plane cuts, and to date there is no precise prescription for calculating them i.e very little is known about the discontinuity across these cuts. However Bronzan and Jones (ref.17) showed that the discontinuity is singular at the end point and that it also vanishes there.

They did this by considering, in the t plane, the separate contributions from the threshold cuts and the cut generated by the l plane cut - in fig(2) CUT 1 and CUT 2 respectively. Here t_e, t_i are the elastic and inelastic thresholds respectively. If $\gamma(t,l)$ is the discontinuity across CUT 2 then we have

$$B(t_1,\ell) - B(t_1',\ell) = 2i\,\gamma(t,\ell) \qquad (2.7)$$

and from elastic unitarity we have

$$B(t_1',\ell) - B(t_2,\ell) = \frac{4i\nu}{\sqrt{t}}^{\ell+\frac{1}{2}} B(t_1',\ell)\,B(t_2,\ell) \qquad (2.8)$$

where $\nu = q^2 = (t-t_e)/4$.

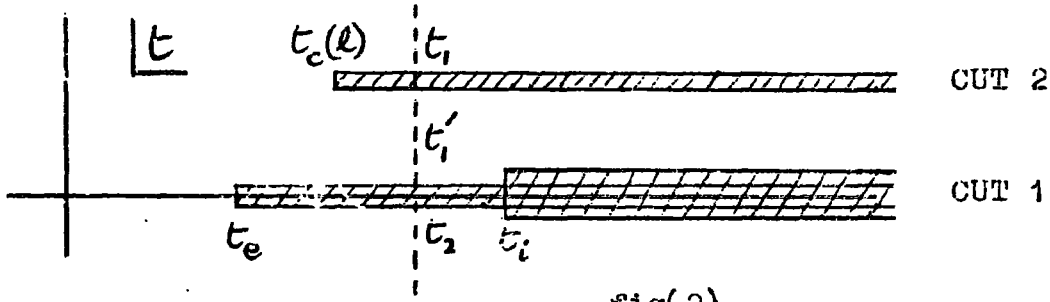

fig(2)

Using these equations they proved that γ must be singular at $t = t_c(1)$ and also that γ vanished at $t = t_c(1)$. It was shown that this implied that the discontinuity of the corresponding cut in the l plane also vanished at its end point.

Without loss of generality we can thus write

$$B(\ell,t) = C\left[t_c(\ell) - t\right]^{\beta} + f(t) \qquad (\beta>0) \qquad (2.9)$$

for t near $t_c(1)$, and where f(t) is regular at $t = t_c(1)$. The contribution of the cut to the full amplitude A(s,t), as $s \to \infty$, is

$$A^{CUT}(s,t) \sim \hat{C}\, s^{\alpha_c(t)} / (\log s)^{1+\beta} \qquad (2.10)$$

and this differs from the usual form by the presence of $\beta > 0$ in the denominator. This is not very important phenomenologically but is very important theoretically. None of the standard methods (discussed later) have this form (they all have $\beta \equiv 0$) and so casts doubt on the theoretical justification for these models.

THE AFS MODEL

The first model for actually calculating cuts was given by Amati, Fubini and Stanghellini (ref.18): - the AFS model.

They considered the equation expressing elastic unitarity in the s channel :-

$$\mathrm{Disc}_s A(s,t) = \frac{q/\sqrt{s}}{32\pi^2\sqrt{s}} \int d\Omega_s \, A_1(s,t_1)\, A_2^*(s,t_2) \qquad (2.11)$$

which holds exactly for $s < s_I$ where s_I is the first inelastic threshold, and where t_1 and t_2 are subject to

$$\delta(t,t_1,t_2) \equiv -(t^2+t_1^2+t_2^2)+2t_1t_2+2tt_1+2tt_2 \geqslant 0 \qquad (2.12)$$

The R.H. side of (2.11) corresponds to the diagram fig.(3a).

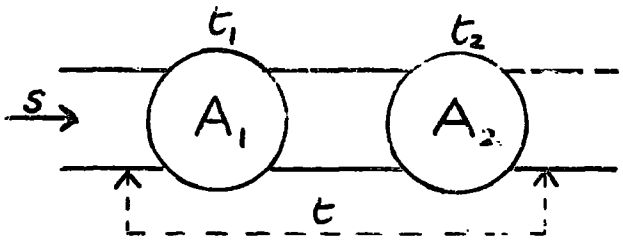

fig.(3a)

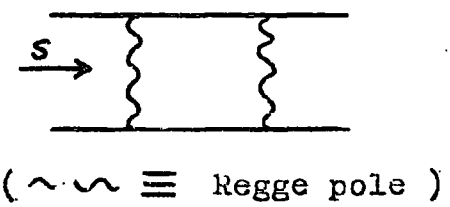

fig.(3b)

Regarding both A_1 and A_2 as given by Regge poles (fig.(3b))

$$A_i(s,t_i) \underset{s\to\infty}{\sim} C_i(t_i)\, s^{\alpha_i(t_i)}$$

we get

$$\mathrm{Disc}_s A(s,t) \sim \iint s^{[\alpha_1(t_1)+\alpha_2^*(t_2)-1]} C_1(t_1) C_2^*(t_2) \frac{\theta(\delta)}{\delta^{1/2}} \, dt_1 \, dt_2 \qquad (2.13)$$

Notice that although (2.11) holds exactly only for $s < s_I$ we have used it for $s \to \infty$ in (2.13).

Assuming the α_i are real the form (2.13) gives a cut with branch point at

$$\alpha_c(t) = \max \left[\alpha_1(t_1) + \alpha_2(t_2) - 1 \right] \qquad (2.14)$$

with t_1 and t_2 subject to $\delta \geqslant 0$. With linear forms for the α's, $\alpha_i(t) = \alpha_i(0) + \alpha_i' t$, and $s \to \infty$, we get

$$\mathrm{Disc}_s A(s,t) \sim F(t)\, s^{\alpha_c(t)} / \log s \qquad (2.15a)$$

where $$\alpha_c(t) = \alpha_1(0) + \alpha_2(0) - 1 + \frac{\alpha_1'\alpha_2'}{\alpha_1' + \alpha_2'} \cdot t \qquad (2.15b)$$

The relation between t, t_1, t_2, at the maximum in (2.14) is

$$(-t_1)^{\frac{1}{2}} + (-t_2)^{\frac{1}{2}} = (-t)^{\frac{1}{2}} \text{ , for maximum.}$$

An attractive property of the AFS model is that the cut contribution does not involve any new parameters - both $F(t)$ and $\alpha_c(t)$ can be expressed in terms of the Regge pole parameters C_i and α_i. Notice however that $F(t)$ involves a complex conjugation C_2^*.

However, as we show below, this AFS cut does not exist on the physical sheet since it is cancelled by higher order unitary contributions. To examine in detail the reasons for this cancellation recourse was made to perturbation theory, where the prescription for calculating the amplitude for a 'Feynman diagram' is known exactly. However the disadvantage here is that, for strong interactions, the perturbation series (for the full amplitude) cannot necessarily be expected to converge, and so the numerical values of individual terms have no special significance. But it is expected that the analytic properties of these terms will exhibit important general properties of the full amplitude. Since complicated Feynmam diagrams are mathematically complicated, the discussion usually confines itself to simple diagrams and iterations and sums of these.

The amplitude for a general ladder diagram can be written

$$F \propto \lim_{\varepsilon \to 0^+} \int \frac{d^4k_1 \ldots\ldots d^4k_j}{\prod_{r=1}^{n} (q_r^2 - m^2 + i\varepsilon)} \qquad (2.16)$$

for equal mass, spinless particles. Here $k_1, \ldots\ldots, k_j$ denote the j independent loop momenta and the q's the momenta of the internal lines.

It can be shown that the leading behaviour of a ladder with n rungs (fig(4a)) is $\frac{g^2}{s}\frac{(K(t)\log s)^{n-1}}{(n-1)!}$ for $s \to \infty$.

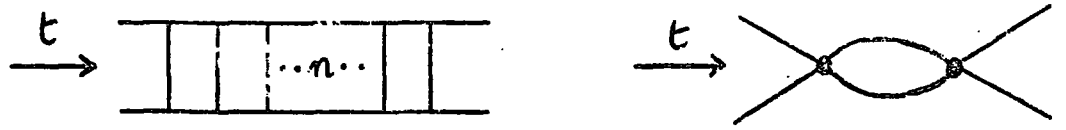

fig(4a) fig(4b)

Here K(t) is a two-dimensional integral over the contracted box diagram fig(4b). If we sum over all ladders, we get the contribution $\sum_{n=1}^{\infty} \frac{g^2}{s}\frac{[K(t)\log s]^{n-1}}{(n-1)!} = g^2 s^{\alpha(t)}, \quad \alpha(t) = -1 + K(t)$

which gives Regge behaviour (ref.19). Thus we have a model for a t channel Regge pole :

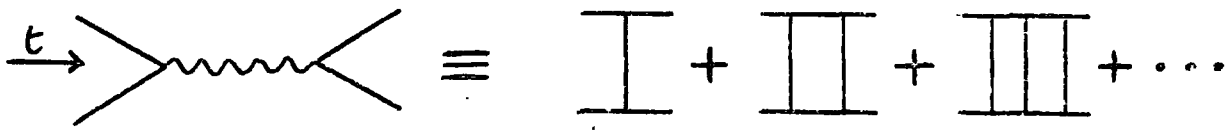

The diagram considered by AFS is essentially that depicted in fig(5a).

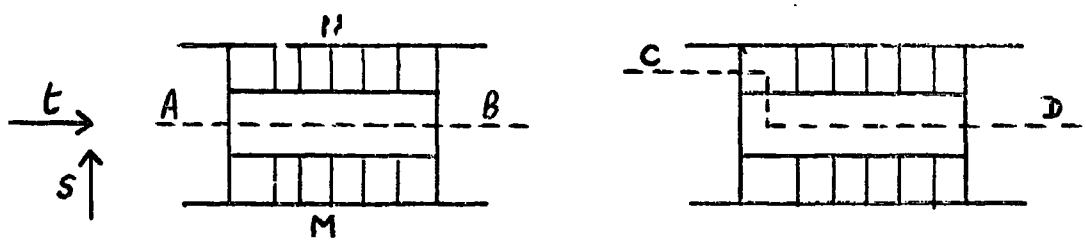

fig(5a) fig(5b)

As a Feyman diagram fig(5a) makes contributions to several 'unitary' diagrams (finite number, if N,M are finite) e.g fig(5a) shows its contribution to the unitary diggram 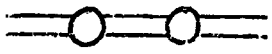 and fig(5b) a contribution to  .

AFS took only the first contribution, and neglected all the others. Recalling the correspondence between ladder sums (Feynman) and Regge poles we would expect that

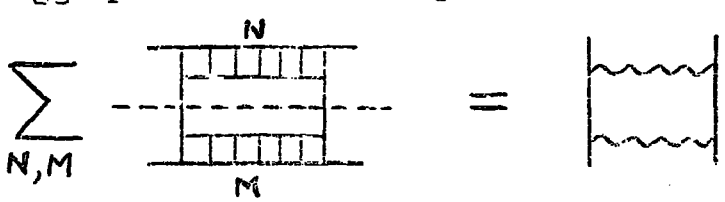

However it can be shown (ref.5) that the asymptotic behaviour of the AFS diagram is log s / s^3 independent of M and N, and so the sum also has this behaviour. This is a fixed cut behaviour and not a moving cut. But retaining only the contributions to the 2 particle unitary diagram seems to give us the moving cut behaviour $s^{\alpha_c(t)}$ log s. Obviously something in the complete contribution has cancelled this. Mandelstam proved this explicitly (ref.20) when he showed that the contribution from fig(5a) was cancelled by a contribution from fig(5b). He went on to show that the cancellation mechanism would not work if instead of the above diagram we considered the "cross" diagram fig(6).

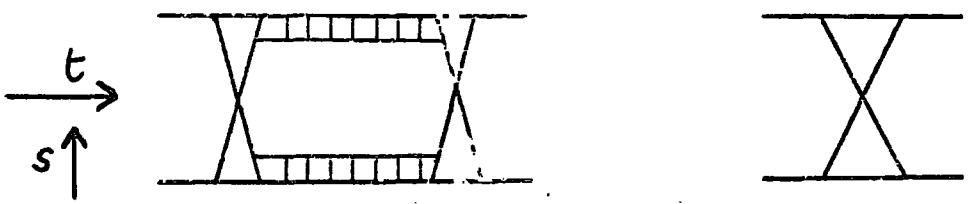

fig(6) fig(7)

It is unlikely that this cut is cancelled by higher order diagrams. The essential property of this diagram is the presence of the third double spectral function. The simplest diagram with a third d.s.f is fig(7) and this has a simple fixed pole at l = -1, from the G.P analysis. The actual diagrams studied by Mandelstam were those of fig(8).

(a) fig(8) (b)

Fig(8a) is simply an iteration of fig(7) and so has a double pole at l = -1. Fig(8b) is really an infinite sum of diagrams and Mandelstam considered the contributions of this sum to the 3 particle intermediate state unitary diagram. He was able to show that

fig(8)b possesed a cut in the l plane whose discontinuity had a double pole at $l = -1$ and that the sum of the diagrams fig(8)a and fig(8)b had no double pole at $l = -1$ on the physical sheet of the l plane. However the sum still possesed a simple pole at $l = -1$ on the physical sheet, and it <u>does</u> have a double pole on the opposite unphysical sheet of the l plane cut. Thus it was shown that the effect of the cut was to prevent the simple pole from becoming an essential singularity via iteration. The same type of reasoning applies to the poles at $l = -3, -5, \ldots$ in the even signature amplitude, and at $l = -2, -4, \ldots$ in the odd signature amplitude, where higher order cuts are presumably available.

Thus it was shown that the AFS diagram did not give rise to a cut on the physical sheet. However it does give a cut on the unphysical elastic sheet of the s plane. This follows immediately from

$$A^{(2)}(s,t) = A^{(1)}(s,t) - 2i\ \mathrm{Disc}_s A(s,t)$$

where $A^{(1)}$ is the amplitude on the physical sheet and $A^{(2)}$ is its continuation through the elastic cut $s_0 < s < s_I$.

Nevertheless there is a similarity between the AFS and Mandelstam diagrams. If for simplicity we consider the diagrams

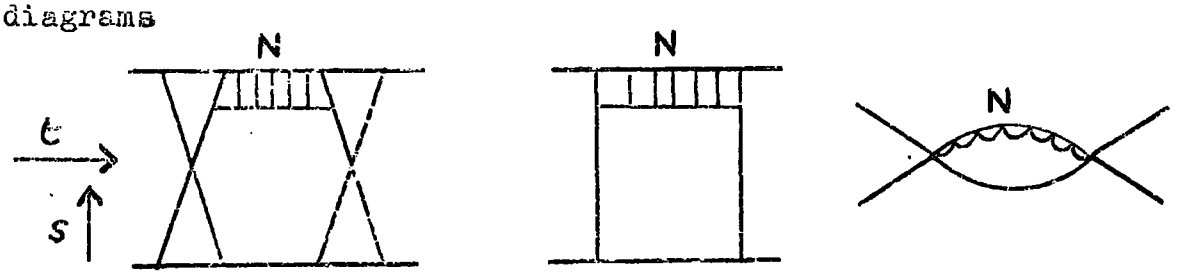

(a) (b) (c)

then it can be shown that (a) has the asymptotic behaviour

$$C_N(t).(\log s)^{N+2}/\ s^2$$

The coefficients $C_N(t)$ are associated with the contracted diagram (c) evaluated with two-dimensional momenta. When we sum over N we get a cut that is analogous to that of (b) on the elastic unphysical sheet. This is plausible because (c) is also the contracted diagram corresponding to (b). Notice however the important difference that the AFS cut involves a complex conjugation while the Mandelstam cut does not. On this basis the 'cross' does not seem to play much of a part, other than actually generating a cut on the physical sheet. This suggests that the 'cross' is a manifestation of something more basic. Intuitively, on the Glauber (ref.21) or Parton picture, we would get the 'cross' structure in a diagram such as

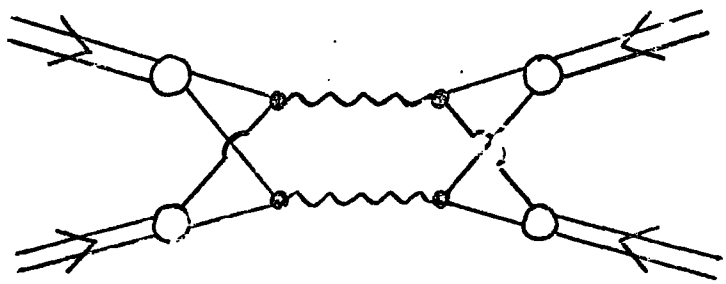

and the cut would then be a result of the compositness of particles. At least it suggests that the existence of cuts depends intimately on the structure of the scattering particles (ref.1).

An illuminating method of discussing the Mandelstam diagram (and others) is the 'Reggeon Calculus' developed by Gribov (ref.22). This is a mixed Feynman-Regge method which avoids the need of having some 'elementary particle' model of Regge poles, such as an infinite sum of ladders. Gribov studied the diagram fig(10) for large s, and found that the discussion was much facilitated by the use of the 'Sudakov' variables (ref.23).

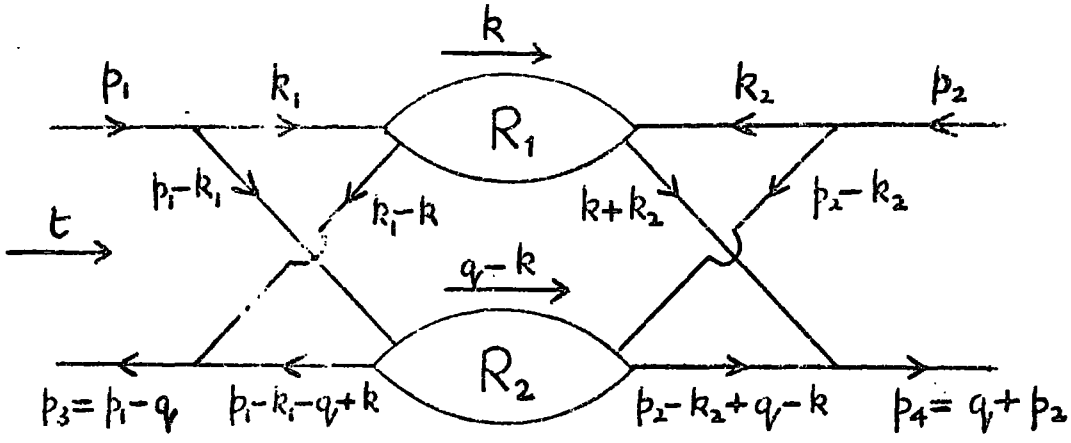

fig(10)

The amplitude for fig(10) is (see eqn.(2.16))

$$A(s,t) = i\lambda^2 \int \frac{d^4k\ d^4k_1\ d^4k_2\ R_1 R_2}{\prod_{r=1}^{8} d_r} \qquad (2.17)$$

where $R_1 = R_1(k_1, k_2, k)$, $R_2 = R_2(p_1-k_1, p_2-k_2, q-k)$ and the d's are the propogators of the internal lines. With suitable assumptions Gribov obtained

$$A(s,t) = \frac{i}{|s|} \int d^2k_\perp\ N^2_{J_1 J_2}(q, k_\perp)\, s^{J_1+J_2}\, \xi_{J_1}\, \xi_{J_2} \qquad (2.18)$$

where ξ_{J_1}, ξ_{J_2} are the usual signature factors, and $N_{J_1 J_2}$ represents the integral over the left-hand cross (the right-hand cross gives a similar result). Taking the discontinuity of (2.18) we have

$$D_s^{\pm} \propto \mathrm{Im}\, A = \frac{1}{|s|} \int d^2k_\perp\ N^2_{J_1 J_2}\, s^{J_1+J_2}\, \mathrm{Re}\left(\xi_{J_1}\, \xi_{J_2}\right) \qquad (2.19)$$

and inserting this in the Froissart-Gribov projection gives

$$A_J \propto \int d^2k_\perp \frac{N^2_{J_1 J_2}\ \mathrm{Re}\left(\xi_{J_1}\, \xi_{J_2}\right)}{J - (J_1 + J_2 - 1)} \qquad (2.20)$$

This gives us the expected cut, whose position is the same as the AFS cut.

A more detailed analysis of $N_{J_1 J_2}$ illustrates well the importance of the 'cross' (or nonzero third double spectral function) We have

$$N(t, t_1, t_2) = \int_{-\infty}^{\infty} ds_1\, A_1(s_1, t, t_1, t_2) \qquad (2.21)$$

where A_1 is the Reggeon-particle scattering amplitude of the left-hand cross.

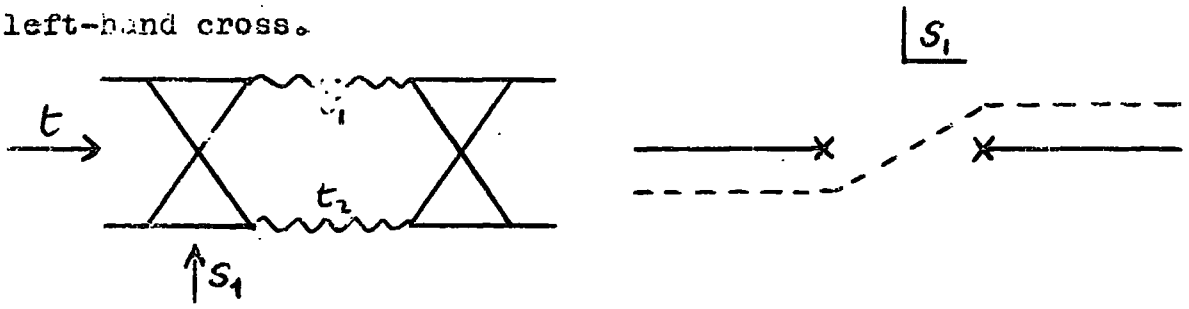

Because of the cross A_1 has a non-zero third d.s.f. i.e it has both left and right-hand cuts. The contour of integration is illustrated above. If there was no cross the amplitude A_1 would only have the right-hand cut and so the contour can be closed in the upper-half plane. Since $A_1 \sim 1/s_1^2$ for large s_1 then N vanishes and so there would be no cut. (A Regge pole behaviour of A_1 amounts to a renormalization of the pole.)

The reason why the usual AFS calculation gives an apparently non-zero result on the physical sheet is that they consider only the on-mass-shell effects. In fact the off-mass-shell part cancels the on-mass-shell contribution. This is demonstrated very simply in the paper by Rothe (ref.24). His method, however, is much less general than Gribov's.

From the above analysis we see that :-

(a) the signature of the cut is given by

$$\mathcal{S} = \mathcal{S}_1 \mathcal{S}_2$$

This follows immediately from (2.18).

(b) from the Sommerfeld-Watson integral, A(s,t) is given by

$$A(s,t) \propto \int_C dJ\, A_J \xi_J s^J = \int d^2k_\perp \int \frac{dJ\, N^2_{J_1 J_2} \xi_J s^J \mathrm{Re}(\xi_{J_1} \xi_{J_2})}{J - (J_1 + J_2 - 1)}$$

and this of course represents a cut in the J-plane starting at

$J_c = \max\,(J_1(k^2) + J_2((q-k)^2) - 1)$ and with discontinuity given by

$$\int d^2k_\perp\, N^2_{J_1J_2}\, \xi_J\, s^J\, \mathrm{Re}\,(\xi_{J_1}\, \xi_{J_2})$$

Neglecting the singularities of $N_{J_1J_2}$ this would give the familiar cut contribution (for large s)

$$A^{\mathrm{cut}}(s,t) \sim s^{\alpha_c(t)}/(\log s) \qquad (\alpha_c \equiv J_c)$$

However as discussed earlier this contradicts the Bronzan-Jones condition, derived from crossed channel elastic unitarity. In this respect the simple cross graph is inadequate. It also fails in that the cut does not perform the necessary duty of properly eliminating the "Gribov disease" of an essential singularity at $J = -1$ (ref.25). The proper incorporation of t channnel unitarity however would require iterations of the simple cross graph. Infact an infinite sum of graphs does correct the above two deficiencies.

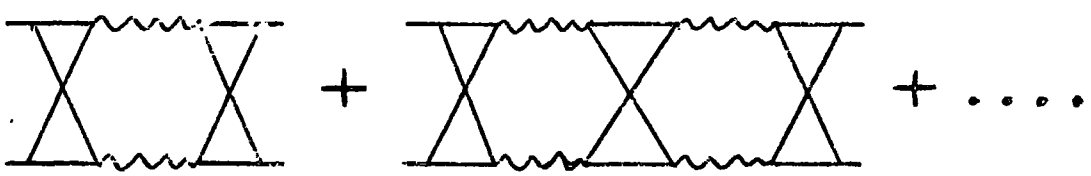

CHAPTER 3

THE ABSORPTION AND EIKONAL MODEL

Although the theory gives us insight into the general properties of cuts, it does not provide a method for calculating them. To remedy this, several models have been proposed, most of which agree to leading order. The basic idea is to write the full amplitude as a power series, identify the lowest order term as the 'Born term' (usually a Regge pole) and the higher order terms as cuts.

As already noted the AFS model was the first and this was an attempt to unitarize the Regge exchange contribution. The unitary equations may be written (in an obvious notation)

$$\mathrm{Im}\, T_{aa} = T_{aa}^{*} \times T_{aa} + \sum_{i \neq a} \int d\Phi_n \, T_{an}^{*} \, T_{an} \quad \text{(elastic)} \quad (3.1)$$

and

$$\mathrm{Im}\, T_{ab} = \mathrm{Re}\left(T_{ab}^{*} \times T_{aa} + T_{bb}^{*} \times T_{ab}\right) + \sum_{n \neq a,b} \int d\Phi_n \, T_{bn}^{*} \, T_{an} \quad \text{(inelastic)} \quad (3.2)$$

For our purposes we may regard a and b as two particle states and n a n-particle state.

The AFS (or multiperipheral) assumption concerning the production amplitudes M_{an} is

$$\sum_{n \neq a} \int d\Phi_n \, M_{an}^{*} \, M_{an} = \mathrm{Im}\, P + \text{low-lying cut}$$
$$\sum_{n \neq a,b} \int d\Phi_n \, M_{an}^{*} \, M_{bn} = \mathrm{Im}\, R_{ab} + \text{low-lying cut} \quad (3.3)$$

where P is the Pomeron (leading contribution for elastic scattering) and R is the leading Regge pole contributions to the scattering $a \to b$.

If we identify T_{an} with M_{an} then equations (3.1) and (3.2) reduce to

$$\begin{aligned} \text{Im } T_{aa} &\approx \text{Im } P + P^* \times P \\ \text{Im } T_{ab} &\approx \text{Im } R_{ab} + 2\text{Re}(P^* \times R_{ab}) \end{aligned} \qquad (3.4)$$

These are the AFS equations. The Regge pole appears as the 'overlap' function. Also note the complex conjugation (ref.26).

If we take P imaginary, P = iIm P, then (3.4) reduce to

$$\begin{aligned} \text{Im } T_{aa} &\approx \text{Im } P + \text{Im } P \times \text{Im } P \\ \text{Im } T_{ab} &\approx \text{Im } R_{ab} + 2\text{Im } P \times \text{Im } R_{ab} \end{aligned} \qquad (3.5)$$

UNITARITY

Thus the 'cut' terms add to the Regge pole terms.

This is to be compared with the Absorption Model result, which we now describe. The absorption effect is due to the existence of many open channels which compete with the one under consideration. In general a single quasi two body production channel constitutes only a small fraction of the total inelastic cross-section. More complex final state configurations also exist with appreciable cross-sections. Intuitivelly one would expect these more complex reactions to be initiated by collisions with small impact parameters (small angular momentum) and thus these collisions would be less likely to participate in the two-body reactions. Thus one would expect that the lower partial waves would be reduced relative to those given by a simple peripheral model, and that the high partial waves are essentially unchanged. This is the absorptive effect. The prescription for taking this into account was given by Sopkovitch (ref.27) and ref.28. viz.

$$A^{J\ ABS.}_{ab}(s) = (S^J_{aa})^{\frac{1}{2}}\, A^J_{ab}(s)\, (S^J_{bb})^{\frac{1}{2}} \qquad (3.6)$$

and the A^J_{ab} is that given by a multiperipheral model (usually a Regge pole).

If we make the usual assumption that

$$S^J_{aa} \approx S^J_{bb} \approx 1 + 2i\rho A^J_{\text{elastic}} \qquad (\rho = 2q_s/s^{\frac{1}{2}})$$

then (3.6) reduces to (ref.1)

$$A^{ABC}_{ab}(s,t) = A_{ab}(s,t) + \frac{i}{8\pi^2 s}\iint_{-s}^{0} dt_1\,dt_2\, A_{ab}(s,t_1)A_{cd}(s,t_2)\frac{\theta(K)}{K^{1/2}} \qquad (3.7)$$

where $K = -(t^2 + t_1^2 + t_2^2) + 2(t_1t_2 + tt_1 + tt_2) + 4tt_1t_2/s$. (3.8)

The form (3.7) holds for large s and small t, t_1, t_2 and the second term corresponds to the diagram

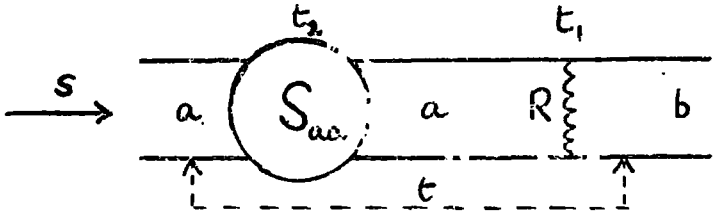

If we use simple Regge pole forms for the amplitudes in the second term, say

$$A(s,t) = -G\,e^{at}\left(\frac{s}{s_c}e^{-i\pi/2}\right)^{\alpha(t)}$$

then we get the contribution (with $\alpha(t) = \alpha(0) + \alpha' t$)

$$\frac{1}{8\pi s}\cdot\frac{G_1G_2}{\alpha_1' + \alpha_2'}\cdot\frac{\left(s/s_0\cdot e^{-i\pi/2}\right)^{\alpha_c(t)}}{\left(\log s/s_0 - i\pi/2\right)} \qquad (3.9)$$

where

$$\alpha_c(t) = \alpha_1(0) + \alpha_2(0) - 1 + \alpha_1'\alpha_2' t/(\alpha_1' + \alpha_2')$$

In deriving (3.9) we used the result (refs.32, 33)

$$\iint_{-s}^{0} dt_1\,dt_2\, e^{b_1t_1 + b_2t_2}\frac{\theta(K)}{K^{1/2}} = \frac{\pi}{A}e^{-\frac{s}{2}(b_1+b_2)}\left[e^{As/2} - e^{-As/2}\right]$$

which we then approximated with

$$\frac{\pi}{(b_1+b_2)}\,e^{b_1b_2t/(b_1+b_2)}$$

Here $A = (b_1^2 + b_2^2 + 2b_1b_2z)^{\frac{1}{2}}$, and $z \approx 1 + 2t/s$. We have also assumed that a_1 and a_2 are small compared with $\log(s/s_0)$.

The cut contribution (3.9) is exactly the kind of term that is expected from Gribov's analysis.

In the above derivation spin was neglected but its inclusion causes no problem. Briefly, we only need to make the change $P_J(z) \to d^J_{\mu\mu'}(z)$ and then use the formula

$$\sum_J (2J+1) d^J_{\mu\mu'}(z) d^J_{\mu_1\mu_2}(z_1) d^J_{\mu''\mu}(z_2) = \frac{2}{\pi} \frac{\theta(\Delta)}{\Delta^{1/2}} \cos(\mu\phi_1 + \mu'\phi_2 + \mu''\phi_3)$$

where $$\Delta(z, z_1, z_2) = 1 - z^2 - z_1^2 - z_2^2 + 2zz_1z_2$$

and the angles ϕ_i are given by (ref.1)

$$e^{i\phi_1} = (z_2 - zz_1 + i\Delta^{1/2})(1-z^2)^{-1/2}(1-z_1^2)^{-1/2} \text{ etc.}$$

The final result is

$$A^{CUT}_{H_s}(s,t) = \sum_{\mu_5\mu_6} \frac{i\rho}{16\pi^2} \iint_{-1}^{+1} dz_1\, dz_2 \left\{ A^{el}_{\mu_1\mu_2\mu_5\mu_6}(z_1,s) A_{\mu_5\mu_6\mu_3\mu_4}(z_2,s) \times \frac{\theta(\Delta)}{\Delta^{1/2}} \cos(\mu\phi_1 + \mu'\phi_2 + \mu''\phi_3) \right\} \quad (3.10)$$

where H_s denotes $(\mu_1\mu_2, \mu_3\mu_4)$, the helicities of the particles (refs.9, 10) and $\mu = \mu_1 - \mu_2$, $\mu' = \mu_3 - \mu_4$, $\mu'' = \mu_5 - \mu_6$

There is one more effect that is usually considered. It was assumed that elastic scattering in the final and initial channels dominated the corrections to inelastic amplitudes. This gave us the expression

$$A^{Abs.}_{ab} \approx A_{ab} + i A_{aa} A_{ab} + i A_{ab} A_{bb} \quad (3.11)$$

If we include other intermediate states ($c \neq a, b$) this generalises to

$$A^{Abs}_{ab} \approx A_{ab} + i(A_{aa}A_{ab} + A_{ab}A_{bb}) + i\sum_{c\neq a,b} A_{ac}A_{cb} \quad (3.12)$$

However there is no rigourous way of estimating this new term. It is assumed (Michigan group, ref.29) that it can be accounted for by multiplying the elastic correction terms by a factor λ, which is expected to be of order 2.

Thus the modified Absorption result is

$$A_{ab}^{Abs} \approx A_{ab} + 2i\lambda A^{el} A_{ab} \qquad (A_{aa} \approx A_{bb} = A^{el}) \qquad (3.13)$$

Note that λ may depend on spin, and in general may be a complex function of s and t. However it is usually assumed to be a real constant.

If we put $A_{ab} = R_{ab}$ (Regge pole) and $A^{el} = i\mathrm{Im}\ P$ then we get (dropping the λ factor for the moment)

$$A_{ab}^{Abs} \approx R_{ab} - 2\mathrm{Im}\ P \times R_{ab} \qquad (3.14)$$

$$\Longrightarrow \quad \mathrm{Im}\ A_{ab}^{Abs} \approx \mathrm{Im}\ R_{ab} - 2\mathrm{Im}\ P \times \mathrm{Im}\ R_{ab} \qquad \text{(Absorptive)}$$

This is to be contrasted with the 'unitarity correction', eqn. (3.5), which has the opposite sign for the cut correction. This difference also arises in the elastic case - the eikonal model of Arnold (ref.30) (to be described below) which gives

$$S_{aa} = 1 + 2iA_{aa} = \exp(2iP)$$

$$\text{and so} \qquad \mathrm{Im}\ A_{aa} = \mathrm{Im}\ P - \mathrm{Im}\ P \times \mathrm{Im}\ P \qquad \text{(Eikonal)} \qquad (3.15)$$

The sign given by the Absorptive-Eikonal model ((3.14), (3.15)) is definitely preferred, both experimentally and theoretically (refs.22, 26).

This contradiction between the two prescriptions was resolved by Caneschi (ref.31, 37) who pointed out that the identification $T_{an} \approx M_{an}$ for the production amplitudes used in deriving the unitarity correction should be replaced by

$$T_{an} = S_{aa}^{\frac{1}{2}} M_{an} S_{nn}^{\frac{1}{2}} \qquad (3.16)$$

since the absorption model seems plausible for inelastic scattering. (3.16) says that the physical production amplitude T_{an} is a multiperipheral amplitude M_{an} with absorptive corrections.

To obtain the first order corrections to the dominant Regge pole contributions we must also take into account corrections of the same order in the production amplitudes T_{an}. It is assumed that the equations (3.3) still hold. We have to decide what to take for S_{nn} and as a first approximation we put $S_{nn} \approx 1$ i.e we assume that absorption in production channels is negligible. Also we take $S_{aa} \approx 1 + 2iP$ which gives $S_{aa}^{\frac{1}{2}} \approx 1 + iP$, so that

$$T_{an} \approx (1 + iP)\, M_{an} \tag{3.17}$$

Putting this in (3.1) and using (3.3) we get

$$\begin{aligned} \text{Im } T_{aa} &= \text{Im } P + P^* \times P - 2\text{Im } P \times \text{Im } P + \ldots \\ &= \text{Im}P + \text{Re } (P \times P) + \ldots \end{aligned} \tag{3.18}$$

which agrees with the eikonal model eqn.(3.15).

For two body inelastic scattering we have

$$T_{an} \approx M_{an} + iM_{an} \times P + iM_{bn} \times R_{ab}$$

and putting this in (3.2) and using (3.3) again we end up with

$$\begin{aligned} \text{Im } T_{ab} &= \text{Im } R_{ab} + 2\text{Re } (R_{ab} \times P^*) - 4\text{Im } R_{ab} \times \text{Im } P + \ldots \\ &= \text{Im } R_{ab} + 2\text{Re } (R_{ab} \times P) + \ldots \end{aligned} \tag{3.19}$$

which agrees with the absorptive prescription (3.14).

Thus the use of absorptive corrections is consistent with unitarity. Absorptive corrections to production amplitudes together with unitarity reproduce the absorptive corrections to the two body inelastic scattering amplitude. Similarly for elastic scattering and the eikonal prescription. Note that the above derivation was independent of P being imaginary.

It is important to point out that the above derivation deals only with the imaginary part of the amplitude - it does not

tell us the corrections to the real part. In this respect the absorptive and eikonal prescriptions go further than unitarity.

THE EIKONAL MODEL

The impact parameter b is defined by the equation

$$J = q_s b = \tfrac{1}{2} \qquad (3.20)$$

where q_s is the c.m 3 momentum.

The partial wave series with spin is

$$A_H(s,t) = 16\pi \sum_J (2J+1)\, A^J_{H_s}(s)\, d^J_{\mu\mu'}(z_s) \qquad (3.21)$$

We make the following replacements in (3.21), which are valid for $|s| \to \infty$ and $|t| \ll |s|$:-

(1) $d^J_{\mu\mu'}(z_s) \longrightarrow J_{\bar\mu}\left[(J+\tfrac{1}{2})\right]$ (Bessel function of order $\bar\mu$)

where $\bar\mu \equiv |\mu-\mu'| \equiv \| \mu_1-\mu_2|-|\mu_3-\mu_4\|$.

(2) $\sum_J \longrightarrow \int_0^\infty q_s\, db \quad (\approx \int_0^\infty \Delta J)$

(3) $A^J_H(s) = (\exp(2i\delta_J(s))-1)/2i\rho(s)$

$\longrightarrow (\exp(i\chi_{H_s}(s,b))-1)/2i\rho(s) \qquad (\rho(s) = \frac{2q_s}{s^{\frac{1}{2}}})$

$\chi_H(s,b)$ is called the eikonal function (see ref.1).

Equation (3.21) then becomes

$$A_{H_s}(s,t) = 4\pi s i \int_0^\infty b\,db \left[1 - e^{i\chi(s,b)}\right] J_{\bar\mu}(b\sqrt{-t})$$

$$= 4\pi s \int_0^\infty b\,db \left[\chi + \frac{i\chi^2}{2!} - \frac{\chi^3}{3!} + \ldots - \frac{i(i\chi)^n}{n!} + \ldots\right] J_{\bar\mu}(b\sqrt{-t}) \qquad (3.22)$$

(Here we have taken $z_s = \cos\theta = 1 + t/2q_s^2$ which gives $\theta \approx \sin\theta \approx (-t)^{\frac{1}{2}}/q_s$ for small t , and so $(J+\tfrac{1}{2})\theta \approx b(-t)^{\frac{1}{2}}$.)

In potential scattering (ref.21) we have

$$\chi_{H_s}(s,b) = \frac{1}{8\pi s}\int_{-\infty}^{0} dt\, J_{\bar{\mu}}(b\sqrt{-t})\, A^{Born}_{H_s}(s,t) \qquad (3.23)$$

and taking the inverse of this we get

$$A^{Born}_{H_s}(s,t) = 4\pi s \int_0^{\infty} b\,db\, \chi_{H_s}(s,b)\, J_{\bar{\mu}}(b\sqrt{-t}) \qquad (3.24)$$

Thus we identify the first term of (3.22) with the 'Born term'. If we regard this as a Regge pole amplitude then the higher order terms will give us cuts.

In elastic scattering we expect the Pomeron P, the P' and possibly the P'' to be the contributing Regge poles. Thus we take

$$A^{Born} = A^{P} + A^{P'} + A^{P''} = A^{E} \text{ say} \qquad (3.25)$$

so that

$$\chi^{E}_{H_s}(s,b) = \frac{1}{8\pi s}\int_{-\infty}^{0} dt\, A^{E}_{H_s}(s,t)\, J_{\bar{\mu}}(b\sqrt{-t}) \qquad (3.26)$$

which gives

$$A^{el}_{H_s}(s,t) = 4\pi s \int_0^{\infty} b\,db\left[\chi^{E}_{H_s} + \frac{i}{2!}\left\{\chi^{E}.\chi^{E}\right\}_{H_s} + \ldots\right] J_{\bar{\mu}}(b\sqrt{-t}) \qquad (3.27)$$

The χ's are of course matrices in helicity space.

The first term of (3.27) gives us back the Regge pole amplitudes, while the second term gives us the first (dominant) cut contribution :

$$A^{CUT(1)}_{H_s} = 2\pi i s \int_0^{\infty} b\,db\left\{\chi^{E}.\chi^{E}\right\}_{H_s} J_{\bar{\mu}}(b\sqrt{-t})$$

$$= \frac{2\pi i s}{(8\pi s)^2}\sum_{\mu''}\iint_{-\infty}^{0} dt_1\,dt_2 \int_0^{\infty} b\,db\, J_{|\mu-\mu''|}(b\sqrt{-t_1}) \times$$

$$\times A^{E}(s,t_1)\, J_{|\mu''-\mu'|}(b\sqrt{-t_2})\, A^{E}(s,t_2)\, J_{\bar{\mu}}(b\sqrt{-t}) \qquad (3.28)$$

For elastic scattering the flip amplitude is very small so we can

take $\mu = \mu' = \mu''$. For the non-flip amplitude $\bar{\mu} = 0$, and by using the formula

$$\int_0^\infty b\,db\, J_{\bar{\mu}}(b\sqrt{-t_1}) J_0(b\sqrt{-t_2}) J_0(b\sqrt{-t}) = \frac{2}{\pi} \frac{\theta(K)}{K^{1/2}} \qquad (3.29)$$

where K is given by (3.8), we get

$$A^{CUT(1)}_{non\text{-}flip} = \frac{i}{16\pi^2 s} \iint_{-\infty}^{0} dt_1\, dt_2\, A^E(s,t_1) A^E(s,t_2) \frac{\theta(K)}{K^{1/2}} \qquad (3.30)$$

Similarly for the higher order cuts.

We can extend the above to inelastic processes with quantum number exchange by adding absorptive corrections.

Thus
$$A^J_H \longrightarrow S^J A^J_H = A^{J\,ABS}_H \qquad (3.31)$$

and writing $S^J = \exp(i\chi_E)$, (χ_E = eikonal for elastic scattering) we have

$$A^{J\,ALS}_H = \exp(i\chi_E)\,(\exp(i\chi_R) - 1)/2i\rho \;,\; \rho = 2q_s/s^{\frac{1}{2}} \qquad (3.32)$$

where χ_R = eikonal for inelastic scattering.

Making this replacement we have the 'Distorted Born Wave' approximation (ref.1) -

$$A_{H_s}(s,t) = 4\pi s i \int_0^\infty b\,db\, e^{i\chi_E}\left[1 - e^{i\chi_R}\right] J_{\bar{\mu}}(b\sqrt{-t}) \qquad (3.33)$$

In expanding

$$i e^{i\chi_E}\left[1 - e^{i\chi_R}\right] \approx \chi_R + i\chi_E\chi_R + \frac{\chi_R}{2!}(i\chi_E)^2 + \ldots.$$

we make the approximation of neglecting the Regge-Regge cuts, since they are lower lying than the Regge-Pomeron cuts. Thus

(3.33) reduces to

$$A_{H_s}(s,t) \approx 4\pi s \int_0^\infty b\,db\left[\chi_R + i\chi_E\chi_R + \frac{\chi_R}{2!}(i\chi_E)^2 + \ldots\right] J_{\bar{\mu}}(b\sqrt{-t}) \qquad (3.35)$$

Comparing this with (3.27) we see that the first cut term has no 2 in the denominator and so the analogous result to (3.30) is

$$A^{cut(1)}_{non\text{-}flip}(s,t) = \frac{i}{8\pi^2 s}\iint_{-\infty}^{0} dt_1\,dt_2\; A^R(s,t_1)\,A^E(s,t_2)\,\frac{\theta(K)}{K^{1/2}} \qquad (3.36)$$

which is exactly the same as the cut term in the absorption model result eqn.(3.7). A_R is of course the Regge pole amplitude for the inelastic process and χ_R is given by

$$\chi^R_{H_s}(s,b) = \frac{1}{8\pi s}\int_{-\infty}^{0} dt\; J_{\bar{\mu}}(b\sqrt{-t})\; A^R_{H_s}(s,t) \qquad (3.37)$$

For the purposes of calculation the forms (3.27) and (3.35) are much easier to handle since they do not involve the quantity $\frac{\theta(\Delta)}{\Delta^{1/2}}\cos(\mu\phi_1 + \mu'\phi_2 + \mu''\phi_3)$, which is difficult to manipulate. Also the higher order terms are much easier to obtain.

It is instructive to consider these results for very simple parameterizations of the Regge poles. If we neglect the P' and P'' we can put

$$A^{\pi}_{++} = i\sigma_T s\,\exp(ct) \quad , \quad c = a + \alpha'_P(\log(s/s_0) - i\pi/2) \qquad (3.38)$$

where we have taken $\alpha_P(t) = 1 + \alpha'_P(t)$, and $s_0 \equiv 1\ (Gev/c)^2$. If we consider πN charge exchange then R = ρ pole, and we take

$$A_{++} = i\,G_1\,e^{c_1 t}\,(e^{-i\pi/2}\cdot s/s_0)$$

$$A_{+-} = i\,(-t)^{\frac{1}{2}}\,G_2\,e^{c_2 t}\,(e^{-i\pi/2}\cdot s/s_0) \qquad (3.39)$$

where

$$c_1 = a_1 + \alpha'_\rho(\log s/s_0 - i\pi/2)$$
$$c_2 = a_2 + \alpha'_\rho(\log s/s_0 - i\pi/2)$$

We use the important formulae (see ref.39)

$$\int_{-\infty}^{0} e^{ct}(-t)^{\frac{\bar\mu}{2}+m} J_{\bar\mu}(b\sqrt{-t})\,dt = (-1)^m \left(\frac{b}{2}\right)^{\bar\mu}\left(\frac{\partial}{\partial c}\right)^m\left[\frac{e^{-b^2/4c}}{c^{\bar\mu+1}}\right]$$

and the inverse (3.40)

$$\int_{0}^{\infty} e^{-b^2/4c}(b^2)^{\frac{\bar\mu}{2}+m} J_{\bar\mu}(b\sqrt{-t})\,b\,db = (-t)^{\frac{\bar\mu}{2}}\left(4c^2\frac{\partial}{\partial c}\right)^m\left[(2c)^{\bar\mu+1}e^{ct}\right]$$

to get the eikonals corresponding to the above amplitudes :

$$\chi^P_{++} = \frac{i\sigma_T}{8\pi c}\cdot e^{-b^2/4c}$$

$$\chi^\rho_{++} = iG_1\left(\frac{s}{s_0}e^{-i\pi/2}\right)^{\alpha_\rho(0)}\frac{e^{-b^2/4c_1}}{8\pi s c_1} \qquad (3.41)$$

$$\chi^\rho_{+-} = iG_2\left(\frac{s}{s_0}e^{-i\pi/2}\right)^{\alpha_\rho(0)}\cdot\frac{b}{2c_2}\cdot\frac{e^{-b^2/4c_2}}{8\pi s c_2}$$

Inserting these in (3.35) we easily get

$$A_{++} = iG_1(\ldots)^{\alpha_\rho(0)}\sum_{n=0}^{\infty}\left(\frac{-\lambda\sigma_T}{8\pi c}\right)^n\frac{1}{n!}\left(\frac{c}{nc_1+c}\right)e^{\chi_n^{(1)}t}$$

$$A_{+-} = iG_2(\ldots)^{\alpha_\rho(0)}\sqrt{-t}\sum_{n=0}^{\infty}\left(\frac{-\lambda\sigma_T}{8\pi c}\right)^n\frac{1}{n!}\left(\frac{c}{nc_2+c}\right)^2 e^{\chi_n^{(2)}t} \qquad (3.42)$$

where $\chi_n^{(1)} = c_1 c/(nc_1+c)$, $\chi_n^{(2)} = c_2 c/(nc_2+c)$.

In (3.42) we have included a λ factor ($e^{i\chi_E} \longrightarrow e^{i\lambda\chi_E}$).

If we just keep the first two terms in (3.42) we get

$$A_{++} \approx iG_1(\ldots)^{\alpha_\rho(0)}\left\{e^{c_1 t} - \frac{\lambda\sigma_T}{8\pi c}\left(\frac{c}{c_1+c}\right)e^{\frac{c_1 c}{c_1+c}\cdot t}\right\}$$

$$A_{+-} \approx iG_2(\ldots)^{\alpha_\rho(0)}\sqrt{-t}\left\{e^{c_2 t} - \frac{\lambda\sigma_T}{8\pi c}\left(\frac{c}{c_2+c}\right)^2 e^{\frac{c_2 c}{c_2+c}\cdot t}\right\}$$

and with $c_1 \approx c_2 \approx c \approx 4$, $\sigma_T = 24$mb., $\lambda = 2$ and $s_0 = 1$ we find that A_{++} has a zero at $t = -0.21$ while A_{+-} has a zero at $t = -0.55$. This is roughly what is required.

We can get an estimate of the cut terms at $t = 0$. If $r = \lambda \sigma_T/(8\pi c) \approx 1.3$ we find at $t = 0$

$$A_{++}(t=0) = i(\ldots)^{\alpha_\rho(0)} G_1 \sum_{n=0}^{\infty} \frac{(-1)^n r^n}{(n+1)!}$$

and so $|\text{Pole}| : |\Sigma \text{cuts}| = 1:1 - (1 - e^{-r})/r \approx 1:0.44$. Thus at $t = 0$ we expect the cut contribution to be 44% of the pole.

The relative sizes of the cut terms are as follows: (with pole = +1)

$C(1) = -0.65$
$C(2) = +0.28$
$C(3) = -0.091$
$C(4) = +0.024$

} and so retaining just three terms gives $\sum$ cuts ≈ -0.46, a good approximation.

With $\lambda = 1$ the corresponding values are

$C(1) = -0.32$
$C(2) = +0.07$
$C(3) = -0.011$

} which gives $\sum$ cuts $\approx$ 25%.

The above estimates show that keeping just the first term may not be a good approximation.

Away from $t = 0$ the cut contribution will decrease slower than the pole e.g comparing the pole and the first cut the effective t dependence is essentially

$$\text{Pole} : \text{Cut} = e^{ct} : e^{ct/2}$$

and so as $|t|$ gets larger, the cut will eventually dominate the pole.

Thus these models differ only very slightly. The eikonal method is more general since it allows one to calculate cuts in elastic scattering (P×P cuts) and Regge-Regge cuts (R×R), and the eikonal 'Distorted Born Wave' prescription gives the P×R cuts. This is to be contrasted with the Absorption model which gives no prescription for calculating P×P or R×R cuts. In our later discussion we confine ourselves to the eikonal method.

In the calculation of cuts one has to make certain assumptions. These are :

(a) nature of input trajectories i.e whether the pole residues contain α factors.

(b) the form of the Pomeron e.g fixed pole (ref.43) or finite slope?

(c) the form of the residue e.g exponential etc.

(d) whether to include Regge-Regge cuts ($R_1 \times R_2$) where neither R_1 or R_2 is the Pomeron.

The central issue is (a).

SENSE - NONSENSE FACTORS

We have seen that in general the partial wave amplitude A^J has fixed poles or inverse square root singularities at wrong-signature nonsense points. However at right-signature nonsense points we can invoke SCR, which thus gives A^J finite at nonsense (ns) points, and $A^J \sim (J-J_0)^{\frac{1}{2}}$ at sense-nonsense (sn) points J_0. So neglecting the third double spectral function effects at wrong-signature we can say that the Regge residue β_H behaves as

$$\beta_H \sim (\alpha - J_0)^{\frac{1}{2}}$$

at sn points, at least for the right-signature points. Then using factorization we have

$$\beta_{ss}\beta_{nn} = (\beta_{sn})^2 \propto (\alpha - J_0)$$

Thus either β_{nn} or β_{ss} vanishes as $(\alpha - J_0)$. The former case is known as the choosing-sense mechanism, in that the trajectory couples to the ss. amplitude and decouples from the nn. amplitude. If $\beta_{ss} \sim (\alpha - J_0)$ then the trajectory is said to be nonsense-choosing.

For the wrong-signature nonsense points the residue in general has fixed poles $(\alpha - J_0)^{-1}$ at nn. points, while at sn. points it behaves as $(\alpha - J_0)^{-\frac{1}{2}}$, and is finite at ss. points. This is the fixed-pole coupling.

The following table gives a summary of the behaviour of the residues and amplitudes as the trajectory passes through a nonsense point J_0 (refs.1,12,35) :

RESIDUE			MECHANISM	
nn	sn	ss		
$(\alpha - J_0)$	$(\alpha - J_0)^{\frac{1}{2}}$	1	Sense-choosing.	right-signature.
1	$(\alpha - J_0)^{\frac{1}{2}}$	$(\alpha - J_0)$	Nonsense-choosing.	right-signature.
$(\alpha - J_0)^{-1}$	$(\alpha - J_0)^{-\frac{1}{2}}$	1	Fixed-pole coupling.	wrong-signature.

AMPLITUDE			MECHANISM	
nn	sn	ss		
$(\alpha - J_0)$	1	$(\alpha - J_0)^{-1}$	Sense-choosing.	right-signature.
1	1	1	Nonsense-choosing.	right-signature.
1	1	1	Fixed-pole coupling.	wrong-signature.

If we neglect the fixed-pole in the residue at the wrong-signature points (weak third d.s.f. effects), the residue behaves as the corresponding right-signature point, and the amplitude is the same except for an extra zero $(\alpha - J_0)$ from the signature factor ξ. Thus, neglecting third d.s.f. effects, the table becomes

MECHANISM	AMPLITUDE		
	nn	sn	ss
Sense-choosing.	$(\alpha - J_0)\xi$	ξ	$(\alpha - J_0)^{-1}\xi$
Nonsense-choosing.	ξ	ξ	ξ

As an example consider πN charge-exchange. Only the ρ Regge pole may be exchanged and $\alpha = 0$ is a wrong-signature point.

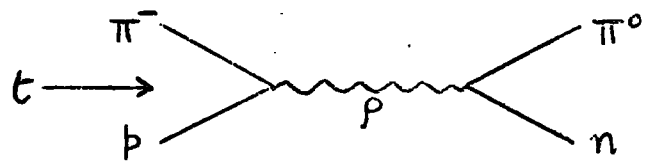

The two amplitudes $A^{(t)}_{++}$ and $A^{(t)}_{+-}$ are ss and sn amplitudes respectively (at $\alpha = 0$). We now have

	MECHANISM	$A^{(t)}_{++}$	$A^{(t)}_{+-}$	
$\alpha = 0$	Sense(S)	1	α	weak third d.s.f. effects
	Nonsense(N)	α	α	
	Fixed-pole coupling(F.P)	1	1	strong third d.s.f. effects

There are two schools of thought on the nature of the pole inputs (refs.1,38).

(a) Argonne School.

The Argonne model (refs.30,34) assumes the existence of WSNZ (wrong signature nonsense zeros) and so the residue of the

Regge pole contains an α factor. So in the convolution which generates the cut (see eqn.(3.7)) A^R has a zero and one would thus expect the integral to be correspondingly smaller due to internal cancellation - 'weak cuts'. Since the cuts interfere destructively (A^{el} being mainly imaginary) their effect is to displace these zeros only slightly. The cut contribution is smaller for helicity flip amplitudes because they do not have the lower partial waves, which require large absorption corrections. Thus zeros in non-flip amplitudes are displaced more than those in flip amplitudes. A by-product of this is that the zero in $d\sigma/dt$ is converted into a dip, as generally required by the data.

In general the structure of differential cross-sections derives from WSNZ in the pole input with cuts being just small corrections.

(b) Michigan school.

In contrast the Michigan model (ref.29) does not assume nonsense zeros. The cuts obtained from the convolution are thus correspondingly stronger and their destructive interference with the pole can generate dips in the differential cross section. To get even stronger cuts they used the λ factor. We have already seen in our example with $\lambda = 2$ that we expect a dip at $t = -0.55$ if the flip amplitude is dominant, and a dip at $t = -0.21$ if the non-flip is dominant. If both are important we expect no dips at all.

Each of these schools have their respective successes in various reactions (see any review of Regge phenomenology e.g ref.36) and their differences are not yet finally settled.

EIKONAL FORMULA FROM PERTURBATION THEORY

The eikonal approximation (eqn.(3.22)) can be derived by considering a certain class of Feynman diagrams - more precisely it involves the following (refs.40,41) :-

(a) we consider generalised ladder graphs only -

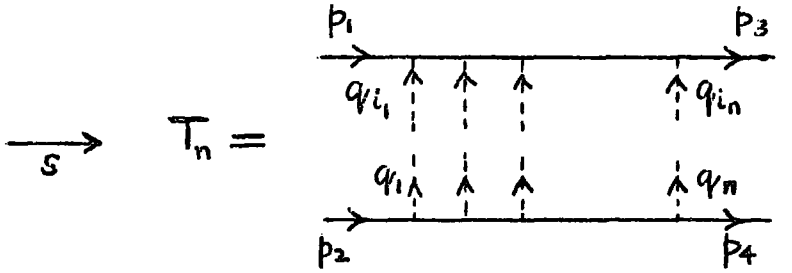

where $(i_1,\ldots,i_n)$ is some permutation of $(1,2,\ldots,n)$.

(b) we drop terms quadratic in q's in the 'nucleon' propogators. We consider scalar particles only i.e a ϕ^3 theory.

The full amplitude is then given by the sum of all such contributions i.e

$$T_{eik} = \sum_{n=1}^{\infty} T_n \text{ , where } \hat{T}_n = \sum_{\text{perms}} T_n$$

It can be shown (see refs.40,41 and references within) that, for large s,

$$\hat{T}_n \propto \frac{1}{(2\pi^2 s)^{n-1}} \cdot \frac{1}{n!} \cdot \int \bar{V}^n(b) . \exp(i\underline{b}.\underline{q})\, d^2\underline{b}$$

where $q = p_3 - p_1$ and $\bar{V}(b) = \frac{1}{(2\pi^2)^2} \int V(\underline{q}_i) \exp(-i\underline{b}.\underline{q}_i)\, d^2\underline{q}_i$

and the $V(\underline{q}_i)$ are the meson propogators.

The sum $\sum \hat{T}_n$ can now be easily done, and gives

$$T_{eik} = \sum \hat{T}_n \propto s \int \exp(i\underline{b}.\underline{q})(e^{i\chi} - 1)\, d^2\underline{b}$$

where χ is given by $\chi \propto V(b)/s$.

Taking $\underline{q}$ as axis we have $\exp(i\underline{b}.\underline{q}) = \exp(ib\sqrt{-t}.\cos\theta)$, and using

$$d^2\underline{b} = b\ db\ d\theta \quad \text{and} \quad J_0(b\sqrt{-t}) = \frac{1}{2\pi}\int_0^{2\pi} \exp(ib\sqrt{-t}.\cos\theta)$$

we finally obtain

$$T_{eik}(s,t) \propto s\int_0^\infty b\ db\ (e^{i\chi} - 1)\ J_0(b\sqrt{-t}) \qquad (3.44)$$

which is the eikonal result derived earlier (eqn.(3.22)).

It can be shown that the form (3.44) is still valid even if $V(q^2)$ had no poles i.e that the particular functional form of V is not essential - we require only an adequate behaviour as $q^2 \longrightarrow \infty$. Thus we could take V to be a sum of ladders i.e a Regge pole, which tallies with our previous eikonal model. Notice however that the generalised ladders are closed under $s \leftrightarrow u$ crossing, so if we require this condition to be satisfied by the kernel $V(q^2)$ then we should also include twisted ladders in our definition of $V(q^2)$. This entails the inclusion of many more diagrams.

The main drawback with the 'generalised ladders' is that they include planar diagrams, which ought not contribute to the cut. Also it would seem that we ought to include t-iterations of the ladders, which correspond to a renormalization of the poles and cuts, and so our input into the eikonal model should be "bare" Reggeons, not the physical Reggeons. The situation is thus rather complicated.

An alternative to the generalized ladders method is given by ref.42 which considers diagrams such as

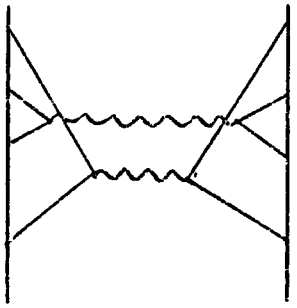

where the two particle form factor of the Regge coupling is exhibited explicitly. The leading order behaviour is obtained from diagrams with 'nested' couplings, which are the non-planar diagrams (the diagram above is equivalent to the Mandelstam diagram). We again obtain the eikonal result.

CHAPTER 4

We apply the general theory to πN charge-exchange. This process is particularly easy since the quantum numbers are such that only one known particle, the ρ, can be exchanged. Indeed this is one of the main reasons why πN scattering has played a major role in high energy phenomenology.

It has been studied by a large number of authors. A πN charge-exchange fit with only a simple ρ pole (ref.44) gives a good fit to the differential cross section but of course zero polarization. Various $\rho + \rho'$ fits have been made (refs.45,46,47) and these give reasonable results. Barger and Phillips (ref.48) used 5 poles (P, P', P'', ρ, ρ') in simultaneously fitting high energy data and finite energy sum rules to the low energy (< 2 Gev) phase shifts, and obtained a very good fit to the elastic and charge-excange data, including a positive peak to the CEX polarization, as required by the new CERN data. Several fits using cuts have been made (see e.g refs. 29,34 49) but these weren't very satisfactory, especially the charge-exchange polarization. Because of the large amount of $d\sigma/dt$ and polarization data, and also some data on the R parameter (ref.50), it has been possible to analyse the πN amplitudes directly at the given energy 6 Gev/c (see refs.51,52). The Barger-Phillips (hereafter denoted BP) amplitudes agree well with these determinations.

We begin with a brief review of the theory of πN scattering (for a fuller discussion see any standard text e.g ref.3). The πN scattering amplitude is the matrix element between Dirac spinors (for the final and initial nucleon states)

of the amplitude

$$T = A(s,t) - \tfrac{1}{2}i\, B(s,t)\, \gamma.(q_1+q_2) \qquad (4.1)$$

where A and B are the invariant amplitudes (scalar) introduced by Chew et al., γ^μ are the Dirac matrices and q_1, q_2 are the pion four-momenta in the initial and final states. The helicity amplitudes T_{++} and T_{+-} are obtained by a suitable choice of the Dirac spinors - eigenstates of spin along the nucleon's direction of motion in the c.m frame (this direction is of course different for the various channels, and the appropriate eigenstates must be worked out for each channel).

In terms of A and B the helicity amplitudes for the t-channel process $\pi N \to N\bar{N}$ are (ref.11)

$$A^{(t)}_{\frac{1}{2}\frac{1}{2},00} = 2p\,(A - mq/p.\cos\theta_t B)$$

$$A^{(t)}_{\frac{1}{2}-\frac{1}{2},00} = qt^{\frac{1}{2}}\sin\theta_t B \qquad (4.2)$$

where $4p^2 = t-4m^2$, $4q^2 = t-4\mu^2$ and $\cos\theta_t = (s-u)/4pq$. (m is the mass of the nucleon, μ the mass of the pion).

It is usual to introduce instead of A the combination $A' = A - mq/p.\cos\theta_t B$. (4.3)

For the s-channel $\pi N \to \pi N$ the helicity amplitudes are

$$A^{(s)}_{\frac{1}{2}0,\frac{1}{2}0} = \cos(\theta/2).\left[2mA + B(s-m^2-\mu^2)\right]$$

$$A^{(s)}_{\frac{1}{2}0,-\frac{1}{2}0} = \sin(\theta/2).\left[A(s+m^2-\mu^2)+mB(s-m^2+\mu^2)\right] \Big/ s^{\frac{1}{2}} \qquad (4.4)$$

where $\cos(\theta/2) = (x^2+st)^{\frac{1}{2}}/x$, $\sin(\theta/2) = (-st)^{\frac{1}{2}}/x$ $(\theta = \theta_s)$

and $x^2 = \left[s - (m+\mu)^2\right]\left[s - (m-\mu)^2\right]$.

If p_L is the momentum of the incident pion in the laboratory frame then it is easy to show that

$$x^2 = 4m^2 p_L^2 \qquad (4.5)$$

Using the result $x^2 + st = (m^2 - \mu^2)^2 - su$ and the identity $4m^2(x^2 + st) - t(s + m^2 - \mu^2)^2 = (4m^2 - t)x^2$ we can write the s-channel helicity amplitudes in terms of the A' and B amplitudes :

$$\begin{aligned} A^{(s)}_{+0,+0} &= \frac{(x^2 + st)}{x}\left[2mA' - \frac{t}{4m^2 - t}(s + m^2 - \mu^2)B\right] \\ A^{(s)}_{+0,-0} &= \frac{(-t)^{\frac{1}{2}}}{x}\left[A'(s + m^2 - \mu^2) - \frac{2m}{4m^2 - t}(x^2 + st)B\right] \end{aligned} \qquad (4.6)$$

where $\pm = \pm\frac{1}{2}$ is the nucleon helicity in the s-channel centre of mass system. We shall drop the 0 subscripts and the (s) superscript in the subsequent formulae, since we shall be dealing only with s-channel amplitudes.

Throughout this chapter we shall be concerned mainly with the charge-exchange reaction $\pi^- p \to \pi^0 n$, and to a lesser extent with the elastic reactions $\pi^{\pm} p \to \pi^{\pm} p$.

The amplitudes for these reactions are not independent but are connected by isospin invariance in the following way :

$$\begin{aligned} A(\pi^{\pm} p \to \pi^{\pm} p) &= A^0 \mp A^1 \\ A(\pi^- p \to \pi^0 n) &= \sqrt{2}\, A^1 \end{aligned} \qquad (4.7)$$

where the superscripts refer to t-channel isospin $I_t = 0, 1$. We shall henceforth work with the amplitudes A^0, A^1.

We parameterize the amplitudes A'^1, B^1 in terms of a ρ Regge pole. The Regge poles which contribute to the A^0

amplitude are the Pomeron P, the P' (or f) and the P''(ref.2). A typical expression for a ρ Regge pole is

$$\rho = -Ge^{at}F(\alpha)\left(\frac{e^{-i\pi\alpha}-1}{\sin\pi\alpha}\right)\left(\frac{s}{s_0}\right)^{\alpha} = iGe^{at}\frac{F(\alpha)\,e^{-i\pi\alpha/2}}{\cos\pi\alpha/2}\left(\frac{s}{s_0}\right)^{\alpha}$$

where we have written the residue $\beta(t)$ as Ge^{at}. $F(\alpha)$ is some function of the trajectory $\alpha_\rho \approx \frac{1}{2} + t$. It contains factors such as $(\alpha+1)$, $(\alpha+3)$ etc. to prevent "ghosts" i.e poles arising from the term $\cos(\pi\alpha/2)$ at $\alpha = -1, -3$ etc (negative t). We are interested in the region $0 > t > -2$ $(Gev/c)^2$ so that we need retain only the factor $(\alpha+1)$ to a good approximation. The factor $(\alpha+1)/\cos(\pi\alpha/2)$ is then a slowly decreasing (with $|t|$) function and to a good approximation may be absorbed into the exponential e^{at} $(a>0)$ for $0>t>-2$. $F(\alpha)$ will also contain a factor α if the ρ chooses nonsense (at $\alpha = 0$). Thus a good approximation to the ρ Regge pole is

$$\rho \approx iGe^{at}\,\alpha\,e^{-i\pi\alpha/2}\left(\frac{s}{s_0}\right)^{\alpha} \qquad (4.8)$$

for a nonsense-choosing ρ.

So for the invariant amplitudes A', B we take

$$2m\,A'(s,t) = A_0\,i\,e^{c_1 t}\left(e^{-i\pi/2}\frac{s}{s_0}\right)^{\alpha_\rho(0)}\alpha_\rho$$

and

$$B(s,t) = B_0\,i\,e^{c_2 t}\,e^{-\frac{i\pi}{2}\alpha_\rho(0)}\left(\frac{s}{s_0}\right)^{\alpha_\rho(0)}\alpha_\rho \qquad (4.9)$$

giving for the full amplitudes

$$A_{++}^{1(\rho)} = i\,\frac{(x^2+st)^{1/2}}{x}\left(e^{-\frac{i\pi}{2}}\frac{s}{s_0}\right)^{\alpha_\rho(0)}\left[A_0\alpha_\rho e^{c_1 t} - \frac{t}{4m^2-t}\,\frac{(s+m^2-\mu^2)}{s}B_0\alpha_\rho e^{c_2 t}\right]$$

$$A_{+-}^{1(\rho)} = \frac{i\sqrt{-t}}{2m}\left(e^{-\frac{i\pi}{2}}\frac{s}{s_0}\right)^{\alpha_\rho(0)}\left[A_0\alpha_\rho\frac{(s+m^2-\mu^2)}{x}e^{c_1 t} - \frac{4m^2 B_0\alpha_\rho}{4m^2-t}\left(\frac{x^2+st}{xs}\right)e^{c_2 t}\right] \qquad (4.10)$$

where $\alpha_\rho(t) = \alpha_\rho(0) + \alpha_\rho' t$

$$c_j = h_j + \alpha_\rho' (\log s/s_0 - i\pi/2) \qquad (j = 1,2)$$

and $s_0 = 1$ (Gev/c)^2 throughout.

The (ρ) superscript is to remind us that the R.H.S is the ρ pole contribution to the full amplitude. The above forms are for a nonsense-choosing ρ. For a sense-choosing ρ there is no α factor in the A_0 terms and for a fixed-pole coupling there are no α factors in either of the A_0 or B_0 terms.

For the purposes of calculating cuts the above forms were simplified by making the approximations

$$x^2 + st \approx x^2 \approx s^2 \ , \ s + m^2 - \mu^2 \approx x \approx s \ , \ 4m^2 - t \approx 4m^2 \qquad (4.11)$$

which are valid for large s and small t. We then get

$$A_{++}^{1(\rho)} \approx i\left(e^{-i\pi/2}\frac{s}{s_0}\right)^{\alpha_\rho(0)}\left[A_0\alpha_\rho e^{c_1 t} - \frac{t}{4m^2}B_0\alpha_\rho e^{c_2 t}\right]$$

$$A_{+-}^{1(\rho)} \approx \frac{i\sqrt{-t}}{2m}\left(e^{-i\pi/2}\frac{s}{s_0}\right)^{\alpha_\rho(0)}\left[A_0\alpha_\rho e^{c_1 t} - B_0\alpha_\rho e^{c_2 t}\right] \qquad (4.12)$$

The normalization of these amplitudes will be given later. Before we can proceed to the calculation of cuts we must first describe the $I_t = 0$ amplitudes A^0_{++}.

$I_t = 0$ AMPLITUDES

Our particular representation of the $I_t = 0$ amplitudes is governed mainly by the requirement of simplicity. We therefore chose to parameterize them directly as Regge poles (without crossing) and used a simple form of the common P + P' parameterization as a starting point. Our procedure was to

regard the $I_t = 0$ B.P amplitudes (ref.48) as "data" and to fit these with our relatively simple representation. To do this we proceeded in two ways :-

Method (a) - in the first we took the $I_t = 0$ amplitudes to be a sum of two terms which look like the Regge Pomeron plus a P' term. Our philosophy here was to regard this simply as a functional representation of the B.P amplitudes without identifying the terms as P and P'. In this sense the question of including PP, PPP,..., P'P, P'PP,...etc. cuts does not arise.

Method (b) - in the second we did identify the terms as P and P' and so we also included the cut terms PP,PPP,...,P'P,P'PP, ... etc.

These methods will be described below.

We required a simple representation (Regge pole X polynomial in t) so that we could calculate the cuts analytically. We expect $\alpha_P(t) = 1 + \alpha'_P\, t$ with $\alpha'_P \approx 0.5$ (Gev/c)$^{-2}$ and $\alpha_{P'}(t) = \alpha_{P'} + \alpha'_{P'}\, t$ with $\alpha_{P'}(0) \approx 0.5$ and $\alpha'_{P'} \approx 1.0$ (Gev/c)$^{-2}$. A rough comparison of this representation with the real and imaginary parts of the B.P $I_t = 0$ amplitudes suggested that a better fit would be obtained by taking a no-compensation P' contribution. This is most clearly seen in the behaviour of the real part of the B.P $I_t = 0$ non-flip amplitude, which for the lower energies at least (up to approximately 6 Gev/c) has a zero around $t \approx -1.0$ (gev/c)^2. This feature can not be reproduced if the $\alpha_{P'}$ factor were absent. Accordingly we chose a no-compensation P' in our fits, even when we included cuts. This in fact agrees with most pole parameterizations of

the $I_t = 0$ amplitudes (see ref.48). The addition of a P'' contribution did not significantly improve the $I_t = 0$ fits, and since its inclusion would have made the cut calculations even more complicated, we felt justified in neglecting it.

Before we describe the methods (a) and (b), we give first the B.P representation of the $I_t = 0$ amplitudes, for the sake of completeness.

B.P AMPLITUDES ($I_t = 0$)

These are given by (ref.48)

$$B.P^{0}_{++} = \frac{(x^2 + st)^{\frac{1}{2}}}{x}\left[2mA'^{0} - \frac{(s + m^2 - \mu^2)t}{4m^2 - t}\,B^{0}\right]$$

$$B.P^{0}_{+-} = \frac{(-t)^{\frac{1}{2}}}{x}\left[(s + m^2 - \mu^2)A'^{0} - \frac{2m(x^2 + st)}{4m^2 - t}\,B^{0}\right] \qquad (4.13)$$

where

$$A'^{0} = \sum_i \left[-\gamma_i\, e^{-i\pi\alpha_i/2}\left(\nu^2 - \nu_0^2\right)^{\alpha_i/2}\right]$$

$$B^{0} = \sum_i \left[-\beta_i \nu\, e^{-i\pi\alpha_i/2}\left(\nu^2 - \nu_0^2\right)^{\alpha_i/2 - 1}\right] \qquad (i = P, P', P''$$

and where $\nu = (s - u)/4m = (s - m^2 - \mu^2)/2m + t/4m$ and $\nu_0 = \mu + t/4m$. The α_i, β_i, γ_i ($i = P, P', P''$) are given by $\alpha_P = 1.0 + 0.36t$, $\alpha_{P'} = 0.56 + 0.86t$, $\alpha_{P''} = t$,

$$\beta_P = 42.5\, e^{2.45t}$$

$$\beta_{P'} = 24.7\, e^{0.17t} \sin(\pi\alpha_{P'}/2)\left[\Gamma(1 - \tfrac{1}{2}\alpha_{P'})\right]^2$$

$$\beta_{P''} = 49.8\, e^{2.31t}$$

$$\gamma_P = 21.6\, e^{6.5t} + 31.1\, e^{1.81t}$$

$$\gamma_{P'} = (22.2 + 16.9\, e^{0.34t}) \sin(\pi\alpha_{P'}/2)\left[\Gamma(1 - \tfrac{1}{2}\alpha_{P'})\right]^2$$

$$\gamma_{P''} = 0$$

We now describe our parameterization of the $I_t = 0$ amplitudes.

OUR MODELS (a) AND (b) OF THE $I_t = 0$ AMPLITUDES

Method (a) - We adopted the following representation :

$$A^{o}_{++} = i\sigma_T s e^{c_3 t} + E_o s_o e^{c_5 t} \alpha_{p'} \left(e^{-i\pi/2} \frac{s}{s_o} \right)^{\alpha_{p'}(o)}$$

$$A^{o}_{+-} = \frac{\sqrt{-t}}{2m} \left[i C_o s e^{c_4 t} + F_o s_o e^{c_6 t} \alpha_{p'} \left(e^{-i\pi/2} \frac{s}{s_o} \right)^{\alpha_{p'}(o)} \right] \qquad (4.14)$$

where $c_3 = b_3 + \alpha'_p (\log s/s_o - i\pi/2)$

$c_5 = b_5 + \alpha'_{p'} (\log s/s_o - i\pi/2)$ etc.

$\alpha_p(t) = 1 + \alpha'_p t$

$\alpha_{p'}(t) = \alpha_{p'}(0) + \alpha'_{p'} t$

and $s_o \equiv 1$ $(Gev/c)^2$ throughout.

The real and imaginary parts of these amplitudes were fitted to their P.P $I_t = 0$ counterparts for t values in the range $0 \geqslant t \geqslant -1$ (at intervals of 0.05) and for the incident pion laboratory momenta

$$p_L = 2.5, 5.0, 6.0, 10.0, 13.3, 18.2 \ (Gev/c)$$

(Recall that $p_L \approx x/2m \approx s/2m$). Results are shown in Fig.6 .

In this fit we have 11 parameters (The actual fitting methods used are described in Chapter 5.) - see Table (1).

Method (b)

This is more complicated because of the addition of cuts. In this case the $I_t = 0$ amplitude is given by

$$A^{o}_{H_s} = 4\pi s \int_0^\infty b\, db \left[\chi^{e}_{H_s} + \frac{i}{2!} \left\{ \chi^{o^2} \right\}_{H_s} + \ldots + \frac{i^{n-1}}{n!} \left\{ \chi^{o^n} \right\}_{H_s} + \ldots \right] J_{\bar{\mu}}(b\sqrt{-t}) \qquad (4.15)$$

For the 'Born' term we again take the forms (4.14) i.e we write

$$A^{o\ Born}_{++} = P_{++} + P'_{++}$$
$$A^{o\ Born}_{+-} = P_{+-} + P'_{+-} \qquad (4.16)$$

where $P_{++} = i\sigma_T s e^{c_3 t}$, $P'_{++} = E_o s_o \alpha_{P'} e^{c_5 t} (e^{-i\pi/2} \cdot s/s_o)^{\alpha_{P'}(0)}$

and correspondingly for P_{+-}, P'_{+-} (eqn.(4.14)).

The eikonal $\chi^o_{H_s}$ is obtained by taking the Fourier-Bessel transform of these 'Born' terms :

$$\chi^o_{H_s} = \frac{1}{8\pi s} \int_{-\infty}^{o} dt\, J_\mu(b\sqrt{-t})\, A^{o\ Born}_{H_s} \qquad (4.17)$$

which gives, by using the result (3.40),

$$\chi^o_{++} = \chi^P_{++} + \chi^{P'}_{++}$$
$$\chi^o_{+-} = \chi^P_{+-} + \chi^{P'}_{+-} \qquad (4.18a)$$

where

$$\chi^P_{++} = \frac{i\sigma_T}{8\pi c_3} e^{-b^2/4c_3}$$

$$\chi^{P'}_{++} = \frac{E_o s_o}{8\pi s c_5} \left(e^{-i\pi/2} \frac{s}{s_o}\right)^{\alpha_{P'}(0)} e^{-b^2/4c_5} \left[\alpha_{P'}(0) - \frac{\alpha'_{P'}}{c_5} - \left(\frac{-b^2}{4}\right)\frac{\alpha'_{P'}}{c_5^2}\right]$$

$$\chi^P_{+-} = \frac{iC_o}{2m \cdot 8\pi} \cdot \frac{b}{2} \cdot \frac{e^{-b^2/4c_4}}{c_4^2} \qquad (4.18b)$$

$$\chi^{P'}_{+-} = \frac{F_o s_o}{2m \cdot 8\pi s \cdot c_6^2} \left(e^{-i\pi/2} \frac{s}{s_o}\right)^{\alpha_{P'}(0)} e^{-b^2/4c_6} \cdot \frac{b}{2} \cdot \left[\alpha_{P'}(0) - \frac{2\alpha'_{P'}}{c_6} - \left(\frac{-b^2}{4}\right)\frac{\alpha'_{P'}}{c_6^2}\right]$$

The first term of (4.15) gives us back the 'Born' term $\Gamma + P'$. The evaluation of the other terms of (4.15), of the form $(i^{n-1}/n!)\{\chi^{o\,n}\}_{H_s}$, is complicated by the fact that the eikonals are actually matrices in helicity space. Thus we write

$$\chi^{\circ} = \begin{pmatrix} \chi^{\circ}_{++} & \chi^{\circ}_{+-} \\ \chi^{\circ}_{-+} & \chi^{\circ}_{--} \end{pmatrix} \tag{4.19}$$

By parity invariance we know that the full amplitude $A^{\circ}_{H_s}$ has the symmetry

$$\begin{aligned} A^{\circ}_{++} &= A^{\circ}_{--} \\ A^{\circ}_{+-} &= -A^{\circ}_{-+} \end{aligned} \tag{4.20}$$

and similarly for $A^{1}_{H_s}$.

We therefore assume that the eikonals $\chi^{\circ}_{H_s}$ also obey this symmetry to ensure that each term of (4.15) will have this symmetry and therefore the whole sum. Thus

$$\chi^{\circ} = \begin{pmatrix} \chi^{\circ}_{++} & \chi^{\circ}_{+-} \\ -\chi^{\circ}_{+-} & \chi^{\circ}_{++} \end{pmatrix} \tag{4.21}$$

Since we know that the non-flip part is much greater than the flip part, which means that $|\chi^{\circ}_{++}| \gg |\chi^{\circ}_{+-}|$, we can neglect terms of order $|\chi^{\circ}_{+-}|^2$ and higher. Thus we get to a good approximation

$$\begin{aligned} \left[(\chi^{\circ})^n\right]_{++} &\approx (\chi^{\circ}_{++})^n \\ \left[(\chi^{\circ})^n\right]_{+-} &\approx n\,(\chi^{\circ}_{++})^{n-1}\chi^{\circ}_{+-} \end{aligned} \tag{4.22}$$

If we were to include λ factors we should multiply the above by $(\lambda^{\circ}_{++})^{n-1}$ and $(\lambda^{\circ}_{++})^{n-2}\lambda^{\circ}_{+-}$ respectively. In our fits they were included and restricted to the range $1 \leqslant \lambda \leqslant 2$ but in fact both λ°_{++} and λ°_{+-} took on the value 1.0 in our best fit, so from now on we will omit them.

We consider first the non-flip cut terms of (4.15).

NON-FLIP CUTS(++) $I_t = 0$

The first cut contribution is given by

$$C^{o}_{++}(1) = 4\pi s \int_0^\infty b\,db\, \frac{i}{2!} \left(\chi^{o}_{++}\right)^2 J_o(b\sqrt{-t}) \qquad (4.23)$$

where $$\left(\chi^{o}_{++}\right)^2 = \left(\chi^{P}_{++}\right)^2 + 2\chi^{P}_{++}\chi^{P'}_{++} + \left(\chi^{P'}_{++}\right)^2$$

In practice all these terms were retained. For the higher order terms ($n > 2$) we made the further approximation

$$\left(\chi^{o}_{++}\right)^n \approx \left(\chi^{P}_{++}\right)^n + n\left(\chi^{P}_{++}\right)^{n-1}\chi^{P'}_{++} \qquad (4.24)$$

i.e we dropped terms of order $(\chi^{P'}_{++})^2$ and higher, since the Pomeron P dominates the P'.

Thus we are left with three types of cut terms to calculate :- $(\chi^{P}_{++})^{n+1}$ and $(n+1)(\chi^{P}_{++})^n \chi^{P'}_{++}$, which contributes to $C^{e}_{++}(n)$, and $(\chi^{P'}_{++})^2$ which contributes to $C^{o}_{++}(1)$ only. We deal with each separately.

(1) MULTI-POMERON CUTS(++)

We have

$$\frac{i^n}{(n+1)!}\left(\chi^{P}_{++}\right)^{n-1} = \frac{i}{(n+1)!}\left(\frac{\sigma_T}{8\pi c_3}\right)\left(\frac{-\sigma_T}{8\pi c_3}\right)^n e^{-(n+1)b^2/4c_3} \qquad (4.25)$$

Doing the integral (4.15) ($4\pi s\int b\,db\ldots$) using the result (3.40) we get the multi-Pomeron contribution

$$P^{(n+1)}_{++} = \frac{i\sigma_T s}{(n+1)} \cdot \frac{1}{(n+1)!}\left(\frac{-\sigma_T}{8\pi c_3}\right)^n e^{c_3 t/(n+1)} \qquad (4.26)$$

(2) MULTI-POMERON ⊗ P-PRIME CUTS(++)

Writing
$$\delta_1 = \alpha_{P'}(0) - \alpha'_{P'}/c_5$$
$$\delta_2 = -\alpha'_{P'}/c_5^2 \qquad (4.27)$$

we have $$\frac{i^n}{(n+1)!}(n+1)\left(\chi^{P}_{++}\right)^n \chi^{P'}_{++} = \left(\frac{-\sigma_T}{8\pi c_3}\right)^n \frac{1}{n!}\frac{E_o s_o}{8\pi s c_5} \times$$
$$\times \left(e^{-i\pi/2}\frac{s}{s_o}\right)^{\alpha_{P'}(o)} e^{-b^2/4h_{53}}\left[\delta_1 + \left(\frac{-b^2}{4}\right)\delta_2\right] \quad (4.28)$$

and so using the result (3.40) we obtain

$$P^{(n)}_{++} \otimes P'_{++} = \frac{1}{n!}\left(\frac{-\sigma_T}{8\pi c_3}\right)^n \cdot \frac{E_o s_o}{c_5} \cdot \left(e^{-i\pi/2}\frac{s}{s_o}\right)^{\alpha_{P'}(o)} \times$$
$$\times\ h_{53}\, e^{h_{53}t}\left[(\delta_1 - h_{53}\delta_2) + t(-\delta_2 h_{53}^2)\right] \quad (4.29)$$

where $$h_{53} = c_5 c_3 / (n c_5 + c_3). \quad (4.30)$$

(3) P-PRIME ⊗ P-PRIME CUT(++)

We have $$\frac{i}{2!}\left(\chi^{P'}_{++}\right)^2 = \frac{i}{2!}\left(\frac{E_o s_o}{8\pi s c_5}\right)^2 \left(e^{-i\pi/2}\frac{s}{s_o}\right)^{2\alpha_{P'}(o)} \times$$
$$\times\ e^{-2b^2/4c_5}\left[\delta_1^2 + 2\delta_1\delta_2\left(\frac{-b^2}{4}\right) + \delta_2^2\left(\frac{-b^2}{4}\right)^2\right] \quad (4.31)$$

and using result(3.40) again we get

$$P'_{++} \otimes P'_{++} = \frac{i}{4}\frac{(E_o s_o)^2}{8\pi s c_5}\left(e^{-i\pi/2}\frac{s}{s_o}\right)^{2\alpha_{P'}(o)} e^{c_5 t/2}\left[v_{11} + v_{12}t + v_{13}t^2\right] \quad (4.32)$$

$$v_{11} = \delta_1^2 - \delta_2 c_5\left(\delta_1 - \delta_2 c_5/2\right)$$

$$v_{12} = \frac{\delta_2 c_5^2}{2}\left(\delta_2 c_5 - \delta_1\right)$$

$$v_{13} = \delta_2^2 c_5^4 / 16.$$

So the total non-flip cut contribution is

$$C^{o}_{++} = \sum_{n=1}^{\infty}\left(P^{(n+1)}_{++} + P^{(n)}_{++} \otimes P'_{++}\right) + P'_{++} \otimes P'_{++} \quad (4.33)$$

and the R.H.S is given by equations (4.26),(4.29) and (4.32).

The total non-flip amplitude is

$$A^{o}_{++} = P_{++} + P'_{++} + C^{o}_{++} \qquad (4.34)$$

where P_{++} and P'_{++} are given in eqn. (4.16).

In practice only the first three terms of the sum in C^{o}_{++} were kept. The real and imaginary parts of A^{o}_{++} as given by (4.34) were then fitted to their B.P counterparts over the same range of t and p_L values used in method (a).

Notice that the cut terms do not introduce any new parameters (apart from λ^{o}_{++}, λ^{o}_{+-}). The results of this fit are given in Table(1) and Fig 6.

To give some idea of the magnitude of these cuts we give a rough estimate of the cuts $P^{(2)}_{++}$, $2P_{++}P'_{++}$ and $P'^{(2)}_{++}$ at p_L = 6 Gev/c and t = 0 , which are to be compared with Im $B.P^{o}_{++}(t = 0) \approx 750$ and Re $B.P^{o}_{++}(t = 0) \approx -150$. We find

$$P^{(2)}_{++} \approx -110i \ , \ 2P_{++}P'_{++} \approx 50(1 - i) \ , \ P'^{(2)}_{++} \approx +18$$

$$\text{i.e} \quad \text{Im } C^{(0)}_{++}(1) \approx -160 \ , \ \text{Re } C^{(0)}_{++}(1) \approx +68 \ .$$

We now indicate the analogous results for the flip cuts.

FLIP CUTS (+-) $I_t = 0$

We have indicated above that we have, to a good approximation,

$$\left[(\chi^{o})^{n}\right]_{+-} \approx n \left(\chi^{o}_{++}\right)^{n-1} \chi^{o}_{+-}$$

We make the further approximation of putting $\chi^{o}_{++} \approx \chi^{P}_{++}$ so that we need to calculate the expression

$$Y^{(n)} = \frac{i^n}{(n+1)!}(n+1)\left(\chi^P_{++}\right)^n\left(\chi^P_{+-}+\chi^{P'}_{+-}\right) \qquad (4.35)$$

to obtain $C^o_{+-}(n)$ from

$$C^o_{+-}(n) = 4\pi s\int_0^\infty b\ db\ Y^{(n)}\ J_1(b\sqrt{-t})$$

We again use the result (3.40) to obtain

$$C^o_{+-}(n) = \frac{\sqrt{-t}}{2m.n!}\left(\frac{-\sigma_T}{8\pi c_3}\right)^n\left[\frac{iC_0 s}{c_4^2}\ h_{43}^2\ e^{h_{43}t} + \right. \qquad (4.36)$$

$$\left. + \frac{F_0 s_0}{c_6^2}\left(e^{-i\pi/2}\frac{s}{s_0}\right)^{\alpha_{\rho'}(0)} h_{63}^2\, e^{h_{63}t}\left(\delta_3 - h_{63}\delta_4(2+h_{63}t)\right)\right]$$

where

$$\delta_3 = \alpha_{\rho'}(0) - 2\alpha'_{\rho'}/c_6 \qquad \delta_4 = -\alpha'_{\rho'}/c_6^2$$

$$h_{43} = c_4c_3/(nc_4+c_3) \qquad h_{63} = c_6c_3/(nc_6+c_3) \qquad (4.37)$$

The total flip amplitude is then given by

$$A^o_{+-} = P_{+-} + P'_{+-} + \sum_{n=1}^{\infty} C^o_{+-}(n) \qquad (4.38)$$

Here again we retained only the first three terms of the sum when fitting the real and imaginary parts of this amplitude to their B.P counterparts. The results are given in Table (1) and Fig.6 .

IMPACT PARAMETER AMPLITUDES FOR $I_t = 0$

We give here the formulae for the impact-parameter amplitudes for the two cases (a) and (b). These are defined by the equation

$$\bar{\chi}^{o}_{H_s}(s,b) = \frac{1}{8\pi s}\int_{-\infty}^{0} dt\; A^{o}_{H_s}(s,t)\, J_{\bar{\mu}}(b\sqrt{-t}) \qquad (4.39)$$

Thus for case (a) we have simply

$$\bar{\chi}^{o(a)}_{+\pm}(s,b) = \chi^{P}_{+\pm} + \chi^{P'}_{+\pm} \equiv \chi^{o(a)}_{+\pm} \qquad (4.40)$$

thus defining $\chi^{o(a)}_{+\pm}$.

For case (b) we have approximately

$$\bar{\chi}^{o(b)}_{++} \approx i\left(1 - e^{i\chi^{o(b)}_{++}}\right)$$

and
$$\bar{\chi}^{o(b)}_{+-} \approx \chi^{o(b)}_{+-} + \frac{i}{2!}2\chi^{o(b)}_{++}\chi^{o(b)}_{+-} + \frac{i^2}{3!}3\left(\chi^{o(b)}_{++}\right)^2\chi^{o(b)}_{+-} + \ldots$$

$$= \chi^{o(b)}_{+-}\, e^{i\chi^{o(b)}_{++}} = \chi^{o(b)}_{+-}\left(1 - i\,\bar{\chi}^{o(b)}_{++}\right) \qquad (4.41)$$

We can now turn to the calculation of the $I_t = 1$ cuts.

$I_t = 1$ CUTS

From the A', B parameterization of the ρ pole (4.12) we can obtain (by using the result (3.40)) the ρ eikonals $\chi^{\rho}_{H_s}$, defined by

$$\chi^{\rho}_{H_s} = \frac{1}{8\pi s}\int_{-\infty}^{0} dt\; A^{\rho}_{H_s}\; J_{\bar{\mu}}(b\sqrt{-t}) \qquad (4.42)$$

We get

$$\chi^{\rho}_{++} = \frac{i}{8\pi s}\left(e^{-i\pi/2}\frac{s}{s_0}\right)^{\alpha_\rho(0)}\left[\zeta_1 + \left(\frac{-b^2}{4}\right)\zeta_2 + \left(\frac{-b^2}{4}\right)^2\zeta_3\right]$$

$$\chi^{\rho}_{+-} = \frac{1}{2m}\frac{i}{8\pi s}\left(e^{-i\pi/2}\frac{s}{s_0}\right)^{\alpha_\rho(0)}\cdot\frac{b}{2}\left[\theta_1 + \left(\frac{-b^2}{4}\right)\theta_2\right] \qquad (4.43)$$

where
$$\zeta_1 = A_0 X_1 e^{-b^2/4c_1} + B_0 X_2 e^{-b^2/4c_2}$$
$$\zeta_2 = A_0 X_3 e^{-b^2/4c_1} + B_0 X_4 e^{-b^2/4c_2}$$
$$\zeta_3 = B_0 X_5 e^{-b^2/4c_2}$$
$$\theta_1 = A_0 Y_1 e^{-b^2/4c_1} + B_0 Y_2 e^{-b^2/4c_2}$$
$$\theta_2 = A_0 Y_3 e^{-b^2/4c_1} + B_0 Y_4 e^{-b^2/4c_2}$$

and where

$$X_1 = \frac{1}{c_1}\left(\alpha_\rho(0) - \frac{\alpha'_\rho}{c_1}\right), \quad X_2 = \frac{1}{4m^2c_2^2}\left(\alpha_\rho(0) - \frac{2\alpha'_\rho}{c_2}\right)$$

$$X_3 = -\alpha'_\rho/c_1^3, \quad X_4 = \frac{1}{4m^2c_2^3}\left(\alpha_\rho(0) - \frac{4\alpha'_\rho}{c_2}\right), \quad X_5 = \frac{-\alpha'_\rho}{4m^2c_2^5}$$

$$Y_1 = \frac{1}{c_1^2}\left(\alpha_\rho(0) - \frac{2\alpha'_\rho}{c_1}\right), \quad Y_2 = \frac{-1}{c_2^2}\left(\alpha_\rho(0) - \frac{2\alpha'_\rho}{c_2}\right)$$

$$Y_3 = -\alpha'_\rho/c_1^4, \quad Y_4 = \alpha'_\rho/c_2^4 \qquad (4.44)$$

Note that these formulae are for a nonsense-choosing ρ. The other cases that we will discuss viz. sense ρ and the fixed-pole coupling, are easily obtained as special cases of this nonsense case.

Since we will eventually use these formulae to compare these different ρ inputs together with the different inputs for the $I_t = 0$ amplitudes (methods (a) and (b)) we shall give below the most general results. These apply directly to a nonsense-choosing ρ input together with method (b) for the $I_t = 0$ amplitudes. The various other models then follow easily from these general results by making a few minor modifications, which we shall indicate at the appropriate place.

We will include the enhancement factors λ_{++}, λ_{+-}

(denoted λ_1, λ_2 respectively) to allow for diffractively produced intermediate states ($\lambda \geq 1$).

We start from the equation

$$A^1_{H_s}(s,t) = 4\pi s \int_0^\infty b\,db \left\{ \chi^e_{H_s} + i\left[\lambda \chi^o \chi^e\right]_{H_s} + \ldots + \frac{i^n}{n!}\left[\lambda (\chi^o)^n \chi^e\right]_{H_s} + \ldots \right\} J_\mu(b\sqrt{-t}) \tag{4.45}$$

The first term just gives us back the ρ pole contribution (4.12). Consider the first cut contribution. As before, we get

$$\begin{aligned} i\left[\lambda \chi^o \chi^e\right]_{++} &= i\lambda_1 \chi^o_{++}\chi^e_{++} - i\lambda_2 \chi^o_{+-}\chi^e_{+-} \\ i\left[\lambda \chi^o \chi^e\right]_{+-} &= i\lambda_2 \chi^o_{++}\chi^e_{+-} + i\lambda_1 \chi^o_{+-}\chi^e_{++} \end{aligned} \tag{4.46}$$

Since $\chi^o = \chi^P + \chi^{P'}$, we make the approximation of neglecting $\chi^{P'}_{+-}$ compared with χ^P_{+-}, so that (4.46) becomes

$$\begin{aligned} i\left[\lambda \chi^o \chi^e\right]_{++} &\approx i\lambda_1 \chi^e_{++}\left(\chi^P_{++} + \chi^{P'}_{++}\right) - i\lambda_2 \chi^P_{+-}\chi^e_{+-} \\ i\left[\lambda \chi^o \chi^e\right]_{+-} &\approx i\lambda_2 \chi^e_{+-}\left(\chi^P_{++} + \chi^{P'}_{++}\right) + i\lambda_1 \chi^P_{+-}\chi^e_{++} \end{aligned} \tag{4.47}$$

For the higher order terms we make the approximation $\chi^o \approx \chi^P$, and we write

$$\begin{aligned} \frac{i^n}{n!}\left[\lambda (\chi^o)^n \chi^e\right]_{++} &\approx \frac{i^n}{n!}\lambda_1 \chi^e_{++}\left(\chi^P_{++}\right)^n \\ \frac{i^n}{n!}\left[\lambda (\chi^o)^n \chi^e\right]_{+-} &\approx \frac{i^n}{n!}\lambda_2 \chi^e_{+-}\left(\chi^P_{++}\right)^n \end{aligned} \tag{4.48}$$

Thus in all we need to calculate the cut contributions from the general terms (4.48), together with the isolated terms

$$i\lambda_1 \chi^{\varrho}_{++}\chi^{P'}_{++}\,,\; i\lambda_2 \chi^{\varrho}_{+-}\chi^{P'}_{++}\,,\; -i\lambda_2 \chi^{P}_{+-}\chi^{\varrho}_{+-}\,,\; i\lambda_1 \chi^{P}_{+-}\chi^{\varrho}_{++} \tag{4.49}$$

We will consider each separately.

NON-FLIP CUTS: $I_t = 1$

(1) MULTI-POMERON ⊗ RHO NON-FLIP CUTS.

χ^{P}_{++} is given in (4.18b) and χ^{ϱ}_{++} by (4.43). We have

$$\frac{i^n}{n!}\lambda_1 \chi^{\varrho}_{++}(\chi^{P}_{++})^n = \frac{i\lambda_1}{8\pi s}\cdot\frac{1}{n!}\left(\frac{-\sigma_T}{8\pi c_3}\right)^n \left(e^{-i\pi/2}\frac{s}{s_0}\right)^{\alpha_\varrho(0)} \times$$
$$\times\, e^{-nb^2/4c_3}\left\{\zeta_1 + \left(\frac{-b^2}{4}\right)\zeta_2 + \left(\frac{-b^2}{4}\right)^2\zeta_3\right\}.$$

Doing the integration in (4.45), using the result (3.40) with $\bar{\mu} = 0$, we obtain, after some manipulation, the contribution

$$C^1_{++}(n) = \frac{\lambda_1 i}{n!}\left(\frac{-\sigma_T}{8\pi c_3}\right)^n \left(e^{-i\pi/2}\frac{s}{s_0}\right)^{\alpha_\varrho(0)} \times$$
$$\times\left\{A_0 e^{h_{13}t}(u_{11}+u_{12}t) + B_0 e^{h_{23}t}(u_{21}+u_{22}t+u_{23}t^2)\right\}$$

(4.50)

where $h_{13} = \dfrac{c_1 c_3}{nc_1 + c_3}$, $h_{23} = \dfrac{c_2 c_3}{nc_2 + c_3}$

and

$$u_{11} = h_{13}(X_1 - h_{13}X_3) \qquad u_{21} = h_{23}(X_2 - h_{23}X_4 + 2h_{23}^2 X_5)$$
$$u_{12} = -h_{13}^3 X_3 \qquad u_{22} = h_{23}^3(4h_{23}X_5 - X_4)$$
$$u_{23} = h_{23}^5 X_5$$

(2) P-PRIME ⊗ RHO NON-FLIP CUT.

This is the term $i\lambda_1 \chi^{\rho}_{++} \chi^{P'}_{++}$. We have

$$i\lambda_1 \chi^{\rho}_{++} \chi^{P'}_{++} = \frac{i^2 \lambda_1 E_0 s_0}{(8\pi s)^2 c_5} \left(e^{-i\pi/2} \frac{s}{s_0}\right)^{\alpha_\rho(0)+\alpha_{P'}(0)} \cdot e^{-b^2/4c_5} \times$$

$$\times \left\{\delta_1 + \left(\frac{-b^2}{4}\right)\delta_2\right\} \cdot \left\{\zeta_1 + \left(\frac{-b^2}{4}\right)\zeta_2 + \left(\frac{-b^2}{4}\right)^2 \zeta_3\right\}$$

We obtain the contribution ($\bar{\mu} = 0$)

$$C^{\rho P'}_{++} = -\frac{\lambda_1 E_0 s_0}{8\pi c_5} \left(e^{-i\pi/2} \frac{s}{s_0}\right)^{\alpha_\rho(0)+\alpha_{P'}(0)} \times \tag{4.51}$$

$$\times \left[A_0 e^{h_{15}t}(f_{11} + f_{12}t + f_{13}t^2) + B_0 e^{h_{25}t}(f_{21} + f_{22}t + f_{23}t^2 + f_{24}t^3)\right]$$

where $h_{15} = \frac{c_1 c_5}{c_1 + c_5}$, $h_{25} = \frac{c_2 c_5}{c_2 + c_5}$

and $f_{11} = h_{15}\left[X_1\delta_1 - h_{15}(X_1\delta_2 + \delta_1 X_3) + 2h_{15}^2 \delta_2 X_3\right]$

$f_{12} = h_{15}^3\left[4h_{15}\delta_2 X_3 - \delta_2 X_1 - \delta_1 X_3\right]$

$f_{13} = h_{15}^5 \delta_2 X_3$

$f_{21} = h_{25}\left[\delta_1 X_2 - h_{25}(X_2\delta_2 + X_4\delta_1) + 2h_{25}^2(X_5\delta_1 + X_4\delta_2) - 6h_{25}^3\delta_2 X_5\right]$

$f_{22} = h_{25}^3\left[4h_{25}(X_5\delta_1 + X_4\delta_2) - (X_2\delta_2 + X_4\delta_1) - 18h_{25}^2\delta_2 X_5\right]$

$f_{23} = h_{25}^5\left[X_5\delta_1 + X_4\delta_2 - 9h_{25}\delta_2 X_5\right]$

$f_{24} = -h_{25}^7 X_5 \delta_2$

δ_1 , δ_2 are given by (4.27) and the X's by (4.44)

(3) EXTRA CONTRIBUTION TO THE NON-FLIP CUT FROM $-i\lambda_2 \chi^P_{+-} \chi^e_{+-}$

This is given by

$$C^{EX}_{++} = \frac{i\lambda_2}{4m^2}\left(\frac{-C_0}{8\pi c_4^2}\right)\left(e^{-i\pi/2}\frac{s}{s_0}\right)^{\alpha_e(0)} \times \tag{4.52}$$

$$\times\left[A_0 e^{h_{14}t}(g_{11}+g_{12}t+g_{13}t^2) + B_0 e^{h_{24}t}(g_{21}+g_{22}t+g_{23}t^2)\right]$$

where $h_{14} = \frac{c_1 c_4}{c_1 + c_4}$, $h_{24} = \frac{c_2 c_4}{c_2 + c_4}$

and the g_{ij}'s are given by

$$g_{11} = h_{14}^2(2Y_3 h_{14} - Y_1) \qquad g_{21} = h_{24}^2(2Y_4 h_{24} - Y_2)$$

$$g_{12} = h_{14}^3(4Y_3 h_{14} - Y_1) \qquad g_{22} = h_{24}^3(4Y_4 h_{24} - Y_2)$$

$$g_{13} = h_{14}^5 Y_3 \qquad g_{23} = h_{24}^5 Y_4$$

Thus the total non-flip amplitude which we used is given by

$$A^1_{++} = A^{1(e)}_{++} + \sum_{n=1}^{\infty} C^1_{++}(n) + C^{eP'}_{++} + C^{EX}_{++} \tag{4.53}$$

where $A^{1(e)}_{++}$ is given by (4.10), $C^1_{++}(n)$ by (4.50), $C^{eP'}_{++}$ by (4.51) and C^{EX}_{++} by (4.52). We expect the contribution C^{EX}_{++} to be small. In practice only a finite number of terms in the infinite sum were retained.

FLIP CUTS: $I_t = 1$

(1) MULTI-POMERON ⊗ RHO FLIP CUTS.

We get these from the general expression

$$\lambda_2 \frac{i^n}{n!} \chi^e_{+-} (\chi^P_{++})^n = \frac{\lambda_2 i}{2m.n!} \cdot \frac{1}{8\pi s} \left(\frac{-\sigma_T}{8\pi c_3}\right)^n \times$$
$$\times \left(e^{-i\pi/2} \frac{s}{s_0}\right)^{\alpha_e(0)} e^{-nb^2/4c_3} \cdot \frac{b}{2} \cdot \left[\theta_1 + \left(\frac{-b^2}{4}\right)\theta_2\right]$$

Doing the integration in (4.45), where now $\bar{\mu} = 1$, we get the contribution

$$C^1_{+-}(n) = \frac{i\lambda_2}{n!} \frac{\sqrt{-t}}{2m} \left(\frac{-\sigma_T}{8\pi c_3}\right)^n \left(e^{-i\pi/2} \frac{s}{s_0}\right)^{\alpha_e(0)} \times$$
$$\times \left[A_0 e^{h_{13}t}(q_{11} + q_{12}t) + B_0 e^{h_{23}t}(q_{21} + q_{22}t)\right] \qquad (4.54)$$

where the coefficients q_{ij} are given by

$$q_{11} = h_{13}^2 (Y_1 - 2h_{13} Y_3) \qquad q_{21} = h_{23}^2 (Y_2 - 2h_{23} Y_4)$$
$$q_{12} = -h_{13}^4 Y_3 \qquad q_{22} = -h_{23}^4 Y_3$$

and h_{13}, h_{23} are given in eqn.(4.50).

(2) P-PRIME ⊗ RHO FLIP CUT.

This is the term $i\lambda_2 \chi^{P'}_{++} \chi^e_{+-}$, which is given by

$$i\lambda_2 \chi^{P'}_{++} \chi^e_{+-} = \frac{-E_0 s_0 \lambda_2}{(8\pi s)^2 2m c_5} \left(e^{-i\pi/2} \frac{s}{s_0}\right)^{\alpha_e(0) + \alpha_{P'}(0)} \times$$
$$\times e^{-b^2/4c_5} \frac{b}{2} \cdot \left[\theta_1\delta_1 + \left(\frac{-b^2}{4}\right)(\theta_1\delta_2 + \theta_2\delta_1) + \left(\frac{-b^2}{4}\right)^2 \theta_2\delta_2\right]$$

and gives the contribution

$$C_{+-}^{e\,p'} = -\frac{E_0 s_c \lambda_2}{8\pi s}\frac{\sqrt{-t}}{2m}\left(e^{-i\pi/2}\frac{s}{s_0}\right)^{\alpha_e(0)+\alpha_{p'}(0)} \times$$

$$\times \left[A_0 e^{h_{15}t}(b_{11}+b_{12}t+b_{13}t^2) + B_0 e^{h_{25}t}(b_{21}+b_{22}t+b_{23}t^2)\right] \qquad (4.55)$$

and the coefficients b_{ij} are given by

$$b_{11} = h_{15}^2\left[Y_1\delta_1 - 2h_{15}(Y_1\delta_2+Y_3\delta_1)+6h_{15}^2 Y_3\delta_2\right]$$

$$b_{12} = h_{15}^4\left[6h_{15}Y_3\delta_2 - Y_1\delta_2 - Y_3\delta_1\right]$$

$$b_{13} = h_{15}^6 Y_3\delta_2$$

$$b_{21} = h_{25}^2\left[Y_2\delta_1 - 2h_{25}(Y_2\delta_2+Y_4\delta_1)+6h_{25}^2 Y_4\delta_2\right]$$

$$b_{22} = h_{25}^4\left[6h_{25}Y_4\delta_2 - Y_2\delta_2 - Y_4\delta_1\right]$$

$$b_{23} = h_{25}^6 Y_4\delta_2 .$$

(3) EXTRA CONTRIBUTION TO THE FLIP CUT FROM $i\lambda_1 \chi_{+-}^{p}\chi_{++}^{e}$

This is given by

$$C_{+-}^{EX} = i\lambda_2\frac{\sqrt{-t}}{2m}\left(\frac{-C_0}{8\pi C_4^2}\right)\left(e^{-i\pi/2}\frac{s}{s_0}\right)^{\alpha_e(0)} \times$$

$$\times \left[A_0 e^{h_{14}t}(a_{11}+a_{12}t) + B_0 e^{h_{24}t}(a_{21}+a_{22}t+a_{23}t^2)\right] \qquad (4.56)$$

where the a_{ij} are given by

$$a_{11} = h_{14}^2 (X_1 - 2h_{14} X_3) \qquad a_{21} = h_{24}^2 (X_2 - 2h_{24} X_4 + 6h_{24}^2 X_5)$$

$$a_{12} = -h_{14}^4 X_3 \qquad a_{22} = h_{24}^4 (6h_{24} X_5 - X_4)$$

$$a_{23} = h_{24}^6 X_5 .$$

Thus the total $I_t = 1$ flip amplitude which we used is given by

$$A_{+-}^1 = A_{+-}^{1(e)} + \sum_{n=1}^{\infty} C_{+-}^1(n) + C_{+-}^{eP'} + C_{+-}^{EX} \qquad (4.57)$$

where $A_{+-}^{1(e)}$ is given by (4.10), $C_{+-}^1(n)$ by (4.54), $C_{+-}^{eP'}$ by (4.55) and C_{+-}^{EX} by (4.56). Again we retained only a finite number of terms in the infinite sum.

The equations above ((4.50) - (4.57)) apply directly for the nonsense-choosing ρ input. To obtain the equations appropriate for a sense-choosing ρ and those for a fixed-pole coupling we need only make changes in the expressions appearing in (4.44). The subsequent formulae remain unchanged. We give these changes below.

SENSE-CHOOSING

$$X_1 = 1/c_1 \ , \quad X_3 = 0 \ , \quad Y_1 = 1/c_1^2 \ , \quad Y_3 = 0 \ . \qquad (4.58)$$

The others remain unchanged.

FIXED-POLE COUPLING

$$X_1 = 1/c_1 \ , \ X_2 = 1/(4m^2 c_2^2) \ , \ X_3 = 0 \ , \ X_4 = 1/(4m^2 c_2^3) \ , \ X_5 = 0$$

$$Y_1 = 1/c_1^2 \ , \ Y_2 = -1/c_2^2 \ , \ Y_3 = 0 \ , \ Y_4 = 0 \ . \qquad (4.59)$$

Recall that eqn.(4.45) is derived from the formula

$$A^1_{H_s}(s,t) = 4\pi s \int_0^\infty b\,db\; e^{i\chi^c}\,\chi^\rho\, J_{\bar{\mu}}(b\sqrt{-t}) \qquad (4.60)$$

and the corresponding expression for the A^0 amplitude is

$$A^0_{H_s}(s,t) = 4\pi s\, i \int_0^\infty b\,db \left[1 - e^{i\chi^c}\right] J_{\bar{\mu}}(b\sqrt{-t}) \qquad (4.61)$$

In the approach adopted in method (a) for the $I_t = 0$ amplitudes (4.61) becomes

$$A^0_{H_s}(s,t) = 4\pi s \int_0^\infty b\,db\; \bar{\chi}^{0(a)}_{H_s}\, J_{\bar{\mu}}(b\sqrt{-t}) \qquad (4.62)$$

where $\bar{\chi}^{0(a)}_{H_s}$ is given by (4.40). Comparing (4.62) with (4.61) shows that for method (a) equation (4.60) reduces to

$$A^1_{H_s}(s,t) = 4\pi s \int_0^\infty b\,db \left[\chi^\rho\left(1 + i\,\bar{\chi}^{0(a)}\right)\right]_{H_s} J_{\bar{\mu}}(b\sqrt{-t}) \qquad (4.63)$$

so that in this case we have only one cut term. Thus when method (a) is adopted for the $I_t = 0$ amplitudes the $I_t = 1$ amplitudes are given by (4.53) and (4.57) with only <u>one</u> term of the infinite sum included. Thus in this case (4.53) and (4.57) reduce to

$$\left.\begin{aligned} A^1_{++} &= A^{1(e)}_{++} + C^1_{++}(1) + C^{eP'}_{++} \\ A^1_{+-} &= A^{1(e)}_{+-} + C^1_{+-}(1) + C^{eP'}_{+-} \end{aligned}\right\} \text{Method (a)} \qquad (4.64)$$

where we have also neglected the small corrections C^{EX}.

Equations (4.64) were the ones used in ref.53.

When method (b) is adopted for the $I_t = 0$ amplitudes the whole sum in (4.53) and (4.57) should be included, but in practice only the first three terms were retained.

$I_t = 1$ IMPACT PARAMETER AMPLITUDES

These are of course defined by

$$\chi^1_{H_s}(s,b) = \frac{1}{8\pi s}\int_{-\infty}^{0} dt\; A^1_{H_s}(s,t)\; \overline{J}_{\bar{\mu}}\left(b\sqrt{-t}\right) \qquad (4.65)$$

Using method (a) for the $I_t = 0$ amplitudes we get

$$\left.\begin{aligned} \chi^1_{++} &= \chi^{\rho}_{++}\left(1 + i\lambda_1 \chi^{o(a)}_{++}\right) \\ \chi^1_{+-} &= \chi^{\rho}_{+-}\left(1 + i\lambda_2 \chi^{o(a)}_{++}\right) \end{aligned}\right\} \text{Method (a)} \qquad (4.66)$$

where we have included the λ factors, and $\chi^{o(a)}_{++}$ is given in (4.40).

For method (b) we have approximately

$$\left.\begin{aligned} \chi^1_{++} &= \chi^{\rho}_{++} + i\lambda_1 \chi^{\rho}_{++}\chi^{o(b)}_{++} + \frac{i^2}{2!}\lambda_1 \chi^{\rho}_{++}\left(\chi^{o(b)}_{++}\right)^2 + \ldots \\ &= \chi^{\rho}_{++}\left(1 - \lambda_1 + \lambda_1 e^{i\chi^{o(b)}_{++}}\right) \\ \chi^1_{+-} &= \chi^{\rho}_{+-}\left(1 - \lambda_2 + \lambda_2 e^{i\chi^{o(b)}_{++}}\right) \end{aligned}\right\} \text{Method (b)} \qquad (4.67)$$

and $\chi^{o(b)}_{++}$ is given by (4.17) when we include cuts in the $I_t = 0$ amplitudes.

DISCUSSION

The above formalism is based on our choice of parameterizing the t-channel amplitudes (A', B) in terms of a ρ Regge pole. We then used crossing to give us the s-channel amplitudes (4.6). This is more exact than using a direct s-channel parameterization, since it correctly takes account of the kinematical factors. Also it is essential for a sense-choosing ρ ,

since the α' factor appears in the B amplitude but not in the A', and this 'mixing' cannot be reproduced by a direct s-channel parameterization. We did in fact try direct s-channel parameterization, together with a few other varieties, namely

$$(1)\quad A^1_{++} = i\left(e^{-i\pi/2}\frac{s}{s_0}\right)^{\alpha_\rho(0)}\left[A_0\alpha_\rho e^{c_1 t} - D_0\alpha_\rho e^{c_2 t}\right]$$

$$A^1_{+-} = i\sqrt{-t}\,(\quad)^{\alpha_\rho(0)} B_0\alpha_\rho e^{c_3 t}$$

$$(2)\quad A^1_{++} = i\left(e^{-i\pi/2}\frac{s}{s_0}\right)^{\alpha_\rho(0)}\left[A_0\alpha_\rho e^{c_1 t} - tD_0\alpha_\rho e^{c_2 t}\right]$$

$$A^1_{+-} = i\sqrt{-t}\,(\quad)^{\alpha_\rho(0)} B_0\alpha_\rho e^{c_3 t}$$

which are to be compared with equations (4.12). All were found to give inferior fits. The s-channel parameterization and the form (1) above gave much poorer fits. It is interesting that the form (2) above, which looks very much like the A', B form (4.12), gave a slightly inferior fit even though it has two extra parameters. The use of the A', B form resulted in much the best fits.

A crucial feature of the A', B parameterization is the appearance of the factor t in the B part of A^1_{++}. The importance of the t factor can be seen as follows. Consider the non-flip amplitude A^1_{++} of (4.12). The magnitude of A_0 is fixed by the $t = 0$ data (i.e $d\sigma/dt$ in the forward direction). As $|t|$ is increased the B_0 term takes over and becomes dominant. However the dominant cut contribution comes from the small $|t|$ region and so is determined by the A' contribution (the cuts from the B part are relativelly small, at least in the range $0 \leq |t| \lesssim 1.0$, even though $|B_0| \gg |A_0|$). Thus we have the

possibility that the A' contribution will die away quickly (i.e h_1 large) thus allowing the pole contribution of the B part to quickly dominate and also giving the dominant cut a slightly steeper slope. There is thus a separation of dominant pole effects from dominant cut effects which can, roughly speaking, adjust themselves independantly to give the best fit. Also, since the pole contribution in B is relatively large for $|t| > 0.2$ the cut contribution is not completely dominant in this region. With direct s-channel parameterization we do not have this freedom.

In the flip amplitude the A' and B terms are on an equal footing in that their cut contributions are similar in form. However since $|B_0| \gg |A_0|$ the dominant pole and cut contributions come from the B term. Because of the factor $\sqrt{-t}$ these flip cuts will be relatively smaller than the non-flip cuts, since the main contribution to the cut comes from the small $|t|$ region.

In general the presence of α factors in the pole input reduces the magnitude of the cuts, since a zero in the pole amplitude will reduce its contribution to the eikonal (eqn.(4.42)). Thus we can expect the strongest cuts in the fixed-pole coupling case, and the weakest in the choosing-nonsense case.

Finally, we give below expressions for the experimental observables, which exhibit the amplitude normalizations and units.

$$\frac{d\sigma}{dt}\left\{mb\left(\frac{Gev}{c}\right)^{-2}\right\} = \frac{0.3893}{64\pi m^2 p_L^2}\left[|A_{++}|^2 + |A_{+-}|^2\right] \quad (4.68)$$

$$\sigma_T = \frac{0.3893}{2m p_L} \operatorname{Im} A_{++}(t=0) \tag{4.69}$$

$$P = \frac{2 \operatorname{Im}(A_{++} A_{+-}^*)}{|A_{++}|^2 + |A_{+-}|^2} \tag{4.70}$$

where m is the mass of the nucleon and p_L is the laboratory momentum of the incident pion. (If q_s is the c.m pion momentum then $sq_s^2 = m^2 p_L^2$).

Our isospin amplitudes are

$$\begin{aligned} A(\pi^{\pm} p \to \pi^{\pm} p) &= A^0 \mp A^1 \\ A(\pi^- p \to \pi^0 n) &= \sqrt{2}\, A^1 \end{aligned} \tag{4.71}$$

With the above normalizations our amplitudes are dimensionless.

CHAPTER 5

GENERAL DISCUSSION AND AMPLITUDE ANALYSIS

There are four main characteristics of πN data which have to be explained:

(i) A dip in $d\sigma/dt$ (CEX) at $t \approx -0.6$ $(Gev/c)^2$.

(ii) A relatively large positive polarization in πN CEX for $|t| \approx 0.4 - 0.5$.

(iii) the so-called 'crossover'. This refers to the fact that

$$\left[\frac{d\sigma}{dt}(\pi^+ p) - \frac{d\sigma}{dt}(\pi^- p)\right]$$

changes sign around $|t| \approx 0.1 - 0.2$, for a large range of energies.

(iv) the mirror symmetry of $\pi^+ p$ and $\pi^- p$ elastic polarization, over a large range of t values (at least up to $|t| \approx +1.5$).

Since the elastic amplitudes depend directly on A^0 while the CEX amplitudes depend only indirectly on A^0 (through the inclusion of cuts) we expect that the properties (iii) and (iv) above would be more sensitive to the structure of the $I_t = 0$ amplitudes.

More precisely, since

$$\frac{d\sigma}{dt}(\pi^{\pm} p) \propto \left\{ \left| A^0_{++} \mp A^1_{++} \right|^2 + \left| A^0_{+-} \mp A^1_{+-} \right|^2 \right\}$$

we have

$$\left[\frac{d\sigma}{dt}(\pi^+ p) - \frac{d\sigma}{dt}(\pi^- p)\right] \propto \left\{ \mathrm{Re}\, A^1_{++}\, \mathrm{Re}\, A^0_{++} + \right.$$
$$\left. + \mathrm{Im}\, A^1_{++}\, \mathrm{Im}\, A^0_{++} + \mathrm{Re}\, A^1_{+-}\, \mathrm{Re} A^0_{+-} + \mathrm{Im}\, A^1_{+-}\, \mathrm{Im}\, A^0_{+-} \right\} \qquad (5.1)$$

By far the most important term here (at least for small $|t|$) is $\mathrm{Im}\, A^0_{++} \mathrm{Im}\, A^1_{++}$, and so a crossover at $|t| \approx 0.1 - 0.2$ implies that $\mathrm{Im}\, A^1_{++}$ should change sign in this region ($\mathrm{Im}\, A^0_{++}$ does not change sign here). Data shows there is no other crossover and so the right hand side of (5.1) should have only the single zero.

We can gain further insight into the expected behaviour of the A^1 amplitudes by considering the expression for the elastic polarization.

Since $P \propto \mathrm{Im}\,(A_{++} A^*_{+-})$ we have

$$P(\pi^{\pm}p) \propto \left[\mathrm{Im}\, A^0_{++}\, \mathrm{Re}\, A^0_{+-} - \mathrm{Re}\, A^0_{++}\, \mathrm{Im}\, A^0_{+-} + \right.$$
$$\left. + \mathrm{Im}\, A^1_{++}\, \mathrm{Re}\, A^1_{+-} - \mathrm{Re}\, A^1_{++}\, \mathrm{Im}\, A^1_{+-}\right] \mp \left[\mathrm{Im} A^0_{++} \mathrm{Re} A^1_{+-}\right.$$
$$\left. - \mathrm{Re} A^0_{++} \mathrm{Im}\, A^1_{+-} + \mathrm{Im} A^1_{++} \mathrm{Re} A^0_{+-} - \mathrm{Re} A^1_{++} \mathrm{Im} A^0_{+-}\right] \tag{5.2}$$

The last two terms in each square bracket are small compared with the first two terms, so we can write

$$P(\pi^{\pm}p) \propto \left[\mathrm{Im} A^0_{++}\, \mathrm{Re}\, A^0_{+-} - \mathrm{Re}\, A^0_{++}\, \mathrm{Im}\, A^0_{+-}\right]$$
$$\mp \left[\mathrm{Im} A^0_{++}\, \mathrm{Re}\, A^1_{+-} - \mathrm{Re}\, A^0_{++}\, \mathrm{Im}\, A^1_{+-}\right] \tag{5.3}$$

The most striking aspect of the elastic polarization data is the almost perfect mirror symmetry of $P(\pi^+ p)$ and $P(\pi^- p)$. This implies that the first bracket in (5.2) is very small compared with the second bracket, even for large $|t|$, which means that A^1_{++} must not approach zero too

quickly as $|t|$ increases. If it does then the symmetry will be badly broken.

The data shows an approximate double zero at $|t| \sim 0.6 - 0.7$. A strong double zero in Re A^1_{+-} (i.e Re A^1_{+-} relatively large for $|t| > 0.7$) would achieve this and indeed this is how the B.P $I_t = 1$ amplitude behaves. This corresponds fairly closely to the amplitude analysis of Halzen-Michael (ref.51) and Kelly (ref. 52). However see later for a fuller discussion.

The expression for the charge-exchange polarization gives

$$P(\pi^- p \to \pi^0 n) \propto \left[\mathrm{Im} A^1_{++} \, \mathrm{Re} A^1_{+-} - \mathrm{Re} A^1_{++} \, \mathrm{Im} A^1_{+-} \right] \quad (5.4)$$

The data shows a zero around $|t| \approx 0.6$–0.7, and since we expect Re A^1_{+-} to have a zero in this region, this implies that one or both of Re A^1_{++}, Im A^1_{+-} should have a zero here. Amplitude analysis gives Im A^1_{+-} a zero at $|t| \approx 0.6$ and Re A^1_{++} a zero at $|t| \approx 0.7 - 0.8$ (cf. Kelly).

Thus zeros in all three of Re A^1_{++}, Re A^1_{+-} and Im A^1_{+-} in this region explains the rather pronounced dip in the CEX differential cross section data, the non-vanishing of Im A^1_{++} making this a true dip, not a zero.

Thus the data and amplitude analysis suggest that we require the following structure :

Im A^1_{++} - a zero at $t \approx -0.15$

$\mathrm{Re}\ A^1_{++}$ - no zero for $|t| \lesssim 0.5$

$\mathrm{Im}\ A^1_{+-}$ - a zero at $t \approx -0.6$

$\mathrm{Re}\ A^1_{+-}$ - approximate double zero at $t \approx -0.6$.

With a ρ trajectory $\alpha_\rho \approx 0.6 + t$, the fixed-pole coupling ρ contribution gives a zero at $t \approx -0.6$ only in the real parts of the amplitudes, while for a sense-choosing ρ we have single zeros at $t = -0.6$ in $\mathrm{Re}\ A'$ and $\mathrm{Im}\ B$, and a double zero in $\mathrm{Re}\ B$. Since the ratio sB/A' is large this means that effectively $\mathrm{Re}\ A^1_{++}$ and $\mathrm{Im}\ A^1_{+-}$ will have a single zero while $\mathrm{Re}\ A^1_{+-}$ will have a double zero. A nonsense-choosing ρ pole gives a double zero in the real parts and a single zero in the imaginary parts of the amplitudes.

Since the general effect of cuts is to pull in zeros it would appear at first sight that the sense and nonsense inputs are to be favoured, at least for the flip amplitude, if the flip cuts are small. In fact no flip cuts at all would seem to be best. The non-flip amplitude could be explained if we had

$$\left|\mathrm{Im\ CUT}_{++}\right| \gg \left|\mathrm{Re\ CUT}_{++}\right| \qquad (5.5)$$

and also

$$\left|\mathrm{Re\ CUT}_{++}\right| \text{ small.}$$

In fact this latter condition was not satisfied in our sense and nonsense fits so that the zero of $\mathrm{Re}\ A^1_{++}$ was pulled in too far. This led to a poor CEX polarization prediction and also meant that both our $\mathrm{Im}\ A^1_{++}$ and $\mathrm{Re}\ A^1_{++}$

were too large at $t \approx -0.6$, thus filling in the dip in the differential cross section.

However both of the above conditions seemed to be satisfied in our fixed-pole coupling (F.P) case. Also the real parts of the cut contributions changed sign at $|t| \approx 0.4 - 0.6$ which meant that the zeros in the real parts were changed into approximate double zeros, even though their magnitudes were too small.

The conditions (5.5) are precisely the effects brought about by the inclusion of the real part of the $I_t = 0$ non-flip amplitude. This can be demonstrated as follows : We can write (see eqn.(4.45))

$$\chi^{CUT}_{++} \approx i \chi^{1}_{++} \chi^{o}_{++} \tag{5.6}$$

where, for the purposes of illustration, we have taken only the first cut term, and neglected $\chi^{1}_{+-} \chi^{o}_{+-}$ and the λ factor.

From (5.6) we get

$$\begin{aligned} \mathrm{Im}\,\chi^{CUT}_{++} &= -\underset{(1)}{\mathrm{Im}\,\chi^{1}_{++}\,\mathrm{Im}\,\chi^{o}_{++}} + \underset{(2)}{\mathrm{Re}\,\chi^{1}_{++}\,\mathrm{Re}\,\chi^{o}_{++}} \\ \mathrm{Re}\,\chi^{CUT}_{++} &= -\underset{(3)}{\mathrm{Re}\,\chi^{1}_{++}\,\mathrm{Im}\,\chi^{o}_{++}} - \underset{(4)}{\mathrm{Im}\,\chi^{1}_{++}\,\mathrm{Re}\,\chi^{o}_{++}} \end{aligned} \tag{5.7}$$

We denote the four terms on the R.H.S by (1),(2), (3),(4) as indicated.

Recall that the actual cut contribution to the full amplitude is given by

$$Cut^{1}_{++} \approx 4\pi s \int_0^\infty b\,db\,(i\chi^{1}_{++}\chi^{0}_{++})J_0(b\sqrt{-t}) \qquad (5.8)$$

To simplify matters we may now confine ourselves to the forward direction, where $J_0(b\sqrt{-t}) = 1$, $(t = 0)$, so that the cut contribution is essentially proportional to the area contained by the curve $i\chi^{1}_{++}\chi^{0}_{++}$. The presence of the factor b does not alter our conclusions.

The first term (1) above has a positive peak at small b, a zero at $b \approx 0.4$ fm., thereafter remaining negative, and the net contribution to Im Cut_{++} is negative. The term (2) is negative for small b, with a zero at $b \approx 1.1$ fm., and positive thereafter. The contribution to Im Cut_{++} is again negative, so the two contributions enhance to strengthen the cut in the imaginary part of the amplitude.

The case with the real part is different. The term (3) has a negative peak at small b and goes rapidly to zero with increasing b. The term (4) has a small negative peak for small b, a zero at around $b \approx 0.4$ fm., a positive bump, and a zero at $b \approx 1.2$ fm. The net effect is to weaken slightly the cut in the real part.

Thus we see the importance of including the real part of the $I_t = 0$ amplitudes. In this way we can expect a separation of zeros in the real and imaginary parts of the $I_t = 1$ non-flip amplitude. This is important to avoid a zero in the charge-exchange polarization around $t = -0.3$, and hence a negative peak at $t \approx -0.5$ (both contrary to data) which were predicted by the older Absorption model fits (e.g refs.29,34).

It should be noted here that since it is the P' that plays the major role in determining the real part of the $I_t = 0$ non-flip amplitude, the extra terms (2) and (4) above stem mainly from the $\rho \otimes P'$ cuts ;- hence the importance of including such cuts.

A similar argument applies to the flip amplitude, giving

$$|\text{Im Cut}_{+-}| \gg |\text{Re Cut}_{+-}|$$

Despite the advantages noted above, the property $|\text{Im Cut}| \gg |\text{Re Cut}|$ also has its disadvantages. The magnitude of the cut has to be relatively large to give the required structure of zeros in the amplitudes. However because of the shallower slope of the cuts the higher $|t|$ data is also important in determining this magnitude. In particular the higher $|t|$ parts ($|t| \gtrsim 0.4$) of the imaginary parts of the amplitudes $A^1_{+\pm}$ can be almost completely accounted for by the cut contributions. This forces the pole contribution in this region to be small. This in turn means that the pole contribution to the real parts of the amplitudes is small, and since $|\text{Re Cut}|$ is too small to make up the difference we find that the real parts of the amplitudes are too small in the high $|t|$ region. Thus we expect the imaginary parts to be well fitted but the real parts to be poorly fitted by this model, and this is indeed found to be so. The model is thus forced to 'explain' the high $|t|$ data essentially using only the imaginary parts. This is a severe restriction especially in fitting the polarization data, which depend sensitively on the interplay between the real and imaginary parts.

This deficiency is most apparent in the high $|t|$ region of the elastic polarization. The most dominant contributions to this come from the terms Im A^0_{++} Re A^1_{+-} and Re A^0_{++} Im A^1_{+-} (see eqn.(5.3)). Since in our model we find Re A^1_{+-} is small, the latter term dominates. However to get the required double zero we need a zero in Re A^0_{++} around $t = -0.6$. This zero does not occur in the B.P $I_t = 0$ amplitude, but the analysis of Kelly (ref.52) gives Re A^0_{++} a zero at $t \approx -0.8$. The model of the $I_t = 0$ amplitudes adopted by Hartly and Kane (ref.54) gives Re A^0_{++} a zero at $t \approx -0.7$ and their magnitude of Re A^0_{++} for $|t| > 0.7$ is relatively large. If Re A^0_{++} does in fact have this zero then the two dominant terms Im A^0_{++} Re A^1_{+-} and Re A^0_{++} Im A^1_{+-} will add consructively for $|t| \gtrsim 0.7$, and if this zero is absent they will interfere destructively for $|t| \gtrsim 0.7$. In the model of Hartley and Kane the term Re A^0_{++} Im A^1_{+-} in fact gives by far the major contribution to the elastic polarization for $|t| \gtrsim 0.7$.

The above suggests that a 'better' model would be to have cuts only in the imaginary parts of the amplitudes. This would accord with our discussion of the unitarity equation and absorption (see Chapter 3), and indeed this type of model has been suggested (ref.55).

In the procedure adopted by us to calculate the elastic polarization we took the actual B.P $I_t = 0$ amplitudes (and not our fit to these amplitudes) so that the two terms above interfered destructively, at least in the range $0.6 \lesssim |t| \lesssim 1.1$. Our elastic polarization is therefore poor

for large $|t|$, because of the non-dominance of the term Im A^{0}_{++} Re A^{1}_{+-}. It will be recalled that for both sense-choosing and nonsense-choosing ρ, the real part of the flip amplitude Re A^{1}_{+-} in a pure pole model (i.e no cuts) does indeed have a double zero at $t \approx -0.6$, and in an attempt to emphasize this double zero we accordingly put $\lambda_2 = 0$ i.e we had non-flip cuts only. This improved the fits slightly, and all our sense and nonsense fits which we describe here had $\lambda_2 = 0$.

We now describe our methods of fitting.

METHODS

Using method (a) for the $I_t = 0$ amplitudes we used only one cut term in the $I_t = 0$ amplitudes, corresponding to the usual absorptive prescription. Using method (b) for the $I_t = 0$ amplitudes we used two slightly different models for the $I_t = 1$ amplitudes corresponding to keeping one or three cut terms respectively. This was to examine if the slightly different cut structures played a significant role. We found that the one cut structure was in fact preferred, and indeed gave the best results of all. (Since |1 Cut| > |3 Cuts| we expected the λ factors to be smaller, and this was indeed the case.)

Thus altogether we examined nine different models for the $I_t = 1$ amplitudes, which we summarize below :

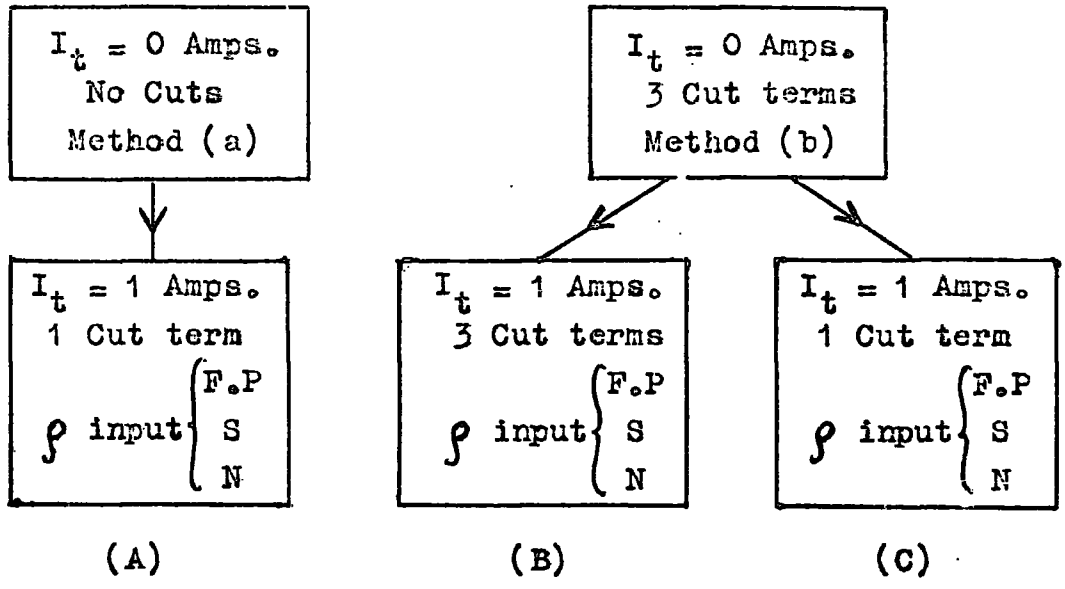

where F.P denotes the fixed-pole coupling, S denotes a sense-choosing and N denotes a nonsense-choosing ρ. These nine models fall into three groups, which we indicate by (A),(B),(C), and within each group we have the three different ρ pole inputs.

The $I_t = 1$ amplitudes obtained from these nine models were used to compare the calculated differential cross section and polarization with the πN charge-exchange data over a range of pion momenta between 5.85 and 18.2 Gev/c and for $0 \leq |t| \leq 2.2$ $(\text{Gev/c})^2$. These amplitudes were then used with the B.P $I_t = 0$ amplitudes to 'predict' the elastic polarization.

In all our least χ^2 minimisations we used the CERN MINUIT program.

I_t = 0 AMPLITUDES

In method (a) we fitted the real and imaginary parts of the expressions (4.14) to their B.P $I_t = 0$ counterparts, for t values in the range $0 \geq t \geq -1.0$ at intervals of 0.05, and for the momentum values p_L = 2.5,5.0,6.0,10.0,13.3,18.2 Gev/c.

In this fit we had eleven parameters

$$\sigma_T,\ E_o,\ C_o,\ F_o, \alpha_P(0),\ \alpha'_P,\ h_3,\ h_4,\ h_5,\ h_6, \alpha'_P$$

At each point we calculated the quantity

$$Q_i = (x_i - y_i)^2 + (y_i/x_i - 1)^2 \qquad (i = 1,2,3,4)$$

where $x_1 = \text{Re } B.P^0_{++}$, $x_2 = \text{Im } B.P^0_{++}$, $x_3 = \text{Re } B.P^0_{+-}$, $x_4 = \text{Im } B.P^0_{+-}$, and the y's are the counterparts of our amplitudes (4.14). The second term in Q_i was included to emphasize any zeros in the B.P $I_t = 0$ amplitudes. We then minimized the quantity

$$\chi^2 = \sum \left[(Q_1 + Q_2) + 100\,(Q_3 + Q_4)\right]$$

where the sum runs over all t points and all energies considered. The factor 100 was included to compensate for the small magnitude of the flip quantities. The results of this minimization are shown in Table(1) and Fig 6.

For method (b), where we now include cut terms, we used exactly the same procedure as above, except that now the y's refer to equations (4.34) and (4.38). The results of this fit are given in Table(1)and Fig 6.

$I_t = 1$ AMPLITUDES

We used our $I_t = 1$ amplitudes (4.53) and (4.57) to fit the πN charge-exchange differential cross section and polarization data. The data used was as follows :

$d\sigma/dt$; p_L = 5.85,5.9,10.0,13.3,13.3,18.2,18.2 Gev/c

and for all t values quoted ($\max|t| = 2.25$ (Gev/c)^2).

$P(\pi^- p \to \pi^0 n)$; $p_L = 5.0,\ 8.0$ Gev/c

and for t values $0 < |t| \leq 1.75$ $(\text{Gev/c})^2$.

The total number of data points used was 115.

We initially fitted the real and imaginary parts of our $I_t = 1$ amplitudes to the corresponding B.P quantities. This was done to avoid any secondary minima in a least χ^2 fit to the experimental data.

In all these fits the solution was encouraged to give a crossover somewhere in the range $0.1 < |t| < 0.2$. This was achieved by adding to the usual χ^2 a quantity proportional to the square of $\left[d\sigma/dt(\pi^+ p) - d\sigma/dt(\pi^- p)\right]$ viz.

$$F^2 = \tfrac{\pi}{4}.10^{-8}\left[\text{Re } A^1_{++}\text{Re } A^0_{++} + \text{Im } A^1_{++}\text{Im } A^0_{++} + \text{Re } A^1_{+-}\text{Re } A^0_{+-} + \text{Im } A^1_{+-}\text{Im } A^0_{+-}\right]$$

evaluated for t values in the range $-0.1 \geqslant t \geqslant -0.2$ at intervals of 0.01, and for each energy considered. The numerical factor above seemed to be a convenient choice. In this way all our models gave a crossover at a value of t in the interval $(-0.1, -0.2)$. This is essentially equivalent to $\text{Im } A^1_{++}$ having a zero at $t \approx -0.2$. It is clear that a crossover in the interval $0.1 \leqslant |t| \leqslant 0.2$ gives a minimum of F^2. The inclusion of this quantity also helps in avoiding secondary minima.

We had 16 polarization data points. These points place a severe restriction on the behaviour of the real and imaginary parts of the amplitudes. To compensate for their small number (as compared to 99 $d\sigma/dt$ data points) and to emphasize their restriction on the amplitudes we accordingly enhanced the

polarization χ^2 by a factor ten.

Thus, for each energy, we calculated

$$\chi^2 = \sum_{\substack{\text{all } t \\ \text{points}}} \left[\chi^2\left(\frac{d\sigma}{dt}\right) + 10\,\chi^2(Pol) \right] + \sum_{\substack{|t|=0.1 \\ \Delta t = 0.01}}^{0.2} F^2$$

and the total χ^2 was $\sum_{\text{all energies}} \chi^2$.

The χ^2 appearing above is defined as usual by

$$\chi^2 = \left(\frac{\text{Experimental - Calculated}}{\text{Error}} \right)^2$$

For each of our models we minimized the quantity $\sum \chi^2$. The actual data χ^2 is of course given by

$$Y^2 = \sum_{\substack{\text{all} \\ \text{energies}}} \sum_{\substack{\text{all } t \\ \text{points}}} \left[\chi^2\left(\frac{d\sigma}{dt}\right) + \chi^2(Pol.) \right]$$

and it is this quantity that we quote in our results.

RESULTS AND CONCLUSIONS

I_t = 0 AMPLITUDES

METHOD (a) : NO CUTS.

As can be seen from Fig. 6 we get quite a good fit to the non-flip amplitude, and a reasonable fit to the flip amplitude. However the flip fit is not really crucial as most of the effects are dominated by the non-flip part.

The fit involves 11 parameters σ_T, E_0, C_0, F_0, α'_P, $\alpha_P(0)$, $\alpha'_{P'}$, h_3, h_4, h_5, h_6, and the following bounds were imposed ;

$$0 < \alpha'_P < 1.0 \ , \ 0.4 < \alpha_{P'}(0) < 0.6 \ , \ 0.8 < \alpha'_{P'} < 1.1 \ .$$

The results are given below.

METHOD (b) : 3 CUT TERMS.

Again we get quite a good fit to the non-flip amplitude, and a reasonable fit to the flip amplitude. The structure of the non-flip fit is slightly different however in that (at 6 Gev/c for example) Re A^{o}_{++} has a zero at $t \approx -0.7$ and another at $t \approx -1.3$, while Im A^{o}_{++} has a zero at $t \approx -1.7$. The zero of Re A^{o}_{++} at $t \approx -0.7$ is in agreement with the analysis of Kelly (ref.52) but is not present in the B.P amplitude. In this fit we also used λ factors, which were bounded by $1 \leq \lambda \leq 2$, but both λ_{++} and λ_{+-} took the minimum value of unity. This fit thus essentially had only the 11 parameters above, subject to the same bounds as method (a). The results are shown in FIG.6 .

The parameter values in the best fit for these two methods are given below.

I_t = 1 AMPLITUDES

Our nine models can conveniently be divided into three groups, denoted (A),(B),(C).

(A) NO CUTS IN I_t = 0 AMPLITUDES FIT.

ONE CUT TERM IN THE I_t = 1 AMPLITUDES FIT.

THREE ρ INPUTS : - F.P, S, N (λ_2 = 0 FOR S, N)

(where F.P denotes fixed-pole coupling, S denotes sense-choosing ρ , and N denotes nonsense-choosing ρ).

(B) 3 CUT TERMS IN $I_t = 0$ AMPLITUDES FIT.

3 CUT TERMS IN THE $I_t = 1$ AMPLITUDES FIT.

THREE ρ INPUTS : - F.P, S, N ($\lambda_2 = 0$ FOR S, N)

(C) 3 CUT TERMS IN THE $I_t = 0$ AMPLITUDES FIT.

1 CUT TERM IN THE $I_t = 1$ AMPLITUDES FIT.

THREE ρ INPUTS : - F.P, S, N ($\lambda_2 = 0$ FOR S, N)

In each $I_t = 1$ amplitudes fit we had eight parameters, the ρ pole parameters A_o, B_o, h_1, h_2, $\alpha_\rho(0)$, α'_ρ and the λ factors λ_1, λ_2 (λ_2 being fixed at zero for all S and N cases).

The 'best fit' parameter values for models (A),(B) and (C) are given in Table (2). In all three cases the parameters were subject to the following bounds :

$$0.45 \leq \alpha_\rho(0) \leq 0.6 \ , \ 0.8 \leq \alpha'_\rho \leq 1.1 \ , \ 1.0 \leq \lambda_{1,2} \leq 2.0$$

and $h_{1,2} \geq 0$ (see ref.49).

The results of model (A) are depicted in Figs.1 - 4 The results of model (C) are also depicted in Figs.1 - 4 where they depart from model (A). The results of model (B) are not given since they are very similar to those of model (C) in all respects.

PARAMETER VALUES FOR THE I_t = 0 AMPLITUDES FIT

	METHOD (a)	METHOD (b)
σ_T	19.92(mb) / 0.3893	21.20(mb) / 0.3893
E_o	− 43.31(mb) / 0.3893	− 77.68(mb) / 0.3893
C_o	5.793(mb) / 0.3893	6.284(mb) / 0.3893
F_o	− 2.736(mb) / 0.3893	− 5.293(mb) / 0.3893
α'_P	0.487	0.543
$\alpha'_{P'}(0)$	0.549	0.544
$\alpha'_{P'}$	1.10	1.08
h_3	2.02	1.08
h_4	0.227	1.25
h_5	2.10	0.012
h_6	0.0	0.0
λ^o_{++}	0.0	1.0
λ^o_{+-}	0.0	1.0

TABLE (1)

PARAMETER VALUES FOR THE $I_t = 1$ AMPLITUDES FIT

Model (A)

	A_o	B_o	h_1	h_2	$\alpha_\rho(o)$	α'_ρ	λ_1	λ_2
F.P	30.4	256	7.40	3.15	0.453	0.8	1.63	1.33
S	36.9	322	7.28	3.11	0.559	0.8	1.71	0
N	20.9	301	4.77	2.43	0.555	0.8	1.48	0

The Data χ^2 were 283, 627, 630 for F.P, S, N respectively.

Model (B)

	A_o	B_o	h_1	h_2	$\alpha_\rho(o)$	α'_ρ	λ_1	λ_2
F.P	29.4	249	6.96	3.11	0.455	0.821	1.46	1.24
S	19.9	300	5.33	2.57	0.558	0.8	1.37	0
N	35.4	318	7.75	3.19	0.563	0.8	1.61	0

The Data χ^2 were 249,596,611 for F.P, S, N respectively.

Model (C)

	A_o	B_o	h_1	h_2	$\alpha_\rho(o)$	α'_ρ	λ_1	λ_2
F.P	28.1	247	7.27	3.11	0.451	0.833	1.15	1.02
S	18.9	297	6.45	2.67	0.561	0.8	1.10	0
N	34.4	318	8.44	3.16	0.570	0.8	1.29	0

The Data χ^2 were 225, 550, 562 for F.P, S, N respectively.

TABLE (2)

It will be seen that in all three models the fixed-pole coupling solution is by far the best, with not much to choose between the sense and nonsense cases, and with model (C) being the best overall.

As can be seen from the fits the general properties of the solutions (A),(B),(C) are very similar, so that the following general remarks will apply to all three.

FIXED-POLE COUPLING SOLUTIONS.

We obtain good fits to the differential cross section data (Fig . 1) , with a dip at $t \approx -0.56$ which seems to be stationary with increasing energy. The fit is slightly too small at large $|t|$ and the smaller energies.

The charge-exchange polarization is also well fitted, except possibly in the very small $|t|$ region, where our fits seem too large. (FIGS. 2(a) and 2(b)).

The crossover is at $t \approx -0.1$ at 5.85 Gev/c and moves out with energy to $t \approx -0.22$ at 18.2 Gev/c. This also seems to be in accord with the elastic data.

Using the B.P $I_t = 0$ amplitudes, the elastic polarization prediction is poor at large $|t|$. As already noted this is due to the smallness of Re A^1_{+-} at large $|t|$. We also used Hartley and Kane's $I_t = 0$ amplitudes (ref.54), where Re A^o_{++} has a zero at $t \approx -0.7$, with our $I_t = 1$ amplitudes to calculate the elastic polarization at 6 Gev/c. This gave a better fit but again the mirror symmetry was quite badly broken.

A similar result was obtained when we used our fit (method (b)) to the $I_t = 0$ amplitudes, which also has a zero in Re A^o_{++} at $t \approx -0.7$.

Both of these were very poor for high $|t|$ ($|t| \gtrsim 1.5$).

SENSE AND NONSENSE SOLUTIONS

These were very similar and so are discussed together. Recall that these solutions had no flip cuts. This meant that Re A^1_{+-} had a double zero at $t \approx -0.6$ and Im A^1_{+-} a single zero. However the pole contribution in this region was so small that $|A^1_{+-}|$ was practically negligible. This again meant that the elastic polarization was badly fitted for high $|t|$ ($|t| \gtrsim 0.7$).

In all the S and N models we obtained a satisfactory crossover : at $t \approx -0.1$ for 5.85 Gev/c, moving out to $t \approx -0.22$ for the sense case, and $t \approx -0.14$ for the nonsense case, at 16.2 Gev/c.

However, in both of these cases, pulling in the zero in Im A^1_{++} also pulled in the zero of Re A^1_{++} too far (at $t \approx -0.35$ for 6 Gev/c in the sense case, and $t \approx -0.27$ for 6 Gev/c in the nonsense case) with the result that Re A^1_{++} was too large at $t \approx -0.6$ and consequently filled in the dip caused by the vanishing of the flip amplitude. As a result our fits to the differential cross section displayed hardly any dip, and were poor at large $|t|$ ($|t| \gtrsim 0.6$). The proximity of the zeros in Im A^1_{++} and Re A^1_{++} gave a poor fit to the charge-exchange polarization, although these fits did not give the large negative peak at $t \approx -0.5$, as predicted by the older absorption fits. As already noted this is due to the inclusion of a real part (essentially P') to the $I_t = 0$ amplitude, which keeps these zeros apart.

The data fits for models (A) and (C) are given in Figs. 1 - 3 . Figs.4(a),(b) show that the $I_t = 1$ phases for the F.P case are in good agreement with recent determinations, and

are similar to the B.P phases, even at low energies where one would expect the approximations used to calculate the cuts to break down. They also show that the imaginary parts are in better agreement than the real parts.

In Figs. 5 we display impact parameter amplitudes at 6 Gev/c for our various fits, where they are compared directly with the forms obtained from the B.P amplitudes. These latter were obtained from Barger and Halzen (ref. 56). (Notice that we have $\chi \approx 2A_J$). These may be compared with the results obtained by Kelly (ref.52), where his definition of impact parameter amplitude differs from ours by a factor 2.

We obtain quite good agreement, bearing in mind the discrepancies between the B.P and Kelly evaluations. We again see that the imaginary parts are in very good agreement, and it is precisely these that are peripheral i.e dominated by contributions around $b \approx 1$ fermi. The real parts are poorly fitted because they are not peripheral, although our fits seem to be. This discrepancy at low b stems mainly from the fact that the real parts of our amplitudes are poor for high $|t|$.

In an attempt to circumvent the above difficulties we made two minor modifications of our treatment. The first concerns the absolute phase of the $I_t = 0$ amplitudes. This is known experimentally only at $t = 0$, from the optical theorem and Coulomb interference measurements (ref.51), and corresponds to predominantly imaginary amplitudes. We may thus include a factor $\exp(iat)$ in these amplitudes without spoiling this result. As far as the $I_t = 1$ amplitudes are concerned this only alters the phases of the cut terms, and

is equivalent to taking complex λ factors $\lambda \rightarrow \lambda \exp(iat)$. Alternatively we could have started with the hypothesis of complex λ factors, on the grounds that there is no need for the P and P' couplings to appear in the same ratio in diffraction processes and elastic processes. Indeed there is evidence from fits to inelastic reactions that the P coupling is less strong in general than its elastic coupling e.g the cross sections of $\pi N \rightarrow \pi N^*$ are much smaller than $\pi N \rightarrow \pi N$ (see ref.57), where the N^* are various $I = \frac{1}{2}$ resonances. There is also evidence from the study of inclusive reactions (see e.g ref.58). However this made only a slight improvement in the fits (χ^2 dropped by approximately by 7%) and made no significant difference to our amplitudes.

The second concerns the validity of the B.P $I_t = 0$ amplitudes, particularly at larger $|t|$. Comparison of the B.P amplitudes with those obtained by Kelly (at 6 Gev/c) shows that the main discrepancy is the behaviour of Re A^0_{++}. Kelly's analysis gives Re A^0_{++} a dip in the forward direction, a zero at $t \approx -0.8$, and a larger magnitude overall. This is in contrast to Re B.P^0_{++} which has no dip, no zero until $t \approx -1.1$ and a smaller magnitude. We thus tried fitting a rough estimate of Kelly's amplitudes with our parameterization (4.14) of the $I_t = 0$ amplitudes at 6 Gev/c. We were not able to reproduce the dip in Re A^0_{++} nor the relatively large magnitude of Re A^0_{++} at small $|t|$. Im A^0_{++} was reasonably well fitted. However we were able to reproduce the zero in Re A^0_{++} at $t \approx -0.8$ and the relatively large magnitude of Re A^0_{++} for $|t| > 0.8$ by including cuts, but then the fit to Im A^0_{++} suffered from having an approximate double zero at $t \approx -0.8$.

With this rather unsatisfactory fit to Kelly's $I_t = 0$ amplitudes we tried fitting the differential cross section data of πN CEX at 5.85 Gev/c. We obtained quite a good fit, but with $d\sigma/dt$ slightly too small at large $|t|$, as in the other fits. The πN CEX polarization prediction gave a positive peak at small $|t|$ and a zero at $t \approx -0.5$. We calculated the elastic polarization using our estimate of Kelly's amplitudes and obtained a good prediction for $|t| \lesssim 0.6$, but for larger $|t|$ the prediction was rather erratic and the mirror symmetry was badly broken. The real and imaginary parts of our $I_t = 1$ amplitudes were rather odd. Im A^1_{++} had a zero at $t \approx -0.35$ but the crossover was at $t \approx -0.1$, while Re A^1_{+-} had neither a single zero nor a double zero at $t \approx -0.5$. Im A^1_{+-} and Re A^1_{++} were both reasonably good.

This analysis illustrates well the sensitivity of the results on the form chosen for the $I_t = 0$ amplitudes and should perhaps serve as a warning against drawing hasty conclusions.

CONCLUSIONS

The work presented in this thesis has assumed throughout that the B.P amplitudes are reliable. In any case they are the best available, and seem to be in accord with the data up to energies of 30 Gev/c or so. On this assumption we conclude that the absorption prescription, with any hypothesis about the choosing mechanism of the ρ pole, is unable to explain the $I_t = 1$ πN amplitudes with complete success, but that the strong-cut model (F.P) is by far the best. We were able to obtain very good agreement for the

imaginary parts of the amplitudes, and this makes contact with our discussion of the unitarity equation and absorption in Chapter 3. The real parts for large $|u|$ were rather poor, especially Re A^1_{+-}, and as a consequence our elastic polarization was rather poor for large $|t|$. The choosing sense and choosing nonsense models, even with non-flip cuts only, suffered from the proximity of the zeros in Im A^1_{++} and Re A^1_{++} which filled in the dip in $d\sigma/dt$ and gave a poor charge-exchange polarization.

It seems unlikely that a better representation of the $I_t = 0$ amplitudes will remedy this defect in the real parts of the $I_t = 1$ amplitudes. It is known of course that our present methods for calculating cuts are incomplete, since the cuts violate the Bronzan-Jones condition (see Chapter 2), but the inference seems to be that until we have a better understanding of cuts the absorption prescription works well for the imaginary parts, and less so for the real parts of the $I_t = 1$ amplitudes, if we exclude extra ad-hoc hypothesis.

FIGURE CAPTIONS

Fig.1 Charge-exchange differential cross-sections. Data from M.A.Wahlig and I.Mannelli, Phys.Rev 168, 1515 (1968) and P.Sonderegger et.al. Phys.Lett. 20, 75 (1966). All curves relate to model (A) except those explicitly labelled (C) which refer to model (C). The S and N curves for model (C) are not shown being only very slightly better than those of (A).

Fig.2 Charge-exchange Polarization. Data from P.Sonderegger CERN 1971. Fig.2(a) gives the results of model (A) while Fig.2(b) gives those of model (C).

Fig.3 $\pi^+ p$ Polarization. Data from M.Borghini et.al. Phys. Lett. 31B, 405 (1970) and Phys.Lett. 36B, 5,493 (1971) The curves apply directly to modal (A). Model (C) fits are practically indistinguishable from these.

Fig.4 The real and imaginary parts of the $I_t = 1$ amplitudes at incident lab. momentum 2.5, 6.0 Gev/c. Note that our amplitudes are dimensionless. The curves apply directly to model (A). Model (C) curves are practically indistinguishable from these, being only slightly better at larger $|t|$ values.

Fig.5 The real and imaginary parts of the $I_t = 1$ impact-parameter amplitudes at incident lab. momentum 2.5, 6.0 Gev/c. Note that $\chi \approx 2A_J$. All curves relate to model (A) or (C) except those explicitly labelled (C) which refer to model (C), being sufficiently different from the model (A) case.

Fig.6 The real and imaginary parts of the $I_t = 0$ amplitudes. It exhibits our fits (a) and (b) to the B.P $I_t = 0$ amplitudes.

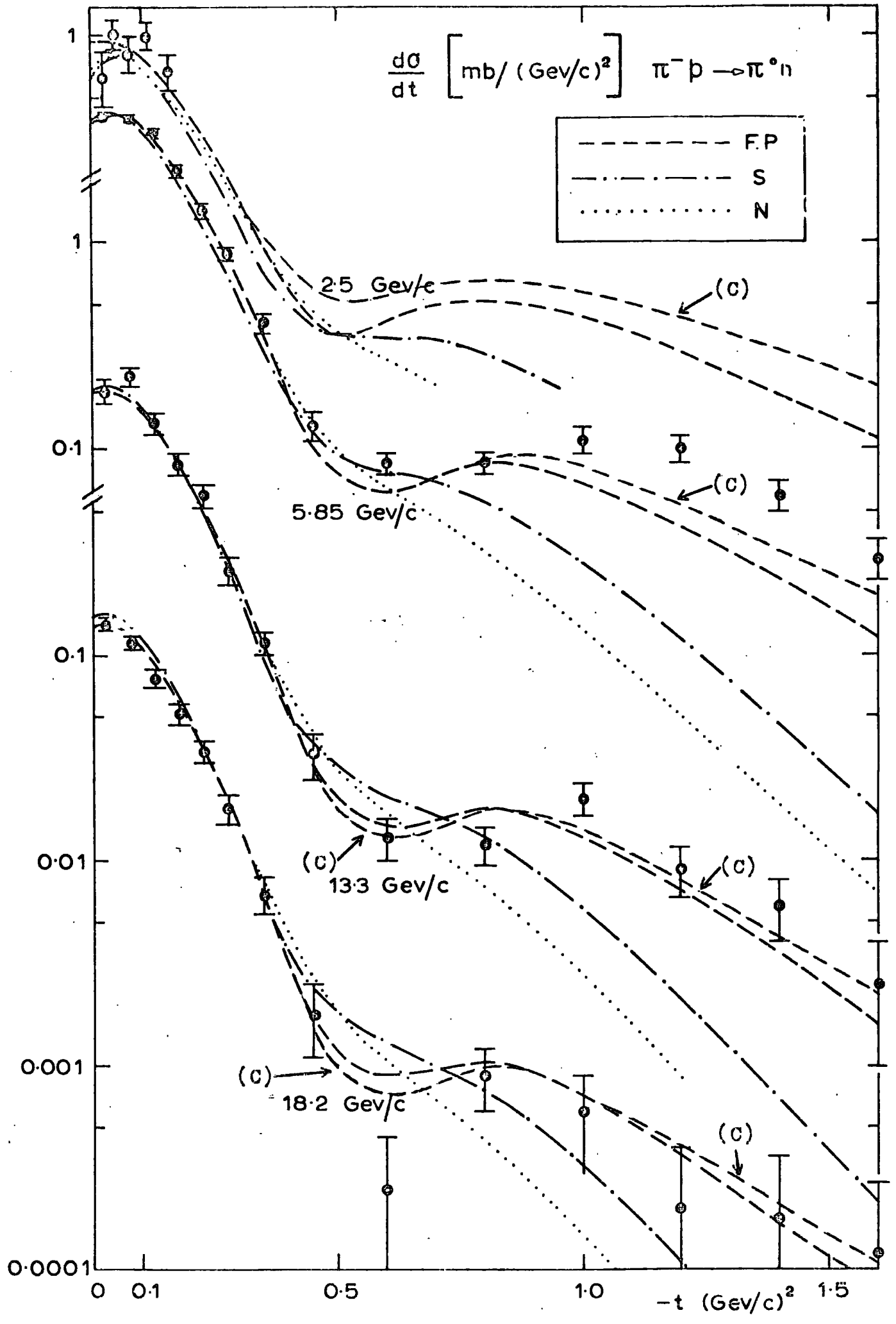
dσ/dt [mb/(Gev/c)²] π⁻p → π°n
F.P
S
N
2·5 Gev/c
(c)
5·85 Gev/c
(c)
13·3 Gev/c
(c)
18·2 Gev/c
(c)
(c)
1
1
0·1
0·1
0·01
0·001
0·0001
0
0·1
0·5
1·0
1·5
−t (Gev/c)²

FIG. 1.

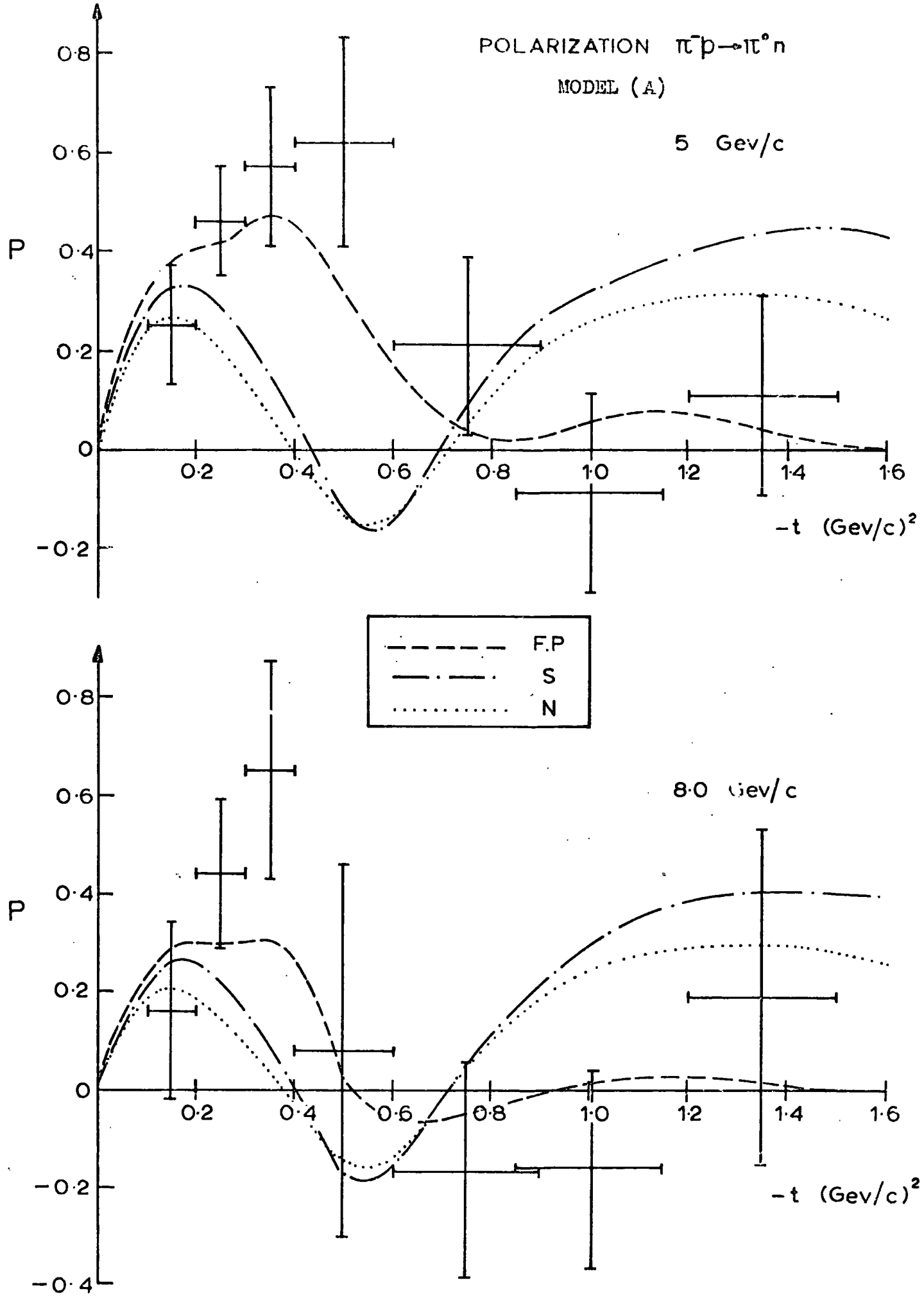
POLARIZATION $\pi^- p \to \pi^0 n$
MODEL (A)
5 Gev/c
P
0·8
0·6
0·4
0·2
0
-0·2
0·2
0·4
0·6
0·8
1·0
1·2
1·4
1·6
-t (Gev/c)²
F.P
S
N
8·0 Gev/c
P
0·8
0·6
0·4
0·2
0
-0·2
-0·4
0·2
0·4
0·6
0·8
1·0
1·2
1·4
1·6
-t (Gev/c)²

FIG. 2.(a)

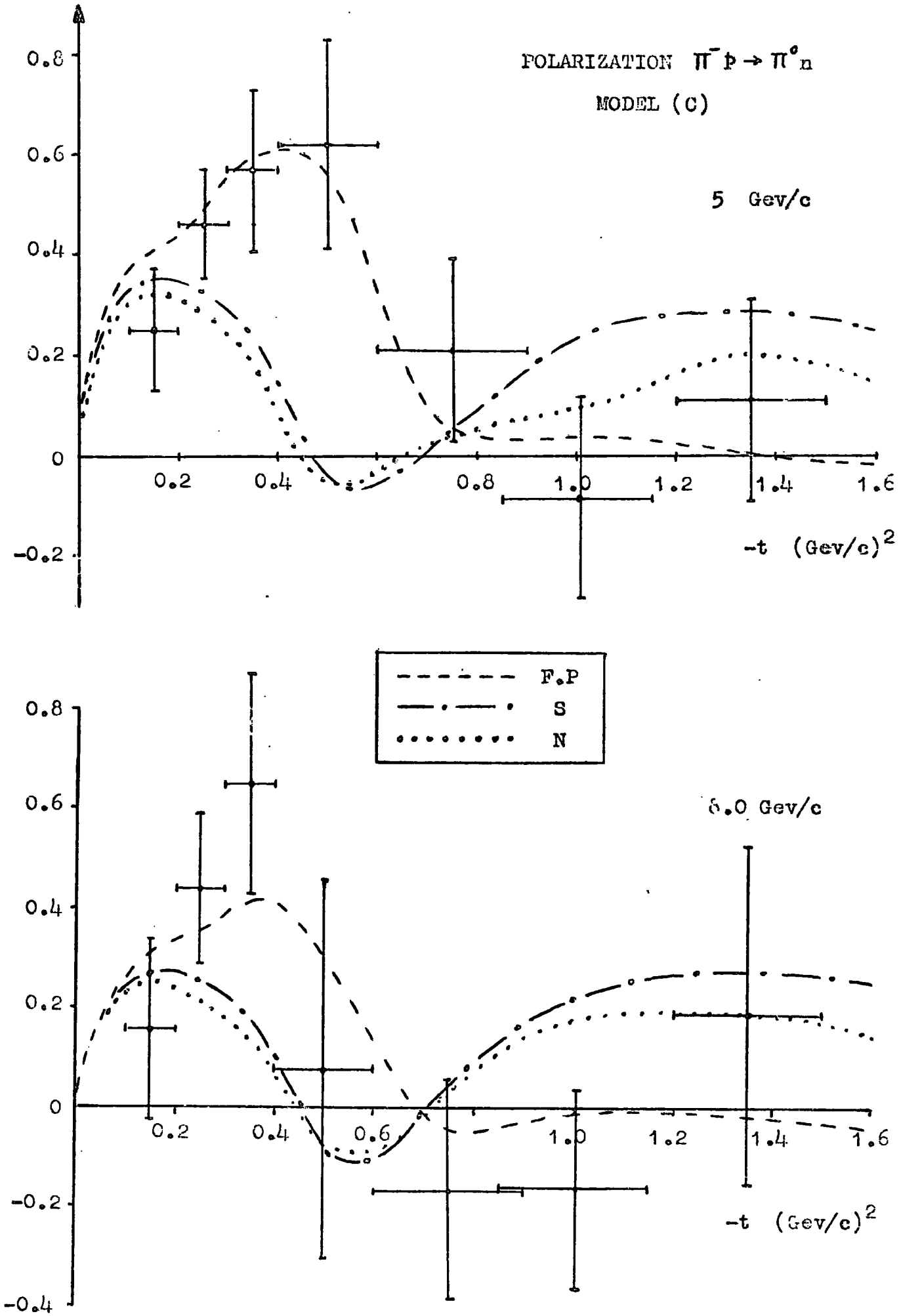
POLARIZATION $\pi^- p \to \pi^0 n$
MODEL (C)
5 Gev/c
0.8
0.6
0.4
0.2
0
-0.2
0.2
0.4
0.8
1.0
1.2
1.4
1.6
-t (Gev/c)^2
F.P
S
N
6.0 Gev/c
0.8
0.6
0.4
0.2
0
-0.2
-0.4
0.2
0.4
0.6
1.0
1.2
1.4
1.6
-t (Gev/c)^2

FIG.2.(b)

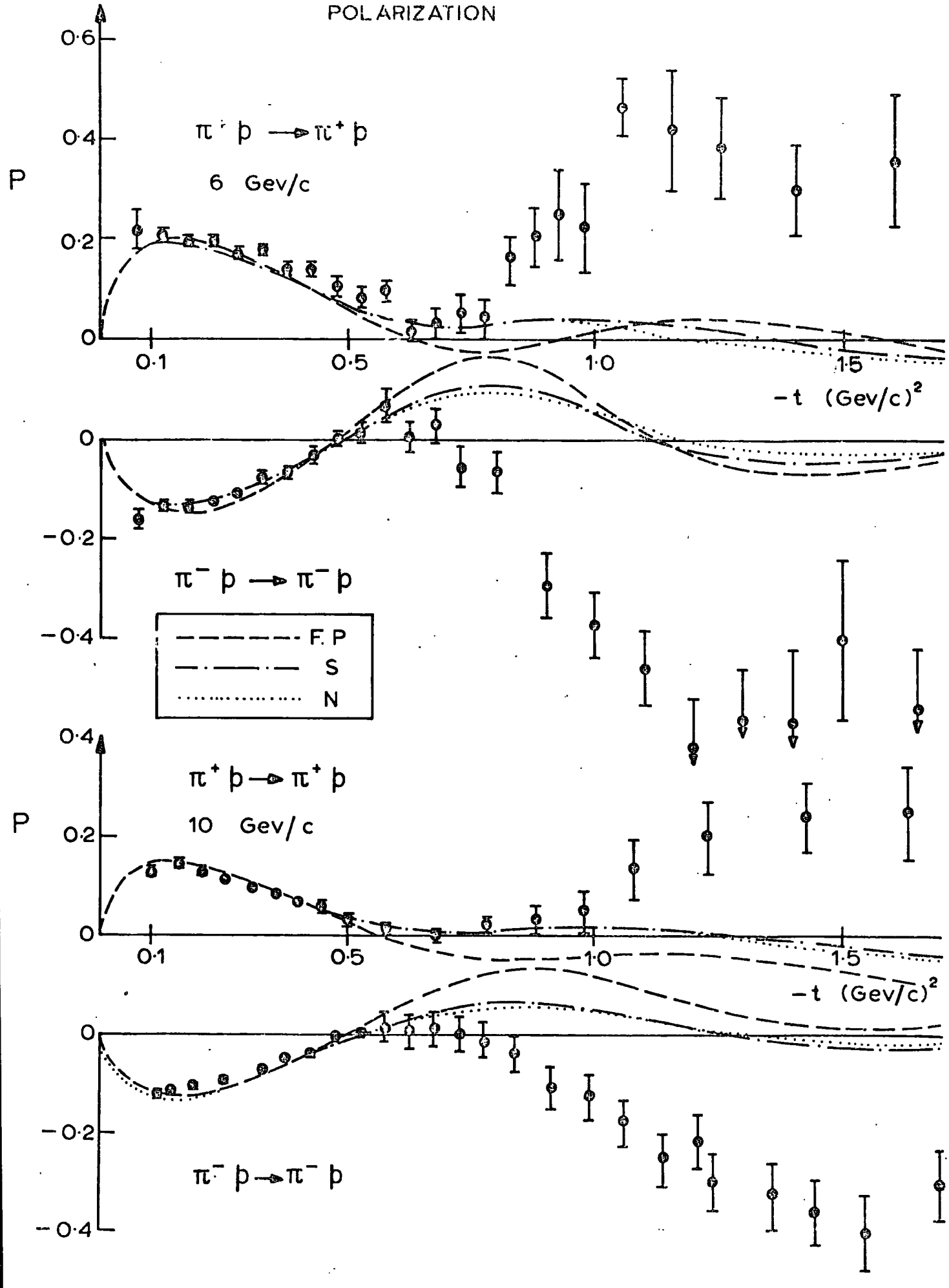
POLARIZATION
P
0·6
0·4
0·2
0
$\pi^- p \rightarrow \pi^+ p$
6 Gev/c
0·1
0·5
1·0
1·5
$-t$ (Gev/c)^2
−0·2
−0·4
$\pi^- p \rightarrow \pi^- p$
F. P
S
N
$\pi^+ p \rightarrow \pi^+ p$
10 Gev/c
$\pi^- p \rightarrow \pi^- p$

FIG. 3.

S-CHANNEL HELICITY AMPLITUDES FOR $I_t = 1$

——— BARGER PHILLIPS
– – – – F.P
—·—·— S
····· N

P_{LAB} = 2·5 Gev/c.

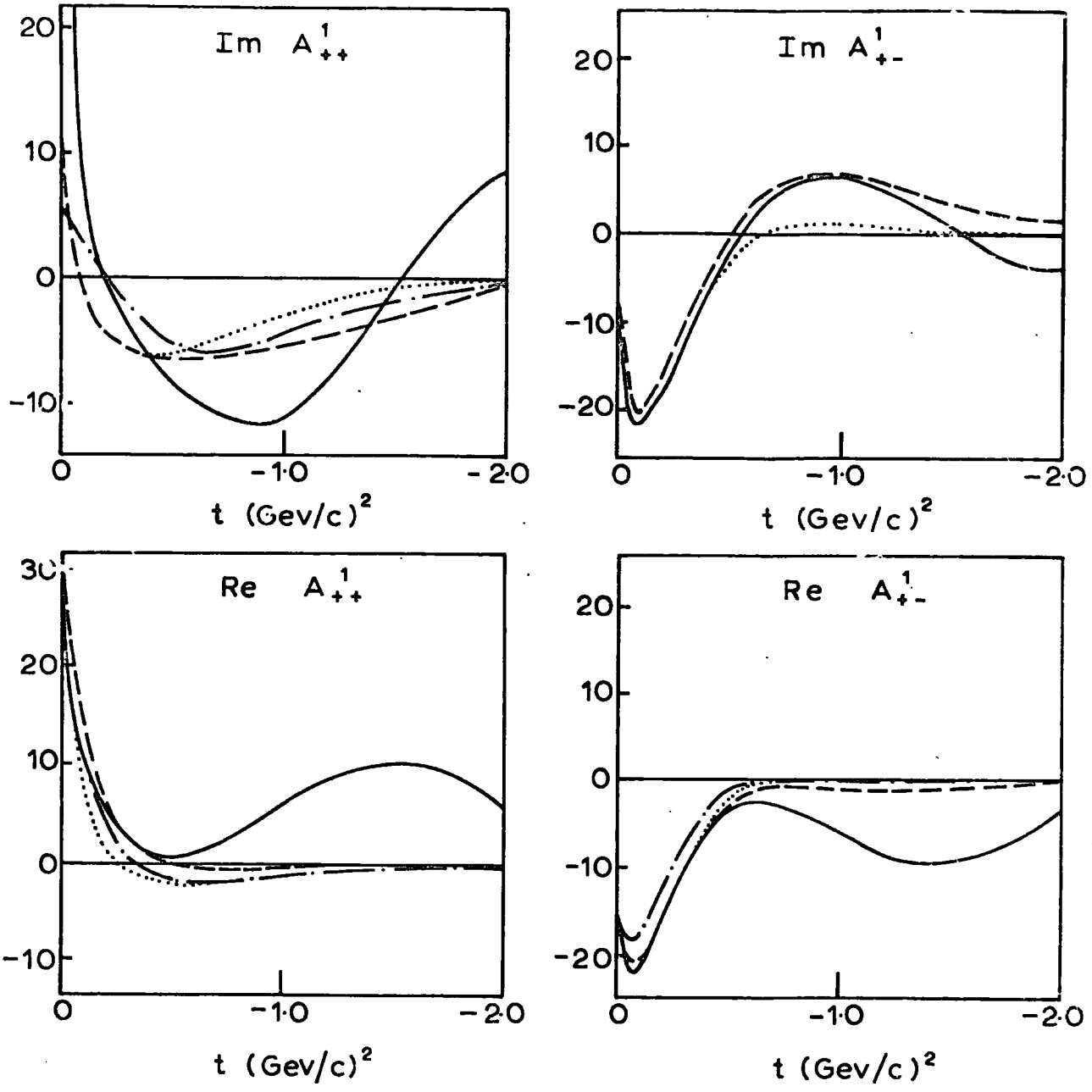

FIG .4 (a).

S-CHANNEL HELICITY AMPLITUDS FOR $I_t = 1$

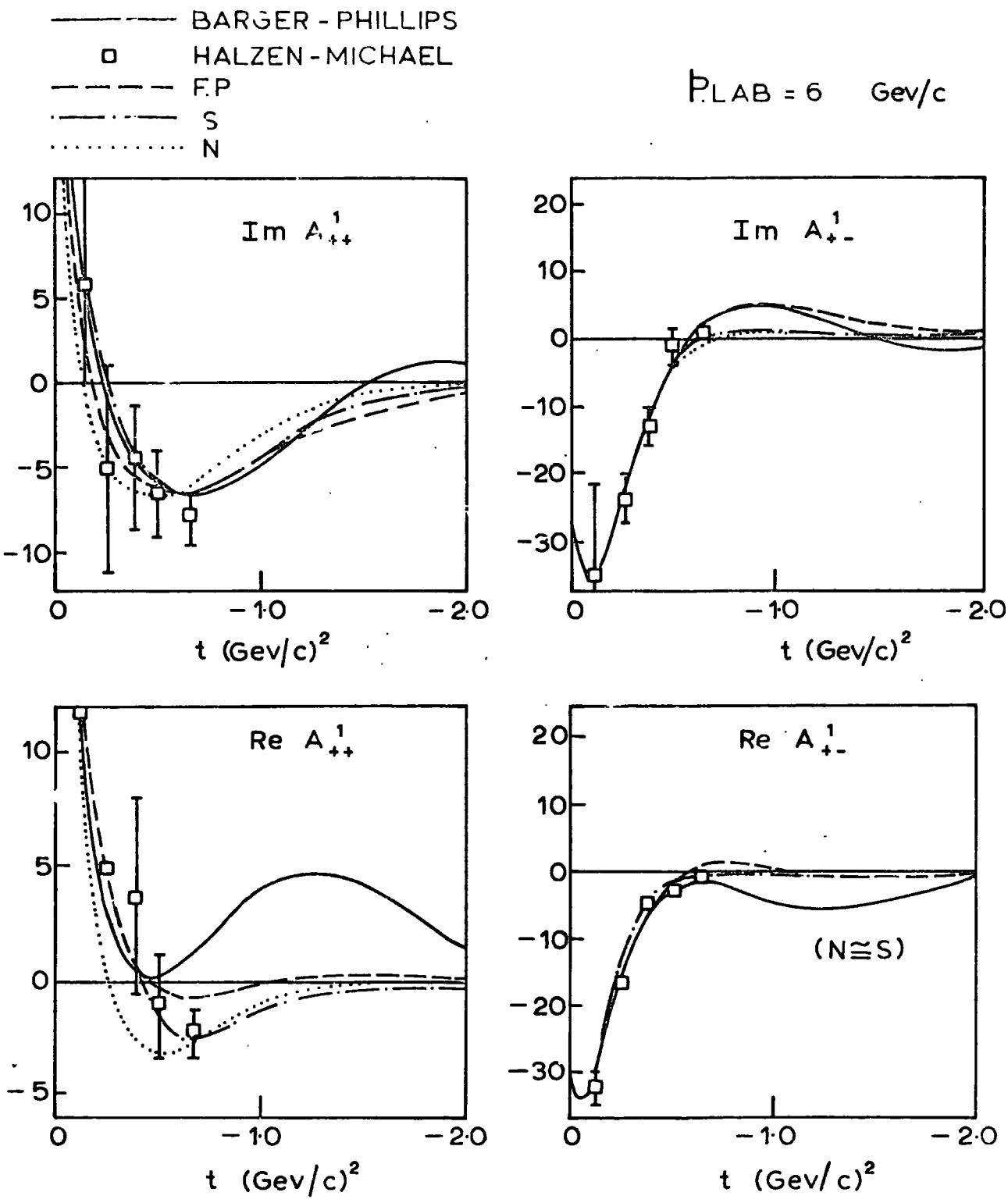

FIG. 4 (b).

$I_t = 1$ π N IMPACT PARAMETER AMPLITUDES.

——— BARGER - PHILLIPS

- - - - - - - - F.P

—·—·— S

. . . . . N

P_{LAB} = 2.5 Gev/c

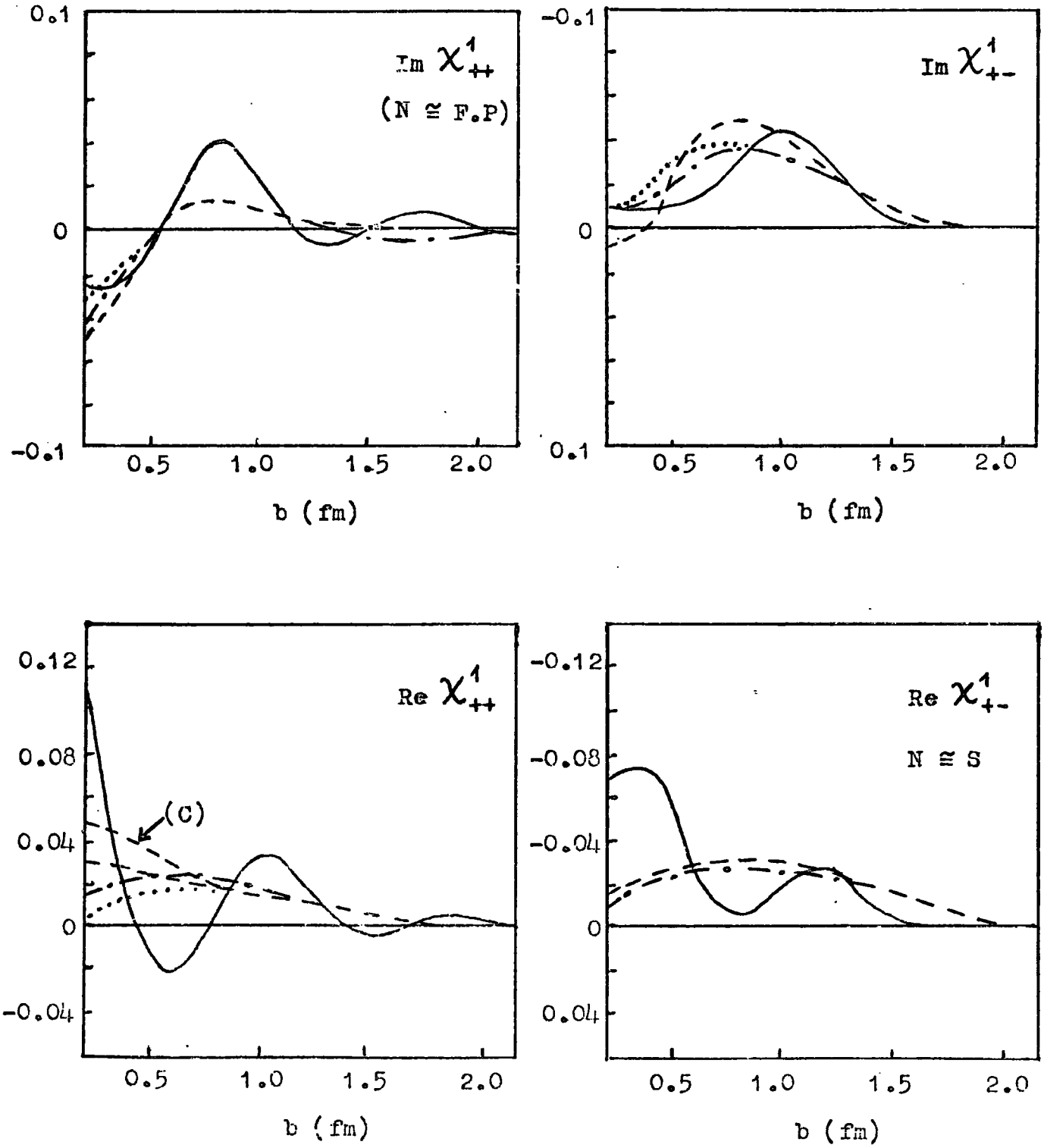

FIG.5(a)

I = 1 πN IMPACT PARAMETER AMPLITUDES.

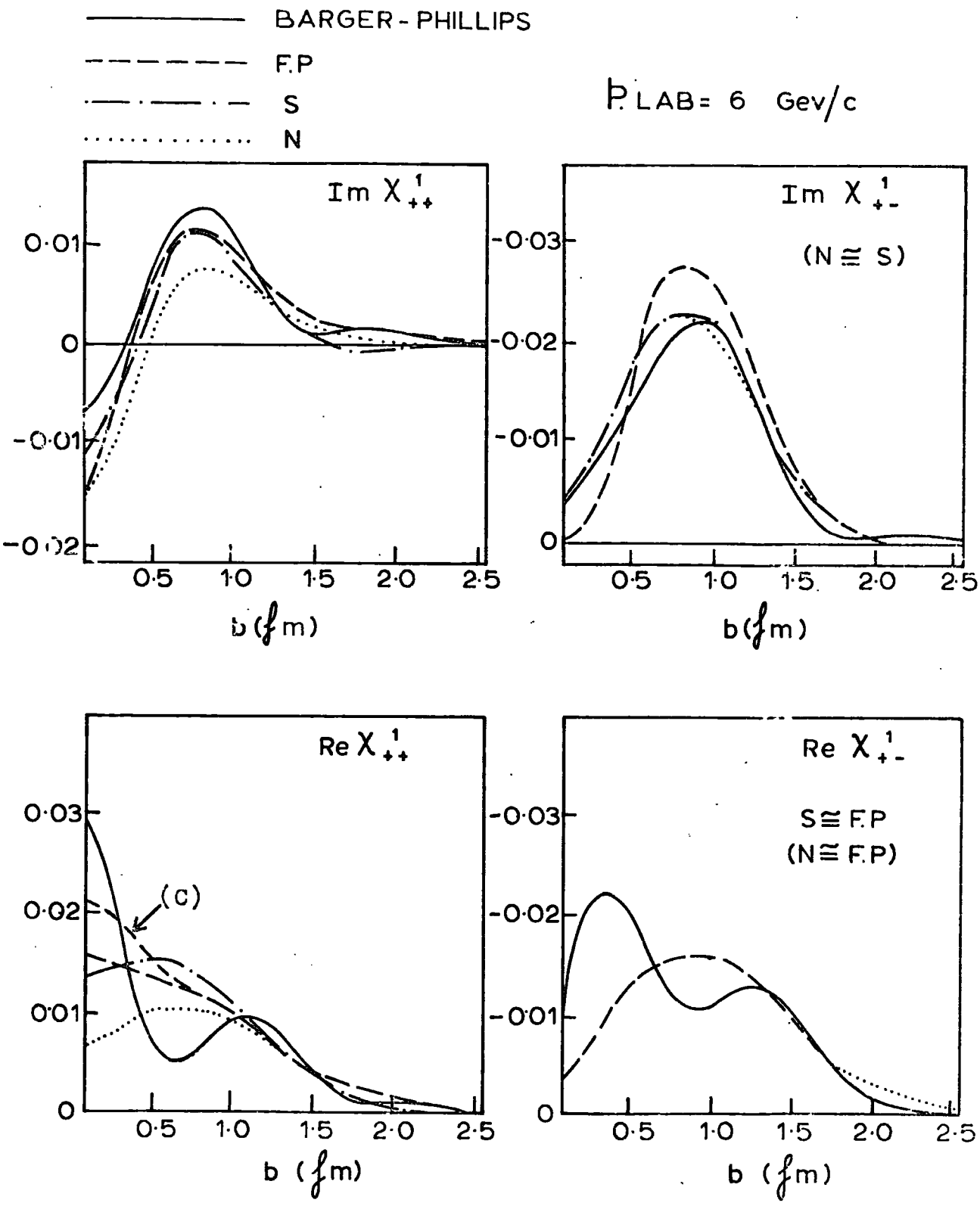

FIG. 5.(b)

S - CHANNEL HELICITY AMPLITUDES FOR $I_t = 0$

——— BARGER - PHILLIPS

□ HALZEN - MICHAEL

– – – – – Method (a) Fit (No Cuts)

. . . . . Method (b) Fit (With Cuts)

p_{LAB} = 6.0 Gev/c

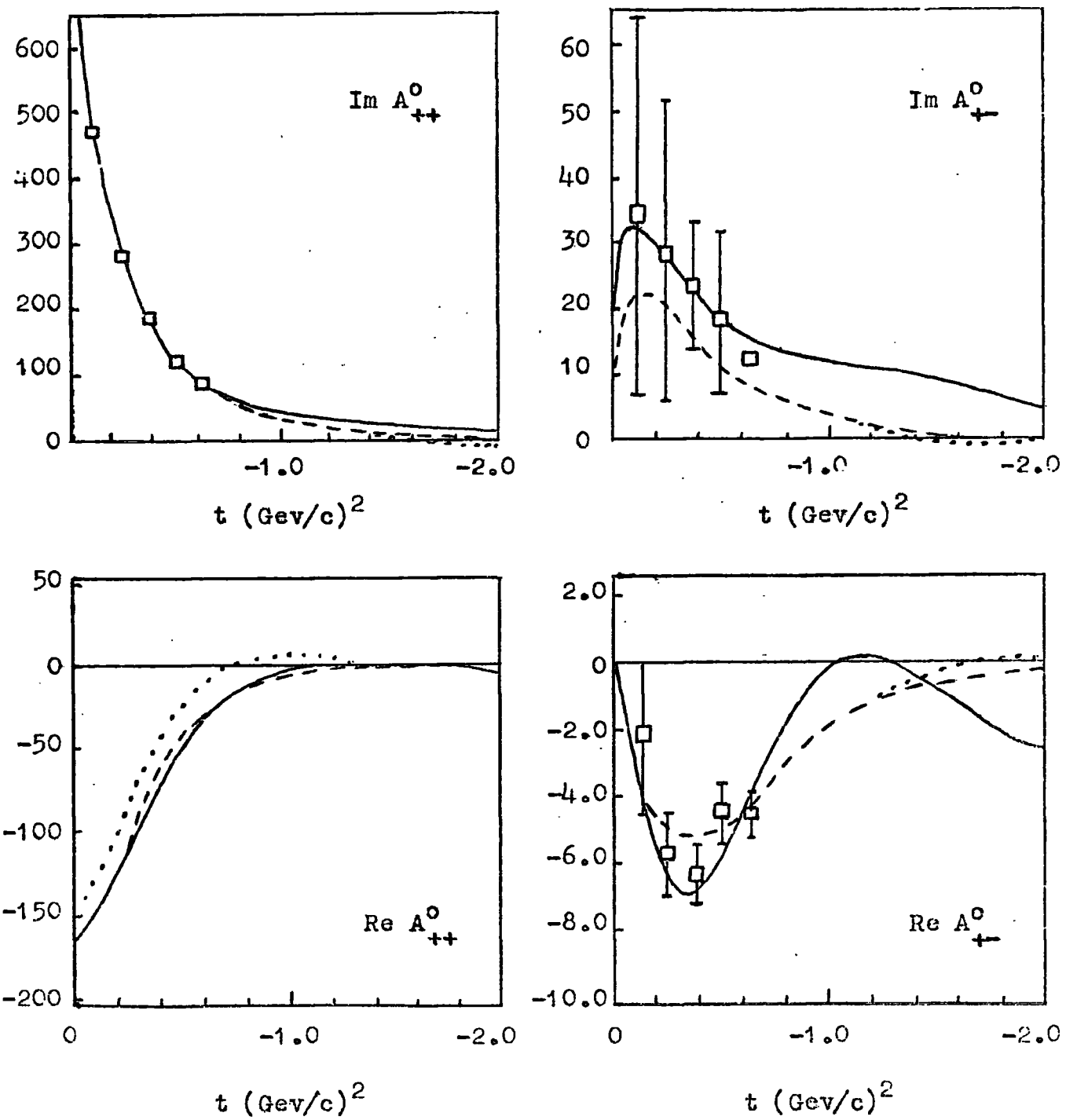

FIG.6

APPENDIX A

We give here the proof of the expression for the discontinuities of the signatured partial wave amplitudes (see eqn.(2.2) of the main text).

We start with the Froissart-Gribov formula

$$A_\ell^{\pm}(t) = \frac{1}{16\pi^2}\int_{z_0}^{\infty} D_s^{\pm}(z',t)\, Q_\ell(z')\, dz' \qquad (A.1)$$

where

$$D_s^{\pm}(z,t) = D_s(z,t) \pm D_u(-z,t) \qquad (A.2)$$

We can write a fixed - s dispersion relation for D_s.

$$D_s(s,t) = \frac{1}{\pi}\int \frac{\rho_{st}(s,t')}{t'-t}\,dt' + \frac{1}{\pi}\int \frac{\rho_{su}(s,u')}{u'-u}\,du' \qquad (A.3)$$

and a fixed-u dispersion relation for $D_u(u,t)$

$$D_u(u,t) = \frac{1}{\pi}\int \frac{\rho_{us}(s',u)}{s'-s}\,ds' + \frac{1}{\pi}\int \frac{\rho_{ut}(u,t')}{t'-t}\,dt' \qquad (A.4)$$

We require $D_u(-z,t)$, and since $z \leftrightarrow -z$ corresponds to $s \leftrightarrow u$ we can write $D_u(-z,t) = D_u(s,t)$, where

$$D_u(s,t) = \frac{1}{\pi}\int \frac{\rho_{us}(s',s)}{s'-u}\,ds' + \frac{1}{\pi}\int \frac{\rho_{ut}(s,t')}{t'-t}\,dt' \qquad (A.5)$$

We put $s' \leftrightarrow u'$ in the first term here, and using $\rho_{su} = \rho_{us}$ we get

$$D_u(-z,t) = \frac{1}{\pi}\int \frac{\rho_{su}(u',s)}{u'-u}\,du' + \frac{1}{\pi}\int \frac{\rho_{ut}(s,t')}{t'-t}\,dt' \qquad (A.6)$$

For simplicity we consider equal mass scalar particles. In this case the boundaries of the spectral functions are given by the condition $K = 0$, where

$$K = K(t,t_1,t_2,s) = t^2+t_1^2+t_2^2-2(tt_1+t_1t_2+tt_2)-tt_1t_2/q_s^2 \quad (A.7)$$

which gives the usual result (see ref.3) that the boundary is given by

$$t = 4t_o + 4t_o^2 / (s - 4m^2) = b(s) \text{ , say.} \quad (A.8)$$

If we include the possibility of bound state poles then $t_o = m^2$ (if not , $t_o = 4m^2$), and we get

$$b(s) = 4m^2 + 4m^4 / (s - 4m^2) . \quad (A.9)$$

In the equal mass case this is the boundary for all the spectral functions.

Thus writing $u = 4m^2 - s - t$, we have

$$D_s^{\pm}(z,t) = \frac{1}{\pi}\int_{b(s)}^{\infty}\left\{\frac{\rho_{st}(s',t) \pm \rho_{ut}(s',t)}{t'-t}\right\}dt' + \frac{1}{\pi}\int_{b(s)}^{\infty}\left\{\frac{\rho_{su}(s,u') \pm \rho_{su}(u',s)}{u'+s+t-4m^2}\right\}du' \quad (A.10)$$

This shows immediately that $D_s(z,t)$ has cuts in t :- the first term has the cut $t \geqslant b(s)$, while the second term has the cut $t \leqslant -s + 4m^2 - b(s)$ i.e

$$t \leqslant -s - 4m^4 / (s - 4m^2) \quad (A.11)$$

Since $s \geqslant 4m^2$ and the maximum of the right-hand side of (A.11) is $-8m^2$, these cuts are therefore

$$t \geqslant 4m^2 \quad \text{and} \quad t \leqslant -8m^2 \quad (A.12)$$

From (A.1) we see that $A_\ell^{\pm}(t)$ must also have these cuts. However $A_\ell^{\pm}(t)$ also has the cuts of $Q_\ell(z)$ viz. the cuts $(-1,1)$ and $(-\infty,-1)$. However we can eliminate the discontinuity for

$z < -1$ by considering instead of $A_\ell^\pm(t)$ the amplitudes $B_\ell^\pm(t)$ where

$$B_\ell^\pm(t) = A_\ell^\pm(t)/q_t^{2\ell} \tag{A.13}$$

and we now have the following result

$$\mathrm{Disc}_t\left[q^{-2\ell}(t+i0)\,Q_\ell\left(1+\frac{2s}{t-4m^2+i0}\right)\right] = \theta(4m^2-s-t)\times$$
$$\times\left(-q^2(t)\right)^{-\ell} i\pi P_\ell\left(-1-\frac{2s}{t-4m^2}\right) \tag{A.14}$$

Since

$$B_\ell^\pm(t) = \frac{1}{16\pi^2}\int_{4m^2}^{\infty}\frac{D_s^\pm(s',t)}{q^{2\ell}}\,Q_\ell\left(1+\frac{s'}{2q^2}\right)\frac{ds'}{2q^2} \tag{A.15}$$

we see that the discontinuity $\frac{1}{2i}\,\mathrm{Disc}_t\left[B^\pm(\ell,t)\right]_{t+i0} = \mathrm{Im}\,B^\pm(\ell,t)$ involves

$$\frac{1}{2i}\mathrm{Disc}_t\left[q^{-2\ell}Q_\ell\,D_s^\pm\right]_{t+i0} = \frac{1}{2i}\mathrm{Disc}_t\left[q^{-2\ell}Q_\ell\right]_{t+i0}\cdot D_s^\pm(s,t-i0) +$$
$$+\left[q^{-2\ell}Q_\ell\right]_{t+i0}\cdot\frac{1}{2i}\mathrm{Disc}_t\left[D_s^\pm(s,t+i0)\right] \tag{A.16}$$

We consider first the discontinuity of (A.15) across the Left-hand cut $t \leq 0$. The first term of (A.16) gives

$$\frac{1}{2i}\frac{1}{16\pi^2}\int_{4m^2}^{\infty}\theta(4m^2-s'-t)\left(-q^2\right)^{-\ell} i\pi P_\ell\left(-1-\frac{2s'}{t-4m^2}\right)D_s^\pm(s',t-i0)\frac{ds'}{2q^2}$$

$$=\frac{1}{32\pi}\int_{4m^2}^{4m^2-t}\frac{ds'}{2q^2}\cdot\frac{1}{(-q^2)^\ell}\cdot P_\ell\left(-1-\frac{2s'}{t-4m^2}\right)D_s^\pm(s',t-i0) \tag{A.17}$$

For the second term of (A.16) we require $\frac{1}{2i}\,\mathrm{Disc}_t\left[D_s^\pm(s',t+i0)\right]_{t\leq}$ and this is given by

$$\left\{\rho_{su}(s',4m^2-t-s') \pm \rho_{su}(4m^2-t-s',s')\right\}\theta\left(-t-s'-\frac{4m^4}{s'-4m^2}\right)$$

where the θ function comes from the condition (A.11).

So the second term gives

$$\frac{1}{16\pi^2}\int_{4m^2}^{\infty}\frac{ds'}{2q^2}\frac{1}{q^{2\ell}}Q_\ell\left(1+\frac{s'}{2q^2}\right)\theta\left(-t-s'-\frac{4m^4}{s'-4m^2}\right)\left\{\rho_{su}(s',4m^2-t-s')\pm\rho_{su}(4m^2-t-s',s')\right\} \tag{A.18}$$

Because of the θ function only those values of s' in the range $[v_-(t),\ v_+(t)]$ will contribute, where $v_\pm(t)$ are the roots of the equation

$$t + s' + 4m^4/(s' - 4m^2) = 0 \tag{A.19}$$

i.e $$v_\pm(t) = \tfrac{1}{2}(4m^2 - t) \pm \tfrac{1}{2}\sqrt{t(t + 8m^2)} \quad .$$

So (A.18) reduces to

$$\frac{1}{16\pi^2}\int_{v_-(t)}^{v_+(t)}\frac{ds'}{2q^2}\frac{1}{q^{2\ell}}.Q_\ell\left(1+\frac{s'}{2q^2}\right)\left\{\rho_{su}(s',4m^2-t-s')\pm\rho_{su}(4m^2-t-s',s')\right\} \tag{A.20}$$

This can be simplified further. Let $\bar{s}' = 4m^2 - t - s'$.

Then if $s' = v_\pm(t)$ then $\bar{s}' = v_\mp(t)$, and so the limits $v_\pm(t) \to v_\mp(t)$ for $s' \to \bar{s}'$. So the second term of (A.20) can be re-written

$$\frac{1}{16\pi^2}\int_{v_+}^{v_-}\frac{-d\bar{s}'}{2q^2}\frac{1}{q^{2\ell}}Q_\ell\left(-1-\frac{2\bar{s}'}{t-4m^2}\right)\rho_{su}(\bar{s}',4m^2-t-\bar{s}') \tag{A.21}$$

$$=\frac{1}{16\pi^2}\int_{v_-}^{v_+}\frac{d\bar{s}'}{2q^2}\frac{1}{q^{2\ell}}Q_\ell\left(1+\frac{\bar{s}'}{2q^2}\right)\left(-e^{-i\pi\ell}\right)\rho_{su}(\bar{s}',4m^2-t-\bar{s}')$$

and so (A.20) becomes

$$\frac{1}{16\pi^2}\int_{v_-(t)}^{v_+(t)}\frac{ds'}{2q^2}\frac{1}{q^{2\ell}}Q_\ell\left(1+\frac{s'}{2q^2}\right)\left[1\mp e^{-i\pi\ell}\right]\rho_{su}(s',4m^2-t-s') \tag{A.22}$$

Thus from (A.22) and (A.17) we get for the left-hand discontinuity

$$\mathrm{Im}\left[B^{\pm}(\ell,t)\right]_{L.H.CUT} = \frac{1}{32\pi}\int_{4m^2}^{4m^2-t} \frac{ds'}{2q^2}\,\frac{1}{(-q^2)^{\ell}}\,P_{\ell}\left(-1-\frac{s'}{2q^2}\right) D_s^{\pm}(s',t-i0) +$$

$$+\frac{1}{16\pi^2}\int_{U_-(t)}^{U_+(t)} \frac{ds'}{2q^2}\,\frac{1}{q^{2\ell}}\,Q_{\ell}\left(1+\frac{s'}{2q^2}\right)\left(1\pm e^{-i\pi\ell}\right)\rho_{su}(s',4m^2-t-s') \qquad (A.23)$$

which is equation (2.2) of the text.

The situation with the Right-hand cut discontinuity is different. There is no term analogous to the first term of (A.23) since for $t \geq 4m^2$ and $s' \geq 4m^2$, $\Theta(4m^2 - t - s') \equiv 0$. The second term would involve $\frac{1}{2i}\,\mathrm{Disc}_t\left[D_s(s',t+i0)\right]_{t\geq 4m^2}$ which is equal to

$$\left\{\rho_{st}(s',t) \pm \rho_{ut}(s',t)\right\}.\,\Theta\left(t-4m^2-\frac{4m^4}{s'-4m^2}\right) \qquad (A.24)$$

and the Θ function comes from the condition $t \geq b(s)$ (see eqn.(A.9)). Thus the discontinuity vanishes unless

$$t \geq 4m^2 + 4m^4/(s'-4m^2)$$

i.e $$s' \geq 4m^2 + 4m^4/(t-4m^2) = v_0(t) \text{ say.} \qquad (A.25)$$

So we have for the Right-hand discontinuity

$$\mathrm{Im}\left[B^{\pm}(\ell,t)\right]_{R.H.CUT} = \frac{1}{16\pi^2}\int_{U_0(t)}^{\infty} \frac{ds'}{2q^2}\,\frac{1}{q^{2\ell}}\,Q_{\ell}\left(1+\frac{s'}{2q^2}\right)\left\{\rho_{st}(s',t)\pm\rho_{ut}(s',t)\right\}. \qquad (A.26)$$

which does <u>not</u> involve a term with a finite range of integration.

REFERENCES

1. 'Regge Theory and Particle Physics' - P.D.B.Collins Physics Reports 1C no.4 (1971)

2. 'Regge Poles in Particle Physics' - P.D.B.Collins and E.J.Squires (Springer, Berlin (1968)).

3. 'Elementary Particle Theory' - A.D.Martin and T.D. Spearman; North Holland (1970)

4. 'The Dynamical S-Matrix' - G.F.Chew ; Benjamin, New York (1966).

5. 'The Analytic S-Matrix' - R.J.Eden et.al ; Cambridge University Press (1966).

6. R.Oehme in 'Strong Interactions and High Energy Physics' - Moorhouse (Ed.) ; Oliver and Boyd, London (1964).

7. M.Froissart, Phys. Rev. 123,1053 (1961)

8. V.N.Gribov and I.Y.Pomeranchuk, Phys. Lett. 2,239 (1962)

9. M.Jacob and G.C.Wick , Ann. Phys. 7,404 (1959)

10. T.L.Trueman and G.C.Wick, Ann. Phys. 26, 322 (1964)

11. G.Cohen-Tannoudji, A.Morel, H.Navalet - Ann. Phys. 46, 239 (1968).

12. F.Arbad and J.D.Jackson, Phys. Rev. 176, 1796 (1968)

13. L.C.Wang, Phys. Rev. 142, 1187 (1966)

14. T.Regge, Nuovo Cimento 14, 951 (1959);18, 947 (1960)

15. Mandelstam and Wang, Phys. Rev. 160, 1490 (1967)

16. C.E.Jones and V.L.Teplitz, Phys. Rev. 159, 1271 (1967)

17. J.B.Bronzan and C.E.Jones, Phys. Rev. 160, 1494 (1967)

18. D.Amati,S.Fubini and A.Stanghellini - Phys. Lett. 1, 29 (1962).

19. J.C.Polkinghorne, Journ. Math. Phys. 4, 503 (1963)

20. S.Mandelstam, Nuovo Cimento 30, 1127,1148 (1963)

21. R.J.Glauber : 'Lectures in Theoretical Physics' Vol.1 - Wiley, New York (1959).

22. V.N.Gribov, JETP 26,414 (1968)

23. V.V.Sudakov, JETP 30, 87 (1956)

24. H.J.Rothe, Phys. Rev. 159, 1471 (1967)

25. P.V.Landshoff, Schladming Lectures 1970.

26. J.Finkelstein and M.Jacob, Nuovo Cimento 56A, 681 (1968)

27. N.J.Sopkovich, Nuovo Cimento 26, 186 (1962)

28. K.Gottfried and J.D.Jackson, Nuovo Cimento 34, 735 (1964)

29. F.Henyey, G.L.Kane, J.Pumplin and M.H.Ross - Phys. Rev. 182, 1579 (1969).

30. R.C.Arnold, Phys. Rev. 153, 1523 (1967)

31. J.Caneschi, Phys. Rev. Lett. 23, 254 (1969)

32. P.J.O'Donovan, Phys. Rev. 185, 1902 (1969)

33. R.J.Rivers, Nuovo Cimento 63A, 697 (1969)

34. R.C.Arnold and M.L.Blackmon, Phys. Rev. 179, 1480 (1969)

35. L.Bertocchi, Heidelberg Conference (1967)

36. R.J.N.Phillips, Acta Physica Austriaca, Suppl.VII 214 (1970) - Springer Verlag.

37. G.E.Hite, Acta Physica Austriaca, Suppl.VII 180 (1970) Springer Verlag.

38. R.J.N.Phillips and G.A.Ringland, Nuc. Phys. B32, 131 (1971)

39. P.D.B.Collins and F.D.Gault, Springer Tracts in Modern Physics 63, 163 (1972)

40. Englert, Nicolotopulos, Prout and Truffin - Nuovo Cimento 64A, 561 (1970)

41. P.Nicolotopulos and M.A.L.Prevost, Nuovo Cimento 69A, 665 (1970)

42. J.L.Cardy, Nuc. Phys. B28, 455,477 (1971)

43. S.C.Frautchi and B.Margolis, Nuovo Cimento 56A, 1155 (1968)

44. F.Arbad and C.B.Chiu, Phys. Rev. 147, 1045 (1966)

45. A.Ahmadzadeh and J.C.Jackson, Phys. Rev. 187, 2078 (1969)

46. S.Y.Chiu, B.R.Desai and D.P.Roy, Phys. Rev. 187,1896 (1969)

47. A.Ahmadzadeh and W.B.Kaufman, Phys. Rev. 188, 2438 (1969)

48. V.Barger and R.J.N.Phillips, Phys. Rev. 187, 2210 (1969)

49. G.Cohen-Tannoudji, A.Morel and H.Navalet - Nuovo Cimento 48A (1967)

50. W.Rarita et.al. Phys. Rev. 165, 1615 (1968)

51. F.Halzen and C.Michael, Phys. Lett. 36B, 367 (1971)

52. R.L.Kelly, Phys. Lett. 39B,635 (1972)

53. P.D.B.Collins and R.A.Swetman, Lettere al Nuovo Cimento vol.5,n.12 793 (1972)

54. B.J.Hartley and G.L.Kane, Phys. Lett. 39B, 531 (1972)

55. H.Harari, Phys. Rev. Lett. 26, 1400 (1971)

56. V.Barger and F.Halzen - Wisconsin preprint.

57. E.W.Anderson, Phys. Rev. Lett. 25, 699 (1970)

58. Chan Hong Mo - Oxford Conference, April 1972.